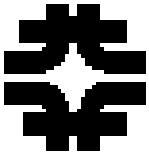

1/05/10
TD-10-001

LARP LQS01 Magnet Test Summary

G. Chlachidze, G. Ambrosio, N. Andreev, E. Barzi, R. Carcagno, S. Caspi, D. Dietderich, H. Felice, P. Ferracin, A. Ghosh, V.V. Kashikhin, M.J. Kim, M.J. Lamm, F. Lewis, F. Nobrega, I. Novitski, D. Orris, G.L. Sabbi, J. Schmalzle, C. Sylvester, M. Tartaglia, J.C. Tompkins, G. Velev, P. Wanderer, A.V. Zlobin

Content:

1. Introduction

LQS01 is the first Nb_3Sn Long Quadrupole assembled by the US LHC Accelerator Research Program (LARP) [1]. It has 3.3-m long coils and a shell-based structure [2]. The LQS01 coils were made of 27-strand Rutherford cable with 0.7-mm Nb_3Sn strand based on the "Restack Rod Process" (RRP) of 54/61 sub-element design. Details of the design, coil fabrication, magnet assembly and instrumentation can be found in [3]. Description of the magnet also can be found in [4].

The test of LQS01 had a special relevance because it was the first attempt to meet the LARP goal (set in 2005) of 200 T/m field gradient in a Nb_3Sn Long Quadrupole. The magnet started training at 9.7 kA, and reached 11.2 kA current (corresponding to the 200 T/m) at the 31st quench.

The test took more time than usual because of trips in quench detection system induced by larger-than-expected voltage spikes at low currents, and because of the recovery time (~ 1-2 hours) after high-current quenches. Nonetheless LQS01 reached the 200-T/m goal, and most of the test plan was completed (magnetic measurements, ramp-rate dependence study, as well as protection heater and spike studies). Most of the test was done at 4.5 K and 3.0 K, and only two quenches were performed at 1.9 K.

Training history, strain-gauge data, and temperature dependence showed that the quench training was strongly affected by low pre-stress in the inner layer. Analysis of the strain-gauge data after pre-load [2] and after cool-down, together with FE modeling, showed that this non-optimal pre-stress distribution could be caused by a mismatch between coil outer diameter (OD) and structure inner (ID) diameter. The computed stress could degrade the coil at currents higher than the target. Therefore it was decided to interrupt the training, and resume it with the nominal pre-stress distribution after disassembly and reassembly.

The LQS01 magnet was installed into the VMTF dewar and it was electrically checked by November 11th, 2009. Cool down started on November 12th and the VMTF dewar was filled with liquid helium on November 17th. Test was started on November 18th and was completed on December 18th. Finally the LQS01 magnet has been removed from the VMTF dewar on January 7th, 2010.

2. Instrumentation

The LQS01 magnet was built using coils 6, 7, 8 and 9. Each coil is equipped with 4 protection heaters and 1 spot heater. For the first time in LARP magnets, protection heaters are installed on both the outer and inner layers; heaters in technological quadrupole (TQ) models were only placed on the outer surface of the outer coil.

Protection heaters were made of stainless steel with 6.2-6.7 Ohm resistance at room temperature. Since only limited number of wires is provided for strip heater connection at VMTF it was decided to connect protection heaters in 4 groups. In each group all heaters on the same coil layer and at the same side (lead end or return end) are connected in parallel (see Fig. 1). Two heaters, both on the outer layer return end in coils 7 and 9, failed the heater-to-coil hipot test and were removed from the magnet protection. Another heater on the outer layer lead end of coil 9 also exhibited compromised insulation during

the hipot test at room temperature. This heater was wired separately in order to use it only if the "cold" hipot test was successful. Eventually this heater was connected in parallel to other heaters of the outer layer lead end at the heater distribution box (not in the magnet) and successfully was used for the magnet protection. Protection heater wiring is shown in Attachment I.

Because of all described above, LQS01 heater groups had different resistances. In order to provide similar decay times for all 4 groups of heaters (~ 32 ms) we used 2 additional "dummy" resistors connected in parallel or series to the groups with missing heaters. Heater firing units were operated at 300-350 V and 19.2 mF of capacitance. Peak current in the individual heaters during the test varied from 45 to 52 A.

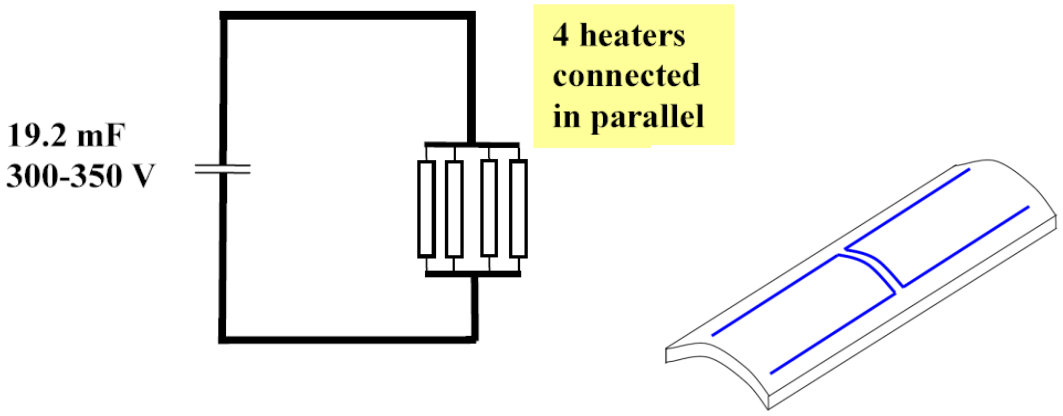

Fig. 1. LQS01 protection heaters.

Voltage tap system in LQS01 covers the inner and outer coil layers, pole turn, multi-turn and splice sections (see Fig. 2). There are 13 voltage taps on the inner layer and 7 voltage taps on the outer layer. Only one voltage tap, **B7** in coil 9 was found open before the cool down. LQS01 magnet schematic with inter-coil connections is shown in Attachment II.

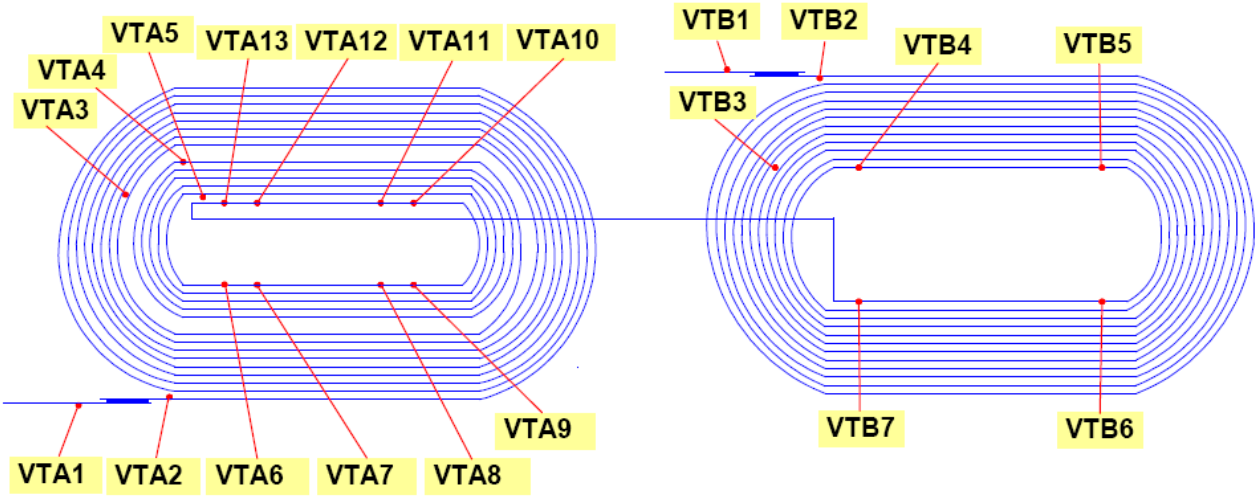

Fig. 2. LQS01 voltage tap locations for the inner (left) and outer (right) layers.

56 strain gauges (SG) were installed on shell, coils and rods for monitoring mechanical strain and calculating coil stresses during the magnet construction and testing. Each gauge consists of active and temperature-compensating gauges connected into a full-bridge circuit. Prior to the test we lost only one SG mounted on the rod in sector D (next to coil 9, see Attachment II). During the cool-down we lost another SG on the rod in sector B (coil 7). SG data were continuously monitored during the mechanical work before the test at Fermilab using the portable SG readout system provided by the LBNL.

In addition to the standard set of the dewar temperature sensors 5 additional resistive temperature devices (RTD) were mounted at top, middle and bottom of the magnet outer skin (*Cernox cx43235, cx43233, cx50629, cx53864* and *cx53825* sensors respectively), and were insulated from the surrounding gas to provide a better indication of the cold mass temperature during cool down and warm up.

The magnetic measurement warm bore was instrumented with a quench antenna for localization of quenches. We used two different quench antennas during this test. The "KEK/HGO" quench antenna consists of three stationary coil segments each 35 cm long and separated by 10.5 cm long couplings. Each coil is made with four windings that are sensitive to normal and skew sextupole and octupole magnetic flux changes, at a radius of 23 mm. The total length of the "KEK" quench antenna is about 120 cm and is not enough to cover even half of the magnet; when installed, it was roughly centered in the LQS01. Another experimental quench antenna was built using 16 pc-board (PCB) circuits, each 4 cm long, distributed evenly with 20 cm spacing along the whole length of the magnet. As the warm bore tube extended only ~2 m into the magnet bore, four of the PCB probes were actually installed in the magnet bore at the return end and were operating in liquid helium.

Quench detection, magnet protection and strain gauge systems at VMTF were modified in preparation for the LQS01 test. These modifications, which are described briefly below, were fully validated in a test using TQM03b, a TQ coil in the Fermilab Mirror magnet structure.

2.1 Quench Detection System

A quench detection system with adaptive thresholds was developed for the test of magnet LQS01. The FPGA-based quench management system allows to set different thresholds in 10 different current regions. This FPGA system currently provides only half-coil and whole-coil quench detection and sends the trigger signal to the quench logic module (QLM) in the VME-based system. Thus, the VME-based system still remains the main one; in the future both VME and FPGA systems will be independent and run in parallel. A block diagram of the quench detection system at VMTF is shown in Fig. 3.

One analog quench detection (AQD) module that is part of the VME system also was modified, to set a current-dependent threshold for the half-coil voltage difference. However, its granularity and flexibility is far less than the one provided by the FPGA system.

2.2 Magnet protection system

The VMTF magnet protection system was redesigned in order to accommodate the large number of protection heaters used in LQS01. It includes 4 heater firing units (HFU)

for protection heaters and 2 HFUs for spot heaters. The distribution box for configuring HFU to heater connections was redesigned to accommodate up to 8 strip heaters and 4 spot heaters. A new module was designed and built for switching operation modes and organizing logic signal communication between HFUs and the QLM.

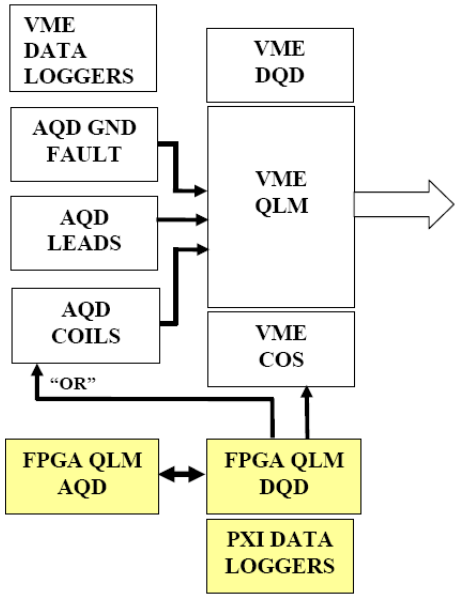

Fig. 3. Quench detection system at VMTF.

The power system grounding scheme was also changed, by moving the single ground point from the negative power lead to one symmetric between positive and negative leads, via passive resistive components. This limits the coil voltage to ground, to half the previous 1000 V limit (defined by Imax * Rdump). A 60 mΩ dump resistor was used, with dump delay set to 1 ms, for energy extraction during quench events. Further improvement using an active ground fault detection scheme is planned in the future.

2.3 Strain gauge readout system

SG readout system at VMTF was modified in order to increase resolution and the maximum current provided to the individual gauge. 1.2 mA of current available in the old configuration resulted in very small voltage signals from LQS01 strain gauges connected into the full-bridge circuit.

One single SG scan was replaced with 4 scans running in parallel – the number of SG per scan was reduced and therefore the maximum available current was increased up to ~ 2.0 mA. A new 4-channel current source was designed and built for the SG system. In the new configuration we can read up to 64 SG in total. This parallel configuration also allowed the sampling rate to be increased – slow scan data now can be saved with a 5-6 s interval.

3. Quench History

The magnet test program started with quench training at 20 A/s ramp rate at 4.5 K temperature. The quench detection threshold for the Half-coil signal was set to 750 mV at the beginning. The 1st half-coil signal is formed by coils 8 and 7, and the 2nd half-coil signal by coils 6 and 9.

Large voltage spikes at low currents resulted in several trips at the beginning of test. Voltage spike data system (VSDS) also confirmed that more and larger spikes are observed in LQS01 magnet than expected from tests of other magnets built with the same type of superconductor. More details about the voltage spike study are presented in Section 11.

From past experience we knew that voltage spikes are smaller at high ramp rates, therefore we started using high ramp rates to avoid low current trips. While looking for the optimal ramp rate, the magnet quenched few times at a ramp rate of 200 A/s. Later on we started using 200 A/s ramp rate only up to 3000 A and then switched to lower ramp rates: 50 A/s up to 5000 A, 20 A/s up to 9000 A and 10 A/s until the quench. At the same time all quench detection thresholds were adjusted. The half-coil thresholds for the FPGA-based system are shown in Fig. 4 (left). Thresholds in the VME-based system also were set accordingly.

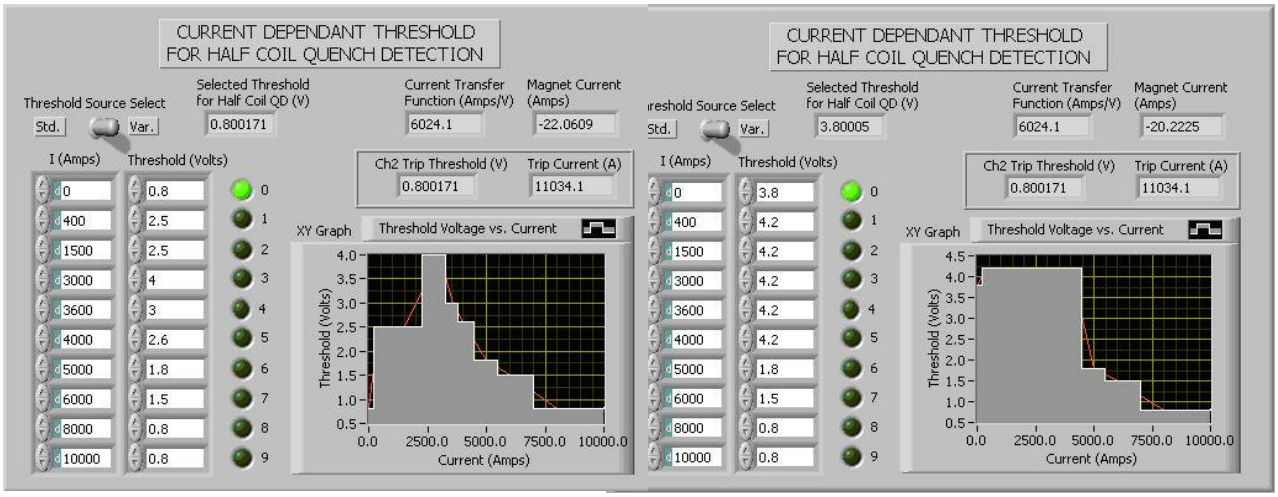

Fig.4. Current dependent quench detection thresholds used in the FPGA-based system for training (left) and for the ramp rate dependence study (right)

The full quench history is presented in Fig. 5 and also in Tables 1 and 2. Training at 4.5 K started with a quench at 9744 A. This quench also showed that the cryogenic refrigeration system compressors could not handle the high pressure gas returned from VMTF after releasing huge stored energy (~ 650 kJ at 10kA). A special procedure was developed to vent the highest pressure helium gas flow to atmosphere, avoiding the system trips. As a consequence, the recovery time between quenches increased to 1-2 hrs

depending on the test temperature and the rate at which quench testing could occur was limited to about 6 quenches per day at 4.5 K.

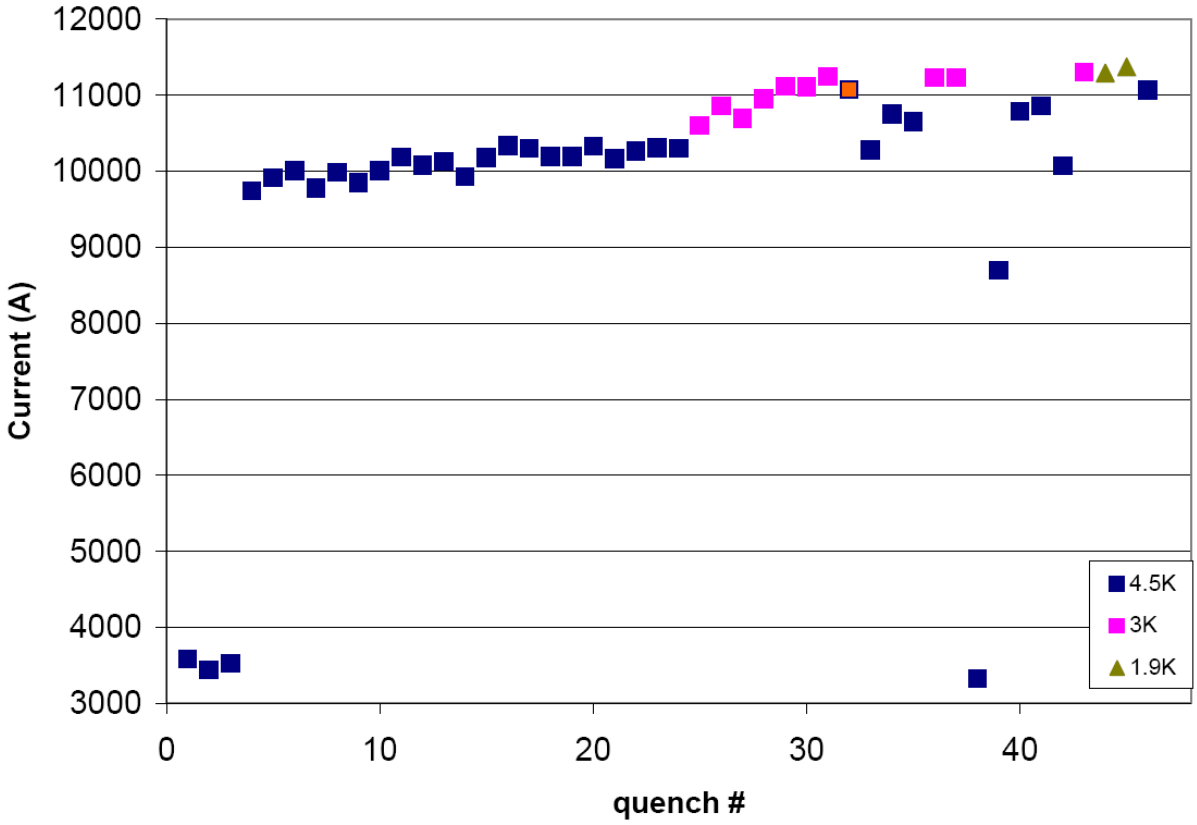

Fig. 5. LQS01 quench history.

Start of the quench training at 4.5 K was rather slow and all quenches were located in the high field region – in the pole-turn segments **A11-A12 and A7-A8**. All 4 coils were participating in the training. According to the run plan it was decided to continue testing at a lower temperature.

In the past some TQ coils exhibited delamination of the insulation on the inner layer surface after 1.9 K test, which is thought to be caused by superfluid helium penetration and expansion. This could be especially critical for LQS01 since this magnet is equipped with protection heaters on the inner layer, and trapped helium might lead to heater-to-coil voltage breakdown. Therefore the magnet was cooled down to only 3.0 K for lower temperature training.

Training at 3 K started with a quench at 10605 A, and after 6 quenches LQS01 reached ~ 11250 A, which corresponds to the target 200 T/m gradient. At this moment it was decided not to go to higher current, even though the training was not completed. The magnet training history, strain-gauge data, and temperature dependence suggested that the quench performance was affected by much lower pre-stress than expected in the inner layer (even though skin and rod gauges showed the expected stresses in the structure). Although the coil strain gauge readings were not completely understood, modeling of the

coil mechanics indicated that a non-optimal pre-stress distribution could degrade the coil at higher currents.

LQS01 was warmed back up to 4.5 K and a few quenches at about 10.7 kA confirmed that the quench current increased after the short training at 3 K.

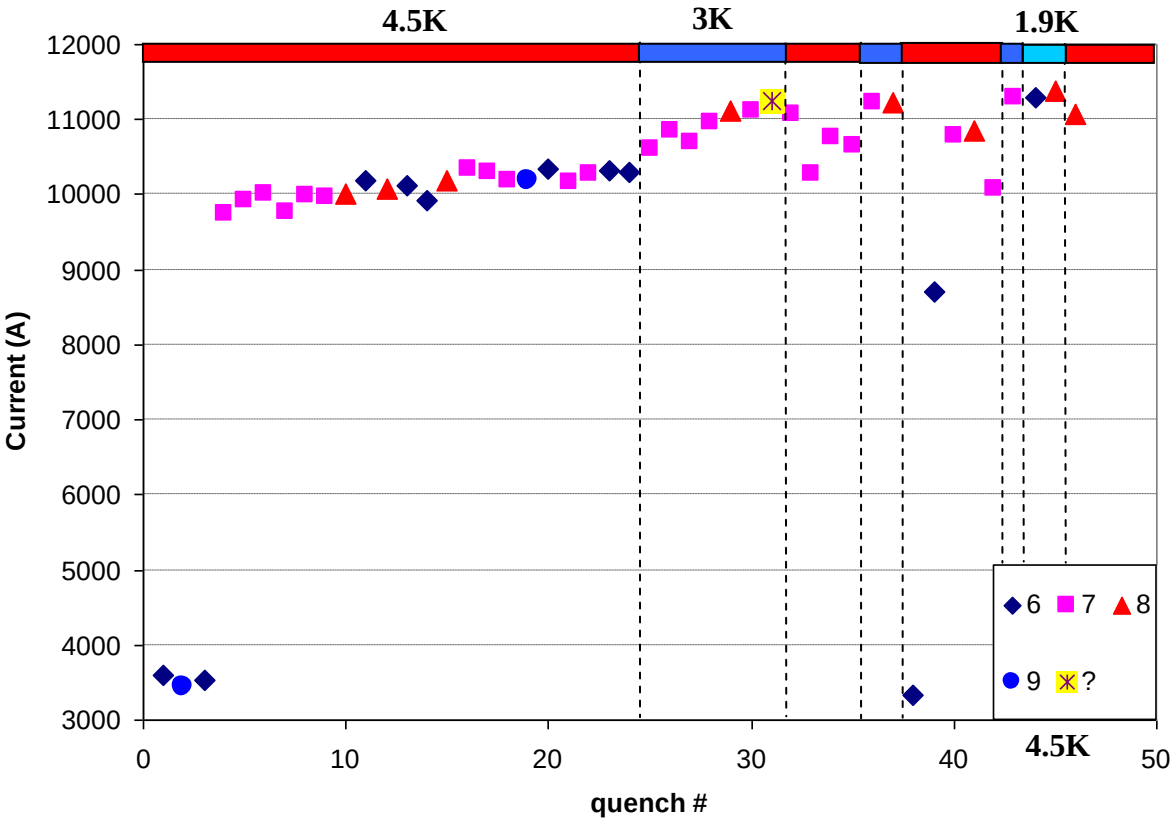

Fig. 6. LQS01 quench history with quench locations. Colored bars are used to indicate test temperature. Data were lost for quench # 31.

Magnetic measurements were done on December 8th at 4.5 K and then high quench currents were confirmed at 3 K next day. A voltage spike study was then performed at different ramp rates, with the main goal to determine proper quench detection thresholds for the 4.5K ramp rate dependence quench study that followed. The updated thresholds are shown in Fig. 4 (right).

Since training at 3 K was successful and there was no indication of damage to coils, LQS01 was cooled down to 1.9 K. Only two quenches were performed at 1.9 K and these quenches at 11.3 kA and 11.4 kA were consistent with the magnet performance at 3 K. The maximum quench current reached in this test was 11372 A at 1.9 K (quench #45). In the last quench at 4.5 K LQS01 reached 11068 A, which is significantly higher than previous quenches at this temperature.

LQS01 quench history with quench locations is shown in Fig. 6. Most quenches developed in coil 7 both at 4.5 K and 3 K. Quench multiplicity in all coils is summarized in Fig. 7. 46 quenches were performed in total (excluding the heater study) and all of them (except for high ramp rate quenches) developed in the innermost turn around the pole in the inner layer.

For quench localization we mainly used the "KEK" quench antenna, even though it covered only the central portion of the magnet. The new quench antenna based on the pc-board circuits was not sensitive enough to the quench development, as a quench signal was detected for only a couple of events. Either a new design or changed orientation in the warm bore will be necessary for their successful use.

We lost data for only one quench, number 31. No particular reasons were found for this failure and as a preventive measure we should restart data logger node in every 1-2 weeks.

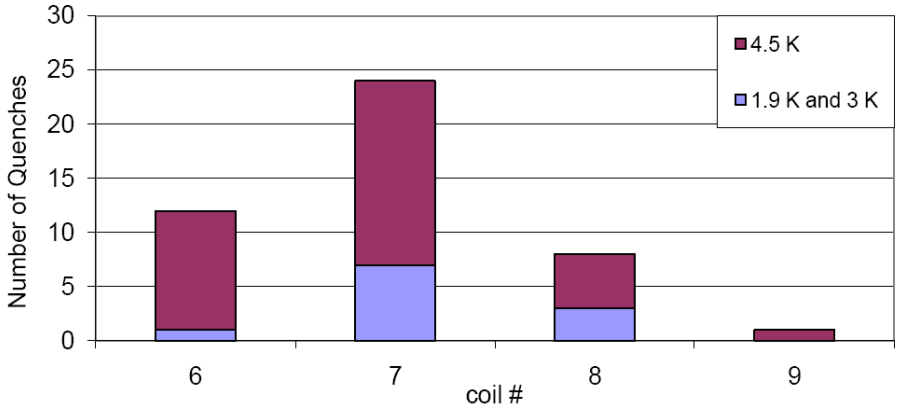

Fig. 7. Quench multiplicity in coils

4. Ramp Rate Dependence

Ramp rate dependence study was performed at 4.5 K after the short training at 3 K. Summarizing plot is shown in Fig. 8. Quenches at a high ramp rates developed in the mid-plane segments of coils 6 (150 A/s and 200 A/s) and 8 (125 A/s). Low ramp rate quenches in pole-turn segments clearly indicate that there is margin for improving the magnet performance.

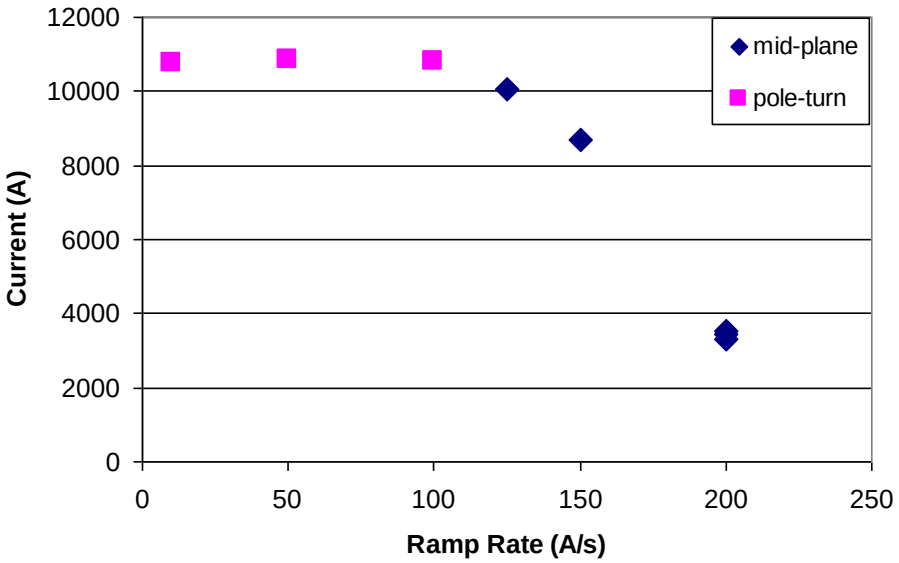

Fig. 8. Ramp rate dependence study at 4.5 K.

Table 1: LQS01 Quench History with comments

#	File	#	I (A)	dI/dt (A/s)	t_{quench} (s)	MIITs ($10^6 A^2$ sec)	QDC	T (K) Mag. cent	T (K) Mag. top	Comments
1	lqs01.Quench.091119173523.688		1009	50			HcoilHcoil	4.34	4.43	manual trip at 1000 A
2	lqs01.Quench.091119183438.948		1122	50	-0.0021	0.18	HcoilHcoil	4.43	4.43	ramp to 3kA trip at 1.1 kA, 4.5 K
3	lqs01.Quench.091119185139.084		1312	20	-0.0042	0.25	HcoilHcoil	4.43	4.43	ramp to 3kA, quench at 1.3 kA, 20 A/s, 4.5K
4	lqs01.Quench.091119195704.430		3000	200	-0.4867	5.58	HcoilHcoil	4.44	4.45	HFU1 test mode (250V, 19.2mF), HFU2 protection mode, 4.5K
5	lqs01.Quench.091119203606.841		3000	200	-0.1176	2.23	HcoilHcoil	4.43	4.43	HFU2 induced quench 350V/19.2 mF, HFU1 in protection mode - 250 V/19.2mF, at 3kA, 4.5K
6	lqs01.Quench.091119210314.357		3403	200	-0.5626	8.13	HcoilHcoil	4.43	4.43	quench at 3.5kA, 200A/s, 4.5K
7	lqs01.Quench.091119211254.431		3379	200	-0.0195	1.54	HcoilHcoil	4.43	4.44	quench at 3375 A, 200 A/s, 4.5K
8	lqs01.Quench.091120145710.849		1041	200	-0.6210	0.86	WcoilGnd	4.42	4.42	ramp at 50 A/s, quench at 1.1kA
9	lqs01.Quench.091120152321.612	**1**	3586	200	-0.0186	1.68	HcoilHcoil	4.42	4.42	ramp rate 200 A/s, quench at 3584 A. 4.5 K
10	lqs01.Quench.091120155842.272	-	1041	200	-0.0120	0.17	GndRef	4.42	4.42	ramp to 5kA, 200A/s, quench at 1kA
11	lqs01.Quench.091120163002.427	**2**	3442	200	-0.0206	1.59	HcoilHcoil	4.42	4.43	ramp rate 200 A/s, quench at 3.5kA, 4.5 K
12	lqs01.Quench.091120171043.746	-	3135	200	-0.0024	1.18	WcoilIdot	4.43	4.43	quench at 3.1 kA, 200 A/s, 4.5 K
13	lqs01.Quench.091120173529.964	**3**	3525	200	-0.0214	1.66	HcoilHcoil	4.42	4.42	quench at 3.5kA, 200A/s
14	lqs01.Quench.091120181315.364	-	967	300	-0.0122	0.15	HcoilHcoil	4.43	4.42	(Wcoil-I) trip in FPGA system at 300 A/s
15	lqs01.Quench.091120182926.811		5000	50	-0.0006	2.71	HcoilHcoil	4.43	4.43	HFU1 test at 300V, 19.2 mF, HFU2 in protection

16	lqs01.Quench.091120190331.447		5000	50	-0.1589	6.70	HcoilHcoil	4.43	4.43	HFU1 test mode: 200 V, 19.2 mF, HFU2 protection, 5kA
17	lqs01.Quench.091120193620.618		5000	50	-0.0007	2.76	HcoilHcoil	4.43	4.45	HFU1 quench 250V/19.2mF, 5kA, 4.5K
18	lqs01.Quench.091120195217.812		6500	50	-0.0210	4.13	HcoilHcoil	4.45	4.45	HFU2 (300V/19.2mF), 6500 A, 4.5K
19	lqs01.Quench.091121152448.769		5000	50	-0.0496	3.72	HcoilHcoil	4.43	4.43	HFU1 (300V) in protection, HFU2 testing 300V, both at 19.2mF, 4.5K
20	lqs01.Quench.091121161433.242		6500	50	-0.0004	3.86	HcoilHcoil	4.43	4.43	HFU1 testing 200V, HFU2 protecting 350V, 19.2mF both, 4.5K
21	lqs01.Quench.091123152423.223		8000	20	-0.0109	4.36	HcoilHcoil	4.43	4.44	HFU2 (350 V/19.2mF) quench at 8kA, 4.5K
22	lqs01.Quench.091123170052.023		8000	20	-0.0004	4.35	HcoilHcoil	4.43	4.43	HFU1 testing 300V,19.2mF. 8kA, 4.5K
23	lqs01.Quench.091123173422.433	**-**	3229	20	-0.0190	1.51	HcoilHcoil	4.46	4.46	quench at 3.3kA, 4.5K
24	lqs01.Quench.091123184910.352	**4**	9744	20	-0.0136	5.90	HcoilHcoil	4.46	4.45	quench at 9.7kA, 20 A/s (200A/s to 3kA, 4.5K
25	lqs01.Quench.091123193852.329	**5**	9915	20	-0.0136	5.95	HcoilHcoil	4.47	4.47	quench at 9.9 kA, 4.5kA
26	lqs01.Quench.091124153452.604	**6**	10006	20	-0.0088	5.53	HcoilHcoil	4.44	4.43	quench at 10kA, 20 A/s (200A/s to 3kA, 50A/s to 5kA), 4.5K
27	lqs01.Quench.091124174540.414	**-**	1048	200	0.0010	0.16	GndRef	4.43	4.42	trip at 1kA, 200 A/s, 4.5K
28	lqs01.Quench.091124183528.589	**7**	9774	20	-0.0144	6.01	HcoilHcoil	4.43	4.43	quench at 9764A, 20A/s, 4.5K
29	lqs01.Quench.091124193818.628	**8**	9986	20	-0.0129	5.93	HcoilHcoil	4.45	4.46	quench at 9.9kA, 20A/s, 4.5K
30	lqs01.Quench.091125104959.339	**-**	986	200	-0.0141	0.16	WcoilIdot	4.43	4.43	200A/s up to 3 kA
31	lqs01.Quench.091125105902.956	**-**	3306	50	-0.0190	1.57	HcoilHcoil	4.43	4.43	Quench at 3.3kA, 50A/s to 5kA, 4.4K
32	lqs01.Quench.091125112819.572	**-**	3269	50	-0.0351	1.71	WcoilIdot	4.43	4.43	quench at 3260A, 50A/s, 4.5K
33	lqs01.Quench.091125115416.812	**9**	9852	20	-0.0125	5.84	HcoilHcoil	4.44	4.44	quench at 9.8 kA, 20 A/s, 4.5K
34	lqs01.Quench.091125125507.763	**10**	10007	10	-0.0122	5.88	HcoilHcoil	4.44	4.44	ramp rate 10 A/s (200A/s to 3kA, 50A/s to 5kA, 20A/s to 9kA), 4.5K

35	lqs01.Quench.091125140215.849	-	1079	200	-0.0137	0.18	WcoilIdot	4.43	4.42	quench at 1080A, 200A/s, 4.5K
36	lqs01.Quench.091125141304.322	-	3374	50	-0.0288	1.74	HcoilHcoil	4.44	4.43	quench at 3.2kA, 50A/s, 4.5K
37	lqs01.Quench.091125143841.809	**11**	10185	10	-0.0172	6.45	HcoilHcoil	4.44	4.44	quench at 10.2kA, 10 A/s, 4.5K
38	lqs01.Quench.091125154601.533	-	957	200	0.0010	0.13	WcoilIdot	4.43	4.42	quench at 980A, 200 A/s, 4.5K
39	lqs01.Quench.091125160445.822	**12**	10075	10	-0.0120	5.89	HcoilHcoil	4.44	4.43	quench at 10.1kA, 10 A/s, 4.5K
40	lqs01.Quench.091130100600.822	-	942	200	-0.5279	0.68	WcoilIdot	4.43	4.43	Trip at 1kA, 200A/s, 4.42K (200A/s requested upto 3kA)
41	lqs01.Quench.091130105227.028	**13**	10128	10	-0.0129	6.00	HcoilHcoil	4.43	4.43	quench at 10.1kA, 10A/s (200A/s upto 3kA, 50A/s to 5kA, 20A/s to 9.5kA), 4.4K
42	lqs01.Quench.091130114150.681	**14**	9932	10	-0.0146	6.09	HcoilHcoil	4.46	4.46	quench at 9.9kA, 10 A/s (as previous ramp), 4.4K
43	lqs01.Quench.091130122056.141	-	992	164	-0.1624	0.32	WcoilGnd	4.45	4.45	quench at 1kA, 50 A/s, 4.5K
44	lqs01.Quench.091130123649.096	**15**	10178	10	-0.0116	5.87	HcoilHcoil	4.44	4.45	quench at 10.2kA, 10A/s, 4.4K
45	lqs01.Quench.091130135421.621	-	3435	50	-0.0111	1.59	WcoilIdot	4.43	4.43	quench at 3.5kA, 50 A/s, 4.5K
46	lqs01.Quench.091130141504.526	**16**	10337	10	-0.0111	5.87	HcoilHcoil	4.43	4.43	quench at 10.3kA, 10 A/s, 4.4K
47	lqs01.Quench.091130151646.966	**17**	10298	10	-0.0111	5.84	HcoilHcoil	4.43	4.43	quench at 10.3kA, 10 A/s, 4.5K
48	lqs01.Quench.091130155020.767	**18**	10194	10	-0.0113	5.83	HcoilHcoil	4.44	4.44	quench at 10.2kA, 10A/s, 4.5K
49	lqs01.Quench.091202121526.970	**19**	10194	10	-0.0115	5.84	HcoilHcoil	4.44	4.43	quench at 10.2kA, 10A/s, 4.4K
50	lqs01.Quench.091202132250.867	**20**	10332	10	-0.0125	6.00	HcoilHcoil	4.43	4.43	quench at 10.3kA, 10A/s, 4.4Kual"
51	lqs01.Quench.091202143707.470	**21**	10165	10	-0.0097	5.65	HcoilHcoil	4.43	4.43	quench at 10.2kA, 10A/s, 4.5K
52	lqs01.Quench.091202152250.608	**22**	10265	10	-0.0106	5.78	HcoilHcoil	4.46	4.46	quench at 10.25kA, 10A/s, 4.4K
53	lqs01.Quench.091202160251.890	**23**	10312	10	-0.0118	5.91	HcoilHcoil	4.45	4.46	quench at 10.3kA, 10A/s

54	lqs01.Quench.091202164344.403	**24**	10298	10	-0.0116	5.88	HcoilHcoil	4.45	4.46	quench at 10.2kA, 10A/s
55	lqs01.Quench.091203100356.483	**25**	10605	10	-0.0094	5.95	HcoilHcoil	3.05	3.18	quench at 10.6kA, 10A/s, 3.1-3.2 K
56	lqs01.Quench.091203115343.640	**26**	10860	10	-0.0101	6.18	HcoilHcoil	3.11	3.22	quench at 10.9kA, 10A/s, 3.1-3.2 K
57	lqs01.Quench.091203134030.884	**-**	3124	50	-0.0155	1.39	WcoilIdot	2.97	3.04	quench at 3.1 kA, 50 A/s, 3K
58	lqs01.Quench.091203135341.586	**27**	10696	10	-0.0091	6.06	HcoilHcoil	3.05	3.20	quench at 10.7 kA, 10 A/s, 3.0-3.12 K
59	lqs01.Quench.091204092122.138	**-**	3196	50	-0.0146	1.44	WcoilIdot	3.01	3.01	trip at 3.2kA, 3K, 50A/s
60	lqs01.Quench.091204093809.062	**28**	10956	10	-0.0080	6.02	HcoilHcoil	3.03	3.15	quench at 11kA, 10 A/s, 3K
61	lqs01.Quench.091204112201.707	**-**	1044	200	0.0010	0.16	WcoilIdot	3.06	3.15	trip at 1kA, 200 A/s, 3K
62	lqs01.Quench.091204114308.466	**29**	11115	10	-0.0077	6.00	HcoilHcoil	3.12	3.24	quench at 11.1kA, 10A/s, 3.06-3.17K
63	lqs01.Quench.091204134643.875	**30**	11112	10	-0.0081	6.06	HcoilHcoil	3.04	3.14	quench at 11.1kA, 10A/s, 3K
64	lqs01.Quench.091204151818.582	**31**	11247	10						Lost Data
65	lqs01.Quench.091204163111.605	**32**	11074	10	-0.0084	6.02	HcoilHcoil	4.17	4.42	quench at 11.1kA, 10A/s, 3.8-4.4 K
66	lqs01.Quench.091208160940.055	**33**	10278	10	-0.0102	5.87	HcoilHcoil	4.43	4.43	quench at 10.3 kA, 10 A/s, 4.42K
67	lqs01.Quench.091208171152.223	**-**	3375	50	-0.0399	1.87	WcoilIdot	4.43	4.43	50A/s, trip at 3.2kA+00
68	lqs01.Quench.091208173138.500	**34**	10752	10	-0.0092	5.86	HcoilHcoil	4.44	4.43	quench at 10740A, 10A/s, 4.4K
69	lqs01.Quench.091208182543.335	**-**	918	200	-0.2064	0.32	HcoilHcoil	4.45	4.45	Wcoil-Idor trip
70	lqs01.Quench.091208184026.612	**35**	10648	10	-0.0095	5.86	HcoilHcoil	4.44	4.44	quench at 10.6 kA, 10 A/s, 4.4K
71	lqs01.Quench.091209101137.969	**36**	11230	10	-0.0060	5.84	HcoilHcoil	3.03	3.13	quench at 11.2kA, 10A/s, 3K
72	lqs01.Quench.091209114103.546	**37**	11232	10	-0.0071	5.99	HcoilHcoil	2.99	3.10	quench at 11.2kA, 10 A/s, 3K
73	lqs01.Quench.091209164314.875	**-**	1287	-20	-0.0059	0.28	HcoilHcoil	4.42	4.43	quench at 1.2kA (ramp down) spike study, 4.4K
74	lqs01.Quench.091209170833.217	**-**	3010	50	-0.0428	1.55	HcoilHcoil	4.43	4.43	quench at 3kA, spike study, 50 A/s, 4.4K
75	lqs01.Quench.091210170023.948	**-**	2187	50	-0.0095	0.69	HcoilHcoil	4.45	4.44	spike study, 50 A/s, quench at 2kA
76	lqs01.Quench.091210174257.308	**-**	2035	20	-0.0286	0.68	HcoilHcoil	4.45	4.45	spike study, 20A/s

77	lqs01.Quench.091210180107.256	-	1665	20	-0.0031	0.39	HcoilHcoil	4.44	4.45	spike study, trip at 1600 A, 20 A/s
78	lqs01.Quench.091210181527.519	-	1965	20	-0.0021	0.53	HcoilHcoil	4.44	4.44	spike study: 20A/s, trip at 1.9kA, 4.4K
79	lqs01.Quench.091210182729.082	-	1701	20	-0.0718	0.61	HcoilHcoil	4.44	4.45	spike study, 20A/s, trip at 1.6kA, 4.4K
80	lqs01.Quench.091210184506.546	-	2084	20	-0.0101	0.63	HcoilHcoil	4.44	4.45	spike study, trip at 2kA, 20A/s, 4.4K
81	lqs01.Quench.091210185543.829	**38**	3328	200	-0.0179	1.49	DQD Hcoil	4.45	4.44	spike study, 200 A/s, quench at 3.3K, 4.4K
82	lqs01.Quench.091210191642.121	-	526	-50	-0.0787	0.09	HcoilHcoil	4.45	4.46	spike study, 150 A/s, trip at 500 A when ramping down
83	lqs01.Quench.091210195043.124	-	977	-20	-0.0120	0.19	HcoilHcoil	4.47	4.48	spike study, trip when ramping down at 20 A/s, 4.4K
84	lqs01.Quench.091211112212.395	**39**	8788	150	-0.0017	4.24	HcoilHcoil	4.45	4.46	quench at 8782A, 150 A/s, 4.4K
85	lqs01.Quench.091211132140.352	**40**	10788	100	-0.5209	64.86	HcoilHcoil	4.44	4.45	quench at 10.7kA, 100A/s, 4.4K
86	lqs01.Quench.091211145134.757	-	1493	50	-0.0151	0.34	DQD Hcoil	4.44	4.43	50A/s, trip at 1.4kA, 4.4K DQD Hcoil trip
87	lqs01.Quench.091211152452.170	**41**	10857	50	-0.0094	5.80	HcoilHcoil	4.45	4.45	quench at 10.9kA, 50 A/s, 4.4K
88	lqs01.Quench.091211163811.694	**42**	10071	125	-0.0020	4.55	HcoilHcoil	4.44	4.46	quench at 10.06 kA, 125 A/s, 4.4K
89	lqs01.Quench.091214113702.352		5006	0	-0.0004	2.85	HcoilHcoil	4.43	4.44	5kA, 150 A/s, HFU1 testing 200V, HFU2 protection 350 V. 4.4K
90	lqs01.Quench.091214123425.233		5012	0	-0.0727	4.48	HcoilHcoil	4.44	4.43	5kA, 5min at flattop, HFU1 testing 250V, HFU2 protection 350 V, 4.4K
91	lqs01.Quench.091214144428.309	-	976	244	0.0010	0.14	GndRef	4.43	4.43	ramping at 150 A/s, trip at 970 A
92	lqs01.Quench.091214164955.905	-	1297	268	-0.0141	0.26	WcoilGnd	4.42	4.42	Magnetic Measurements, trip at 1.3 kA
93	lqs01.Quench.091215101046.362		5000	150	-0.0608	4.04	HcoilHcoil	4.44	4.44	HFU1 (250V) test at 5kA, HFU2 (350V) protection, 4.4K No flattop

94	lqs01.Quench.091215111513.311		5000	150	-0.0004	2.84	HcoilHcoil	4.45	4.45	HFU1 testing, 250 V, HFU2 protection 350 V, 5kA, 4.4 K 4min flattop
95	lqs01.Quench.091215113914.361		5000	150	-0.0613	4.06	HcoilHcoil	4.44	4.45	HFU1 test at 5kA, HFU1 A and B with op.polarity, HFU2 protection
96	lqs01.Quench.091215120128.355	-	1067	151	-0.0102	0.18	HcoilHcoil	4.44	4.44	trip at 1kA in WcoilIdot, set threshold to 4V again
97	lqs01.Quench.091215121013.335		6500	150	-0.0343	4.77	HcoilHcoil	4.45	4.45	HFU1 (250V) testing at 6500 A, HFU2 protection at 350V, 4.4K
98	lqs01.Quench.091215124726.151		5000	150	-0.0764	4.51	HcoilHcoil	4.46	4.46	HFU1 tested at 150, 200 and 250 V, 5kA, 4.4K HFU1-B w op. polarity
99	lqs01.Quench.091215173034.918		8000	150	-0.0207	5.21	HcoilHcoil	4.45	4.45	HFU1 test at 8kA, 250V, HFU2 protection 350V, 4.4K
100	lqs01.Quench.091217094932.519	-	1605	200	-0.0137	0.39	HcoilHcoil	2.98	3.02	trip at 1.6kA, 200A/s to 3kA, 3K
101	lqs01.Quench.091217100920.882	**43**	11302	10	-0.0088	6.21	HcoilHcoil	3.04	3.15	quench at 11.3kA, 10A/s, 3K
102	lqs01.Quench.091217142156.986	**44**	11292	10	-0.0094	6.40	HcoilHcoil	1.92	1.93	quench at 11.2kA, 10A/s, 1.9K
103	lqs01.Quench.091217162222.151	**45**	11372	10	-0.0073	6.15	HcoilHcoil	1.84	1.84	quench at 11.4kA, 10 A/s, 1.9K
104	lqs01.Quench.091218101540.005		10000	150	-0.0007	4.95	HcoilHcoil	4.31	4.40	HFU2 induced quench at 10kA, 350 V, HFU1 (300V) in protection, 4.4K
105	lqs01.Quench.091218112440.193		8000	150	-0.0167	4.96	HcoilHcoil	4.46	4.47	HFU1 test at 8kA, 300 V at 19.2 mF, HFU2 (350V) in protection, 4.4K
106	lqs01.Quench.091218122321.687	**46**	11067	10	-0.0070	5.66	HcoilHcoil	4.46	4.46	quench at 11.1kA, 10A/s, 4.5K

Table 2: LQS01 Quench History with parameters for the first two quenching segments

#	File	#	I (A)	dI/dt (A/sec)	t_{quench} (sec)	1st VT seg	t_{rise} (sec)	2nd VT seg	t_{rise} (sec)	T (K) Mag. cent	T (K) Mag. top
1	lqs01.Quench.091119173523.688		1009	50						4.34	4.43
2	lqs01.Quench.091119183438.948		1122	50	-0.0021	9a7_9a6	-0.0032	9a8_9a7	-0.0032	4.43	4.43
3	lqs01.Quench.091119185139.084		1312	20	-0.0042	7a12_7a11	-0.0042	7a5_7a4	-0.0029	4.43	4.43
4	lqs01.Quench.091119195704.430		3000	200	-0.4867	8b3_8b2	-0.1171	8b2_8b1	-0.1169	4.44	4.45
5	lqs01.Quench.091119203606.841		3000	200	-0.1176	8b2b_8b1b	-0.1502	8a2_8a3	-0.0692	4.43	4.43
6	lqs01.Quench.091119210314.357		3403	200	-0.5626	9b1b_9b2b	0.0006	6b2b_6b1b	0.0007	4.43	4.43
7	lqs01.Quench.091119211254.431		3379	200	-0.0195	7a2b_7a1b	-0.0127	6a11_6a12	-0.0125	4.43	4.44
8	lqs01.Quench.091120145710.849		1041	200	-0.6210	8a7_8a8	-0.0046	9a4_9a3	-0.0046	4.42	4.42
9	lqs01.Quench.091120152321.612	**1**	3586	200	-0.0186	6a2_6a3	-0.0191	6b3_6b2	-0.0161	4.42	4.42
10	lqs01.Quench.091120155842.272	-	1041	200	-0.0120	7a12_7a11	-0.1381	6a2_6a3	-0.0154	4.42	4.42
11	lqs01.Quench.091120163002.427	**2**	3442	200	-0.0206	6a2_6a3	-0.0214	6b3_6b2	-0.0214	4.42	4.43
12	lqs01.Quench.091120171043.746	-	3135	200	-0.0024	6a5_6a6	-0.001	qABp_qABn	-0.0003	4.43	4.43
13	lqs01.Quench.091120173529.964	**3**	3525	200	-0.0214	6a2_6a3	-0.0225	6b3_6b2	-0.0225	4.42	4.42
14	lqs01.Quench.091120181315.364	-	967	300	-0.0122	6b4_6b3	-0.0029	9a3_9a2	-0.0028	4.43	4.42
15	lqs01.Quench.091120182926.811		5000	50	-0.0006	9a12_9a11	-0.001	9a3_9a2	-0.0008	4.43	4.43
16	lqs01.Quench.091120190331.447		5000	50	-0.1589	8b2b_8b1b	-0.1592	8a7_8a8	-0.1588	4.43	4.43
17	lqs01.Quench.091120193620.618		5000	50	-0.0007	7b7_7a13	-0.0008	8b6_8b5	-0.0008	4.43	4.45
18	lqs01.Quench.091120195217.812		6500	50	-0.0210	7b2_7b3	-0.0222	8a11_8a12	-0.0185	4.45	4.45
19	lqs01.Quench.091121152448.769		5000	50	-0.0496	7b2_7b3	-0.0444	8a2_8a3	-0.0267	4.43	4.43
20	lqs01.Quench.091121161433.242		6500	50	-0.0004	qABp_qABn	-0.0007	8b6_8b5	-0.0006	4.43	4.43
21	lqs01.Quench.091123152423.223		8000	20	-0.0109	8a11_8a12	-0.0109	7a3_7a2	-0.008	4.43	4.44
22	lqs01.Quench.091123170052.023		8000	20	-0.0004	6a2_6a3	-0.0007	6a3_6a4	-0.0007	4.43	4.43
23	lqs01.Quench.091123173422.433	-	3229	20	-0.0190	8a11_8a12	-0.019	9b1_9b2	-0.019	4.46	4.46

24	lqs01.Quench.091123184910.352	**4**	9744	20	-0.0136	7a13_7a12	-0.0175	7a12_7a11	-0.0124	4.46	4.45
25	lqs01.Quench.091123193852.329	**5**	9915	20	-0.0136	7a8_7a7	-0.0167	7a7_7a6	-0.0133	4.47	4.47
26	lqs01.Quench.091124153452.604	**6**	10006	20	-0.0088	7a12_7a11	-0.0122	7a6_7a5	-0.0035	4.44	4.43
27	lqs01.Quench.091124174540.414	**-**	1048	200	0.0010	7a13_7a12	-0.0112	7a7_7a6	-0.0109	4.43	4.42
28	lqs01.Quench.091124183528.589	**7**	9774	20	-0.0144	7a12_7a11	-0.0159	7a5_7a4	-0.0076	4.43	4.43
29	lqs01.Quench.091124193818.628	**8**	9986	20	-0.0129	7a12_7a11	-0.0153	7a5_7a4	-0.0077	4.45	4.46
30	lqs01.Quench.091125104959.339	**-**	986	200	-0.0141	6a11_6a12	-0.0144	8a7_8a8	-0.0141	4.43	4.43
31	lqs01.Quench.091125105902.956	**-**	3306	50	-0.0190	9a13_9a12	-0.0193	8a11_8a12	-0.019	4.43	4.43
32	lqs01.Quench.091125112819.572	**-**	3269	50	-0.0351	8a7_8a8	-0.0336	8a11_8a12	-0.0315	4.43	4.43
33	lqs01.Quench.091125115416.812	**9**	9852	20	-0.0125	7a12_7a11	-0.0155	7a5_7a4	-0.0076	4.44	4.44
34	lqs01.Quench.091125125507.763	**10**	10007	10	-0.0122	8a11_8a12	-0.0154	8a4_8a5	-0.008	4.44	4.44
35	lqs01.Quench.091125140215.849	**-**	1079	200	-0.0137	8a1b_8a2b	-0.009	7a8_7a7	-0.0088	4.43	4.42
36	lqs01.Quench.091125141304.322	**-**	3374	50	-0.0288	7a12_7a11	-0.0213	7b4_7b5	-0.0211	4.44	4.43
37	lqs01.Quench.091125143841.809	**11**	10185	10	-0.0172	6a7_6a8	-0.0157	6a4_6a5	-0.0072	4.44	4.44
38	lqs01.Quench.091125154601.533	**-**	957	200	0.0010	9a5_9a4	-0.0882	9a6_9a5	-0.0882	4.43	4.42
39	lqs01.Quench.091125160445.822	**12**	10075	10	-0.0120	8a11_8a12	-0.0152	8a4_8a5	-0.0084	4.44	4.43
40	lqs01.Quench.091130100600.822	**-**	942	200	-0.5279	7b3_7b4	-0.0108	7a2_7a1	-0.0106	4.43	4.43
41	lqs01.Quench.091130105227.028	**13**	10128	10	-0.0129	6a7_6a8	-0.0158	6a4_6a5	-0.0082	4.43	4.43
42	lqs01.Quench.091130114150.681	**14**	9932	10	-0.0146	6a7_6a8	-0.0159	6a4_6a5	-0.0077	4.46	4.46
43	lqs01.Quench.091130122056.141	**-**	992	164	-0.1624	7a12_7a11	-0.0447	8b4_8b3	-0.0167	4.45	4.45
44	lqs01.Quench.091130123649.096	**15**	10178	10	-0.0116	8a11_8a12	-0.0147	8a4_8a5	-0.0079	4.44	4.45
45	lqs01.Quench.091130135421.621	**-**	3435	50	-0.0111	6a5_6a6	-0.0115	7a12_7a11	-0.0113	4.43	4.43
46	lqs01.Quench.091130141504.526	**16**	10337	10	-0.0111	7a12_7a11	-0.0143	7a5_7a4	-0.0065	4.43	4.43
47	lqs01.Quench.091130151646.966	**17**	10298	10	-0.0111	7a12_7a11	-0.014	7a5_7a4	-0.0069	4.43	4.43
48	lqs01.Quench.091130155020.767	**18**	10194	10	-0.0113	7a12_7a11	-0.0142	7a5_7a4	-0.0068	4.44	4.44
49	lqs01.Quench.091202121526.970	**19**	10194	10	-0.0115	9a8_9a7	-0.0134	9a5_9a4	-0.0068	4.44	4.43
50	lqs01.Quench.091202132250.867	**20**	10332	10	-0.0125	6a7_6a8	-0.0144	6a4_6a5	-0.0068	4.43	4.43
51	lqs01.Quench.091202143707.470	**21**	10165	10	-0.0097	7a12_7a11	-0.0128	7a5_7a4	-0.0056	4.43	4.43
52	lqs01.Quench.091202152250.608	**22**	10265	10	-0.0106	7a12_7a11	-0.0135	7a5_7a4	-0.006	4.46	4.46
53	lqs01.Quench.091202160251.890	**23**	10312	10	-0.0118	6a7_6a8	-0.015	6a4_6a5	-0.0071	4.45	4.46
54	lqs01.Quench.091202164344.403	**24**	10298	10	-0.0116	6a7_6a8	-0.0148	6a4_6a5	-0.0069	4.45	4.46
55	lqs01.Quench.091203100356.483	**25**	10605	10	-0.0094	7a8_7a7	-0.0123	7a5_7a4	-0.0082	3.05	3.18

56	lqs01.Quench.091203115343.640	**26**	10860	10	-0.0101	7a8_7a7	-0.0127	7a5_7a4	-0.005	3.11	3.22
57	lqs01.Quench.091203134030.884	**-**	3124	50	-0.0155	8a11_8a12	-0.0122	8a7_8a8	-0.0122	2.97	3.04
58	lqs01.Quench.091203135341.586	**27**	10696	10	-0.0091	7a8_7a7	-0.0123	7a5_7a4	-0.0081	3.05	3.20
59	lqs01.Quench.091204092122.138	**-**	3196	50	-0.0146	7a12_7a11	-0.0157	7a6_7a5	-0.0157	3.01	3.01
60	lqs01.Quench.091204093809.062	**28**	10956	10	-0.0080	7a12_7a11	-0.0106	7a5_7a4	-0.0041	3.03	3.15
61	lqs01.Quench.091204112201.707	**-**	1044	200	0.0010	9b3_9b4	-0.0133	9b2_9b3	-0.0125	3.06	3.15
62	lqs01.Quench.091204114308.466	**29**	11115	10	-0.0077	8a11_8a12	-0.0101	8a4_8a5	-0.0077	3.12	3.24
63	lqs01.Quench.091204134643.875	**30**	11112	10	-0.0081	7a12_7a11	-0.0106	7a5_7a4	-0.0067	3.04	3.14
64	lqs01.Quench.091204151818.582	**31**	11247	10							
65	lqs01.Quench.091204163111.605	**32**	11074	10	-0.0084	7a12_7a11	-0.0108	7a5_7a4	-0.005	4.17	4.42
66	lqs01.Quench.091208160940.055	**33**	10278	10	-0.0102	7a12_7a11	-0.014	7a5_7a4	-0.0055	4.43	4.43
67	lqs01.Quench.091208171152.223	**-**	3375	50	-0.0399	9a3_9a2	-0.0399	9a2_9a1	-0.0398	4.43	4.43
68	lqs01.Quench.091208173138.500	**34**	10752	10	-0.0092	7a12_7a11	-0.0117	7a2b_7a1b	-0.0057	4.44	4.43
69	lqs01.Quench.091208182543.335	**-**	918	200	-0.2064	6a4_6a5	-0.0183	6a2_6a3	-0.0162	4.45	4.45
70	lqs01.Quench.091208184026.612	**35**	10648	10	-0.0095	7a12_7a11	-0.012	7a5_7a4	-0.0052	4.44	4.44
71	lqs01.Quench.091209101137.969	**36**	11230	10	-0.0060	7a8_7a7	-0.0086	7a5_7a4	-0.0035	3.03	3.13
72	lqs01.Quench.091209114103.546	**37**	11232	10	-0.0071	8a11_8a12	-0.0096	8a4_8a5	-0.0085	2.99	3.10
73	lqs01.Quench.091209164314.875	**-**	1287	-20	-0.0059	9a2b_9a1b	-0.0059	6b2b_6b1b	-0.0055	4.42	4.43
74	lqs01.Quench.091209170833.217	**-**	3010	50	-0.0428	7a12_7a11	-0.0423	8b2_8b1	-0.042	4.43	4.43
75	lqs01.Quench.091210170023.948	**-**	2187	50	-0.0095	7a12_7a11	-0.0111	6a3_6a4	-0.0109	4.45	4.44
76	lqs01.Quench.091210174257.308	**-**	2035	20	-0.0286	9b6_9a13	-0.0028	7a1_9b1	-0.0015	4.45	4.45
77	lqs01.Quench.091210180107.256	**-**	1665	20	-0.0031	7a1_9b1	-0.0032	9b6_9a13	-0.0032	4.44	4.45
78	lqs01.Quench.091210181527.519	**-**	1965	20	-0.0021	7a1_9b1	-0.0025	9a9_9a8	-0.0024	4.44	4.44
79	lqs01.Quench.091210182729.082	**-**	1701	20	-0.0718	6a11_6a12	-0.0812	7a8_7a7	-0.0802	4.44	4.45
80	lqs01.Quench.091210184506.546	**-**	2084	20	-0.0101	9b3_9b4	-0.0091	8a11_8a12	-0.0088	4.44	4.45
81	lqs01.Quench.091210185543.829	**38**	3328	201	-0.0179	6b3_6b2	-0.0191	6a2_6a3	-0.0191	4.45	4.44
82	lqs01.Quench.091210191642.121	**-**	526	-50	-0.0787	9a12_9a11	-0.0792	9a5_9a4	-0.0788	4.45	4.46
83	lqs01.Quench.091210195043.124	**-**	977	-20	-0.0120	8a11_8a12	-0.0095	8a13_8b7	-0.0092	4.47	4.48
84	lqs01.Quench.091211112212.395	**39**	8788	150	-0.0017	6a2_6a3	-0.0029	6b3_6b2	-0.0029	4.45	4.46
85	lqs01.Quench.091211132140.352	**40**	10788	100	-0.5209	7a8_7a7	-0.0112	7a5_7a4	-0.0064	4.44	4.45
86	lqs01.Quench.091211145134.757	**-**	1493	50	-0.0151	7a12_7a11	-0.0043	7a13_7a12	-0.0041	4.44	4.43
87	lqs01.Quench.091211152452.170	**41**	10857	50	-0.0094	8a12_8a13	-0.0115	8a11_8a12	-0.0106	4.45	4.45
88	lqs01.Quench.091211163811.694	**42**	10071	125	-0.0020	8a2_8a3	-0.0029	8b3_8b2	-0.0029	4.44	4.46

89	lqs01.Quench.091214113702.352		5000	0	-0.0004	hp_hn	-0.0007	8a7_8a8	-0.0006	4.43	4.44
90	lqs01.Quench.091214123425.233		5000	0	-0.0727	6b2b_6b1b	-0.0736	7a3_7a2	-0.0735	4.44	4.43
91	lqs01.Quench.091214144428.309	**-**	976	244	0.0010	6b4_6b3	-0.0122	9a8_9a7	-0.0105	4.43	4.43
92	lqs01.Quench.091214164955.905	**-**	1297	268	-0.0141	8b1_7b1	0.0001	9a1_6a1	0.0001	4.42	4.42
93	lqs01.Quench.091215101046.362		5000	150	-0.0608	7a8_7a7	-0.0617	7b6_7b7	-0.0617	4.44	4.44
94	lqs01.Quench.091215111513.311		5000	150	-0.0004	8b6_8b5	-0.0007	qABp_qABn	-0.0007	4.45	4.45
95	lqs01.Quench.091215113914.361		5000	150	-0.0613	8b4_8b3	-0.015	8b5_8b4	-0.0131	4.44	4.45
96	lqs01.Quench.091215120128.355	**-**	1067	151	-0.0102	9a13_9a12	-0.0123	7a6_7a5	-0.0118	4.44	4.44
97	lqs01.Quench.091215121013.335		6500	150	-0.0343	9b3_9b4	-0.0096	8b4_8b3	-0.0096	4.45	4.45
98	lqs01.Quench.091215124726.151		5000	150	-0.0764	8b4_8b3	-0.0203	8b5_8b4	-0.0195	4.46	4.46
99	lqs01.Quench.091215173034.918		8000	150	-0.0207	9b3_9b4	-0.0054	8b4_8b3	-0.0054	4.45	4.45
100	lqs01.Quench.091217094932.519	**-**	1605	200	-0.0137	6a10_6a11	-0.019	6a11_6a12	-0.019	2.98	3.02
101	lqs01.Quench.091217100920.882	**43**	11302	10	-0.0088	7a12_7a11	-0.0115	7a5_7a4	-0.005	3.04	3.15
102	lqs01.Quench.091217142156.986	**44**	11292	10	-0.0094	6a6_6a8	-0.0107	6a4_6a5	-0.0066	1.92	1.93
103	lqs01.Quench.091217162222.151	**45**	11372	10	-0.0073	8a12_8a13	-0.0103	8a4_8a5	-0.0074	1.84	1.84
104	lqs01.Quench.091218101540.005		10000	150	-0.0007	6b3_6b2	-0.001	8a2_8a3	-0.001	4.31	4.40
105	lqs01.Quench.091218112440.193		8000	150	-0.0167	9b3_9b4	-0.0062	8b4_8b3	-0.0054	4.46	4.47
106	lqs01.Quench.091218122321.687	**46**	11067	10	-0.0070	8a12_8a13	-0.0108	8a4_8a5	-0.0056	4.46	4.46

5. Temperature Dependence

A ramp rate of 10 A/s was used for the temperature dependence study. Quench current temperature dependence for LQS01 magnet is shown in Fig. 9. Only 2 quenches were performed at 1.9 K and training was not completed neither at 4.5 K, 3 K or 1.9 K, so it is premature to draw firm conclusions. For comparison 4.5 K quenches in Fig. 9 are shown after the initial training at 4.5 K, after the training at 3 K and at the end of test.

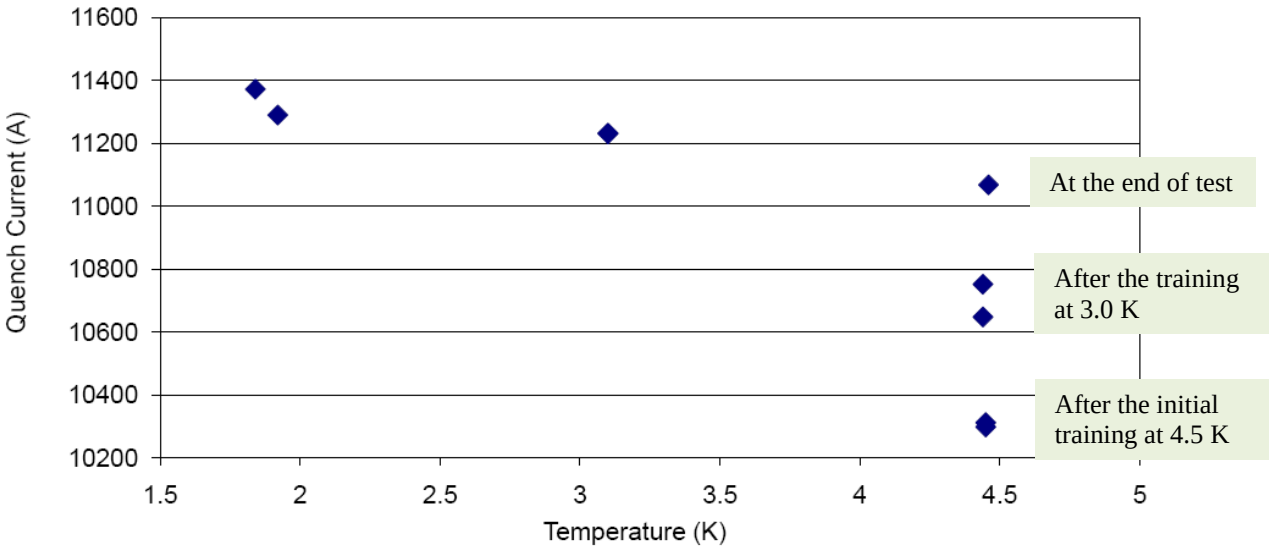

Fig. 9 Quench current temperature dependence at a ramp rate of 10 A/s.

6. Quench Locations

Voltage drop measurements across the voltage tap segments were used to check the length of these segments. The segments and their lengths are listed in Table 3.

Table 3. Voltage tap segment lengths in LQS01 magnet

Segment	length (cm)	Segment	length (cm)
A1-A2	10.2	A11-A12	204.3
A2-A3	7009.1	A12-A13	30.7
A3-A4	1233.3	A13-B7	32.9
A4-A5	2448.8	B7-B6	283.6
A5-A6	40.8	B6-B5	18.1
A6-A7	30.7	B5-B4	283.6
A7-A8	204.3	B4-B3	3655.6
A8-A9	37.5	B3-B2	5542.8
A9-A10	12.6	B2-B1	10.2
A10-A11	37.5		

All training quenches developed in the straight sections of the inner layer pole-turn segments **A7-A8** and **A11-A12**. These segments are about 200 cm long and in most quenches no longitudinal quench propagation to adjacent segments was observed. As a consequence we can not locate precisely the origin of these quenches using voltage tap information. Location of all training quenches is shown in Fig. 10.

For further localization of quenches we used the quench antenna instrumented in the warm bore. The "KEK" quench antenna consists of three stationary coils segments each 35 cm long and separated by 10.5 cm long couplings. The probe was positioned in the bore of the magnet so that the second antenna coil **C2** was about in the middle of magnet, and C1 towards the Lead End. Quench antenna location in the bore and with respect to the long straight section segments **A7-A8** and **A11-A12** is shown in Fig. 11. All training quenches with available quench antenna information are listed in Table 4 that shows also the time difference between the quench-start signal in the quench antenna (QA) and in the voltage taps. No preferred longitudinal location is observed.

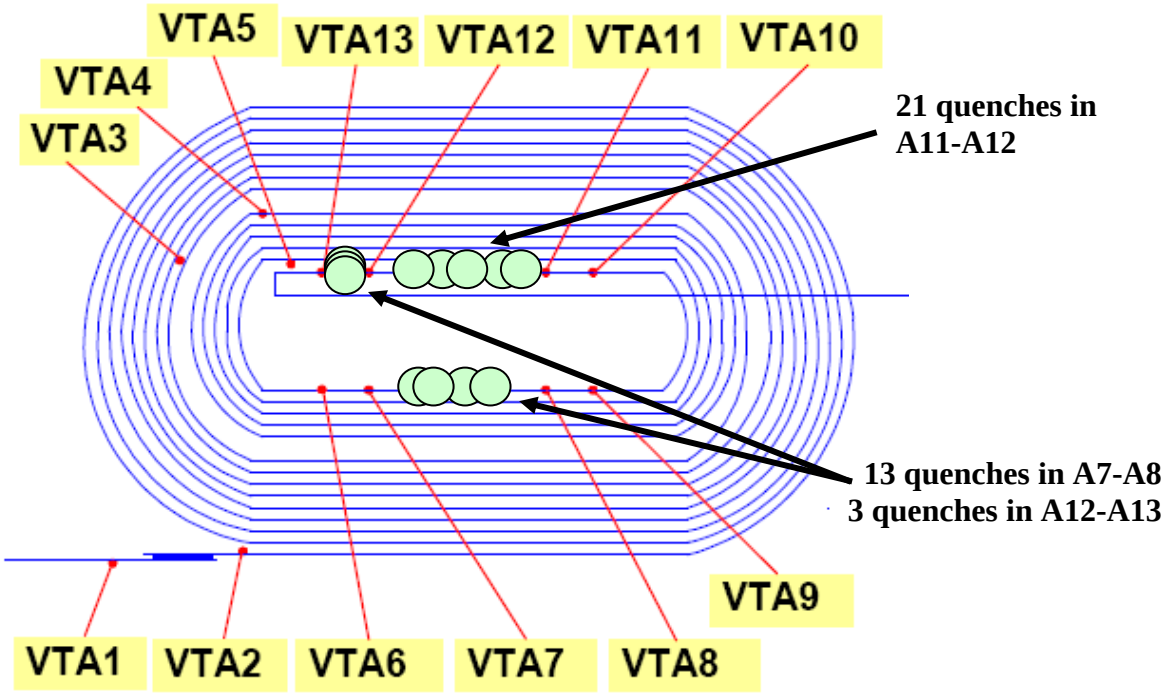

Fig. 10. Location of the training quenches at 1.9 K, 3 K and 4.5 K.

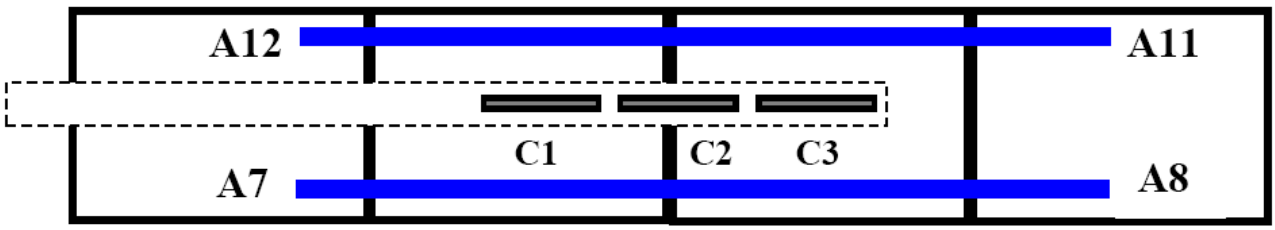

Fig. 11. Quench antenna location in the magnetic measurement warm bore.

Table 4. Quenches with the quench antenna information

#	I (A)	Ramp Rate (A/s)	T (K)	Coil	Segment	QA	Tq-T(QA) (ms)
9	9852	20	4.45	7	A11-A12	C3	1.5
10	10007	10	4.45	8	A11-A12	C1	0.6
11	10185	10	4.45	6	A7-A8	C3	2.3
12	10075	10	4.45	8	A11-A12	C1	1.2
13	10128	10	4.43	6	A7-A8	C3	-0.2
14	9932	10	4.45	6	A7-A8	C3	-8.9
15	10178	10	4.44	8	A11-A12	C1	0.4
16	10337	10	4.45	7	A11-A12	C3	-0.6
17	10298	10	4.43	7	A11-A12	C3	0.1
18	10194	10	4.44	7	A11-A12	C3	0.9
19	10194	10	4.43	9	A7-A8	C1	1.8
20	10332	10	4.43	6	A7-A8	C3	1.4
21	10165	10	4.43	7	A11-A12	C3	-0.4
22	10265	10	4.46	7	A11-A12	C3	0.8
23	10312	10	4.45	6	A7-A8	C3	1.4
24	10298	10	4.45	6	A7-A8	C3	0.4
25	10605	10	3.05-3.2	7	A7-A8	C3	-3.7
26	10860	10	3.1-3.2	7	A7-A8	C1	0.8
27	10696	10	3.05-3.2	7	A7-A8	-	
28	10956	10	3.03-3.15	7	A11-A12	C3	1.8
29	11115	10	3.12-3.24	8	A11-A12	-	
30	11112	10	3.04-3.13	7	A11-A12	-	
32	11074	10	3.7-4.4	7	A11-A12	C1, C2	0.4
33	10278	10	4.43	7	A11-A12	C2	0
34	10752	10	4.44	7	A11-A12	C2	2.5
35	10648	10	4.44	7	A11-A12	C3	0.5
36	11231	10	3.1	7	A7-A8	C3	0.5
37	11232	10	3.1	8	A11-A12	C1	0.4
38	3330	200	4.44	6	B3-B2 & A2-A3	C1, C2	0.9
39	8700	150	4.44	6	B3-B2 & A2-A3	C1	0.6
40	10788	100	4.44	7	A7-A8	C3	6
41	10857	50	4.45	8	A12-A13	C1	0.7
42	10071	125	4.44	8	B3-B2 & A2-A3	C1	0.1
43	11302	10	3.04-3.14	7	A11-A12	C2	0.1
44	11290	10	1.92	6	A7-A8	C3	1.6
45	11372	10	1.84	8	A12-A13	C1	-1.3

7. Protection Heater Test

Protection heater studies were performed at 4.5 K. Protection heater wiring is shown in Attachment I. Outer layer heaters PH-B and PH-D (see Attachment I) were connected to the heater firing units HFU1-A and HFU1-B, and inner layer heaters (PH-A and PH-C) were connected to the HFU2-A and HFU2-B respectively. HFU capacitance was set to 19.2 mF for whole test.

Protection heater delay time as a function of the magnet current is shown in Fig. 12. Full markers show the delay to quench start (i.e., time delay from the heater firing to the quench onset) and open markers show the time delay from heater firing to quench detection.

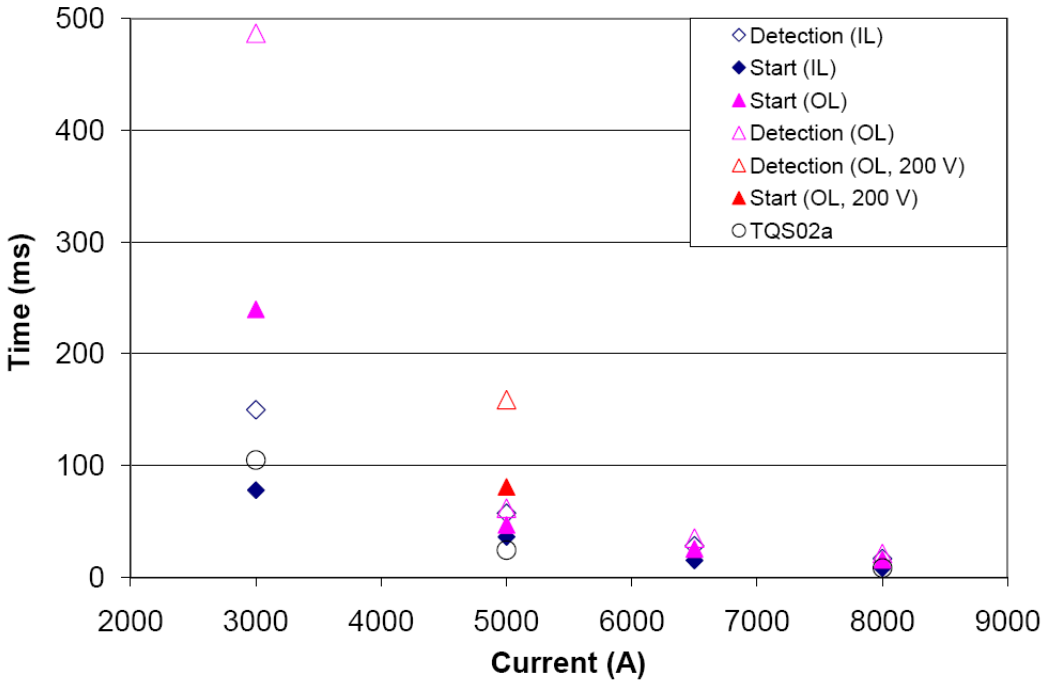

Fig. 12. Protection heater delay time as a function of the magnet current.

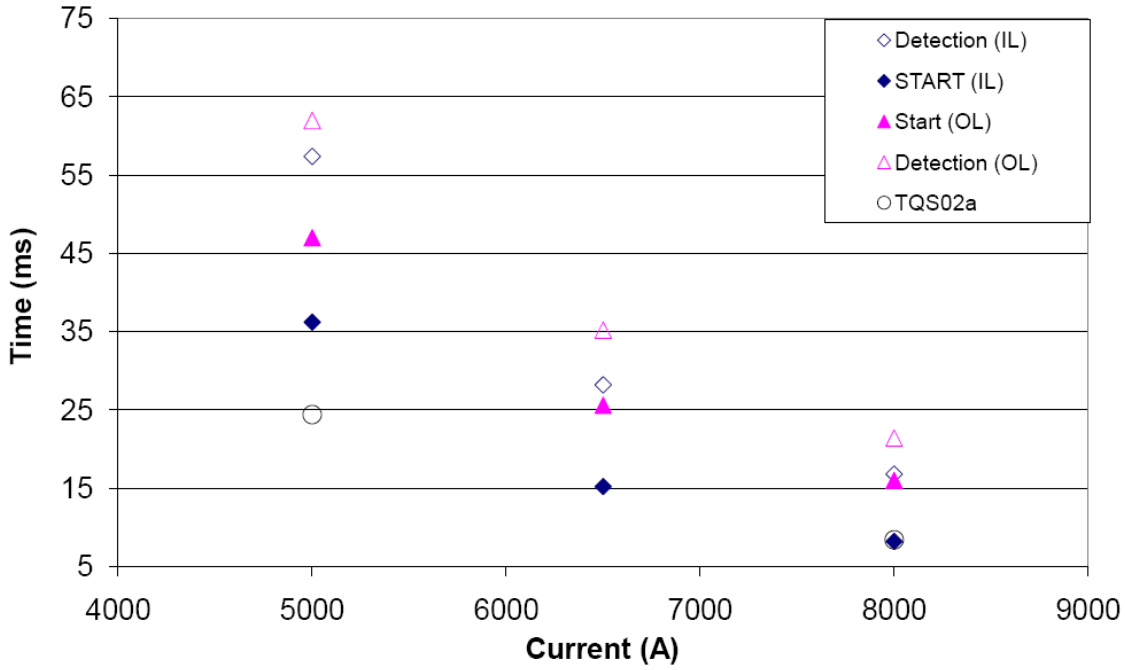

Fig. 13. Protection heater delay time as a function of the magnet current.

All heaters on the outer layer were tested at 250 V, only one test at 5 kA was done at 200 V for comparison. Inner layer heaters were tested at 300 V (tests at 5 kA and 6.5 kA) and 350 V (at 3 kA and 8 kA). Fine resolution plot for tests at a magnet current of 5 kA and above is shown in Fig. 13.

TQS02a protection heater test results also are shown in the same figure for comparison.

8. Strain Gauge Data

The LQS01 mechanical behavior during cool-down, test, and warm-up were monitored with strain gauges mounted on support structure components and coils. The shell was instrumented with half-bridge strain gauges (see Fig. 14) placed on each segment ("S1" to "S4" from the lead end), and distributed on four mid-planes ("T" top, "R" right, "B" bottom, and "L" left). The gauges measured both the azimuthal ("T") and axial ("Z") strain and were all thermally compensated by gauges mounted on aluminum elements.

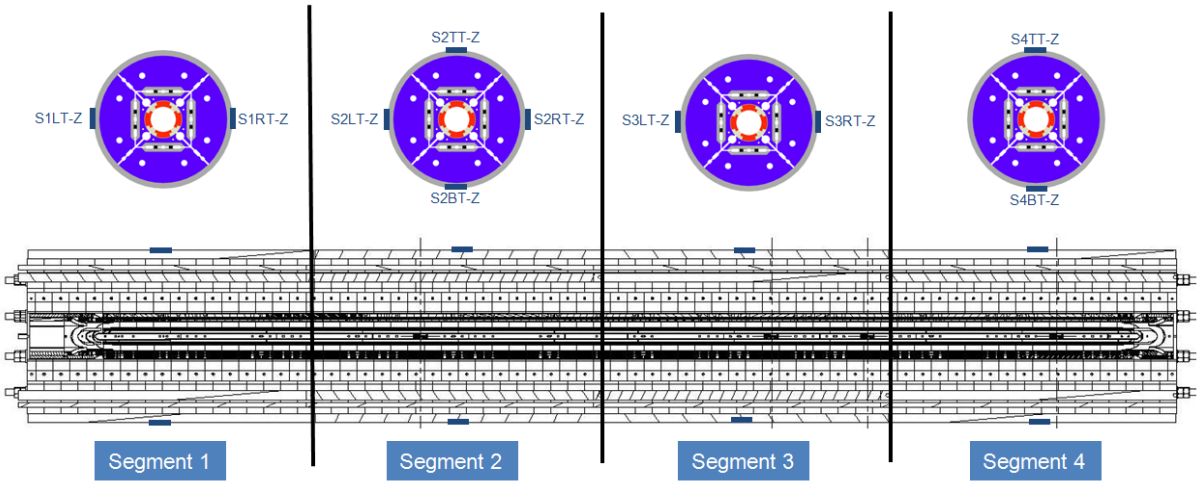

Fig. 14. Locations of the shell strain gauges (blue markers).

Each of the four LQS01 coils ("C"), coil #6-#7-#8-#9, was instrumented with full bridge azimuthal ("T") and axial ("Z") gauges thermally compensated and mounted along four axial locations ("1" to "4" from the lead end) of the inner-layer poles (see Fig. 15).

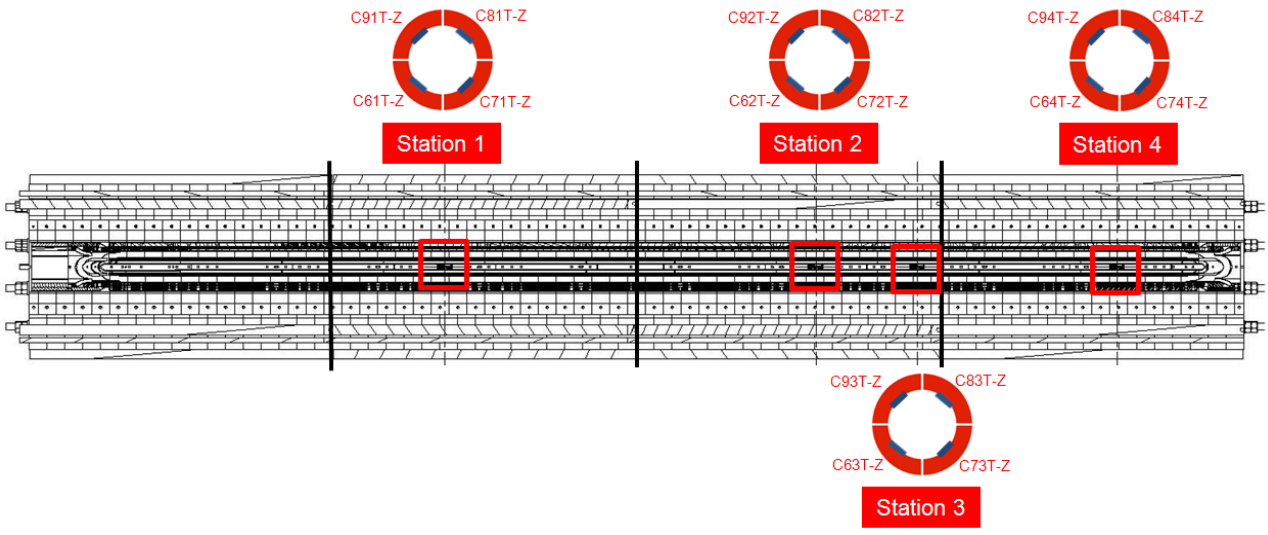

Fig. 15. Locations of the coil strain gauges (blue markers).

Each axial rod was equipped with two half-bridge gauges mounted close to the end plate (lead end), in opposite azimuthal locations to compensate for bending effects (see Fig. 16). The total number of gauges mounted on the LQS01 magnet amounts to 56 gauges.

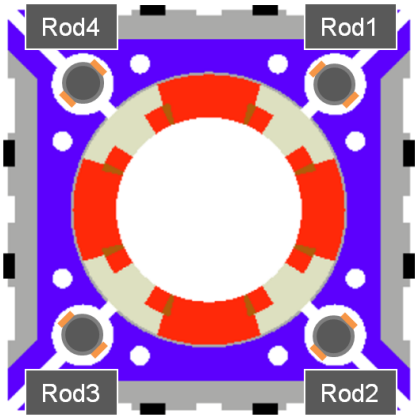

Fig. 16. Locations of the axial rod strain gauges (orange markers).

The plots in Fig. 19-34 and Fig. 37-46 show the strain gauge measurements taken during cool-down (as a function of data point), excitation as a function of current squared I^2), and warm-up (as a function of data point). Correspondence between temperature, time and data points are shown in Fig. 17-18 and Fig. 34-35.

The data are compared with the predictions of a 3D finite element model (described in [2]) of the entire magnet geometry. According to the finite element model, the 293 K and 4.3 K stresses chosen as target values for the shell and rods provide a coil pre-load sufficient to avoid separation between the turns and the Ti-alloy pole pieces up to a gradient of 230-240 T/m.

On the one hand, the shell and the axial rods were pre-loaded respectively to +33 MPa of azimuthal stress (see Fig. 20) and +60 MPa of axial stress (see Fig. 24), and their tensions after cool-down were consistent with the numerical predictions. On the other hand, the room temperature azimuthal stress of -12 MPa measured on the coil poles was lower than the expected -49 MPa (see Fig. 26), and no significant increase of compression was observed during cool-down. This discrepancy between computed and measured values was not observed in the LQSD data [2]. The lack of coil pre-load in the coil inner layer was confirmed by the strain measurements during excitation (see Fig. 31 to Fig. 34), which showed, in the last part of the current ramp, a "plateau" indicating separation between coil turns and pole pieces. The causes of this unexpected low pre-load are currently under investigations.

8.1 Cool-down

During cool-down (see Fig. 17 and 18)

- the shell strain-stress changed as follows
  - Azimuthal microstrain (Fig. 19): from +459 ±114 to +1630 ±117
  - Azimuthal stress (Fig. 20): from +34 ±8 to +146 ±6 MPa
  - Axial microstrain (Fig. 21): from -100 ±106 to +28 ±203
  - Axial stress (Fig. 22): from +4 ±7 to +49 ±15 MPa
- the rod strain-stress changed as follows
  - Axial microstrain (Fig. 23): from +393 ±38 to +939 ±50
  - Axial stress (Fig. 24): from +79 ±7 to +197 ±11 MPa
- the coil pole strain-stress changed as follows
  - Azimuthal microstrain (Fig. 25): from -22 ±69 to -179 ±104
  - Azimuthal stress (Fig. 26): from +3 ±12 to -25 ±19 MPa
  - Axial microstrain (Fig. 27): from -139 ±157 to -3 ±257
  - Axial stress (Fig. 28): from +19 ±23 to -7 ±38 MPa

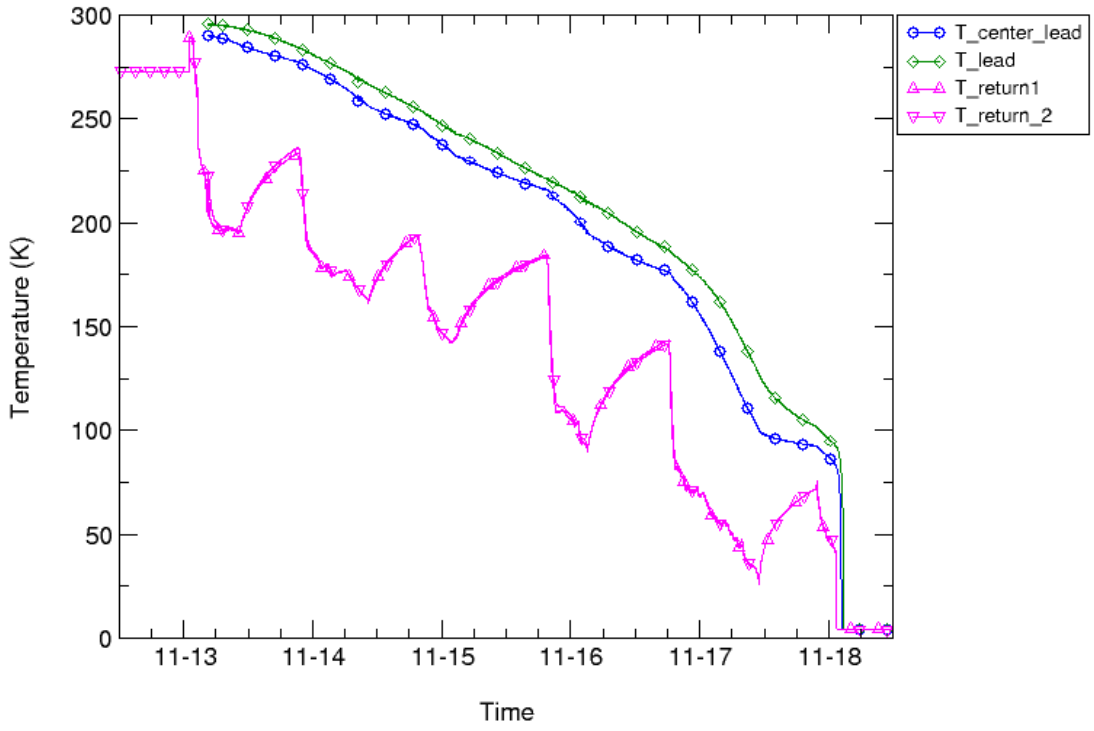

Fig. 17. Temperature of the shell measured during cool-down vs. time.

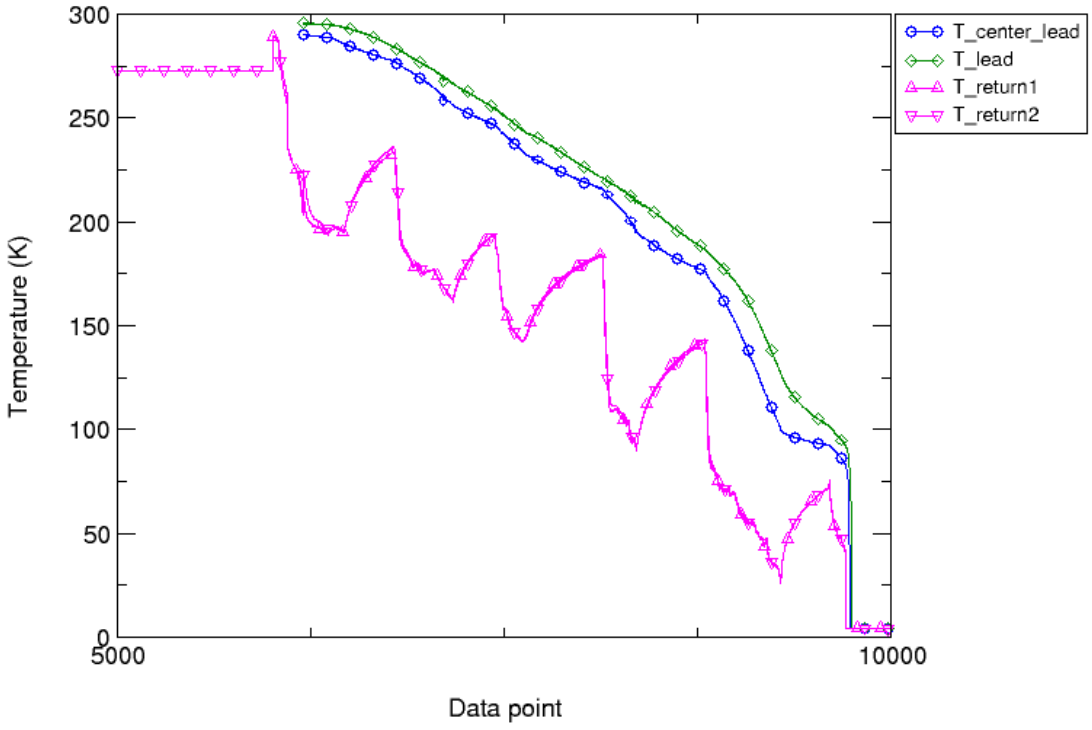

Fig. 18. Temperature of the shell measured during cool-down vs. data point.

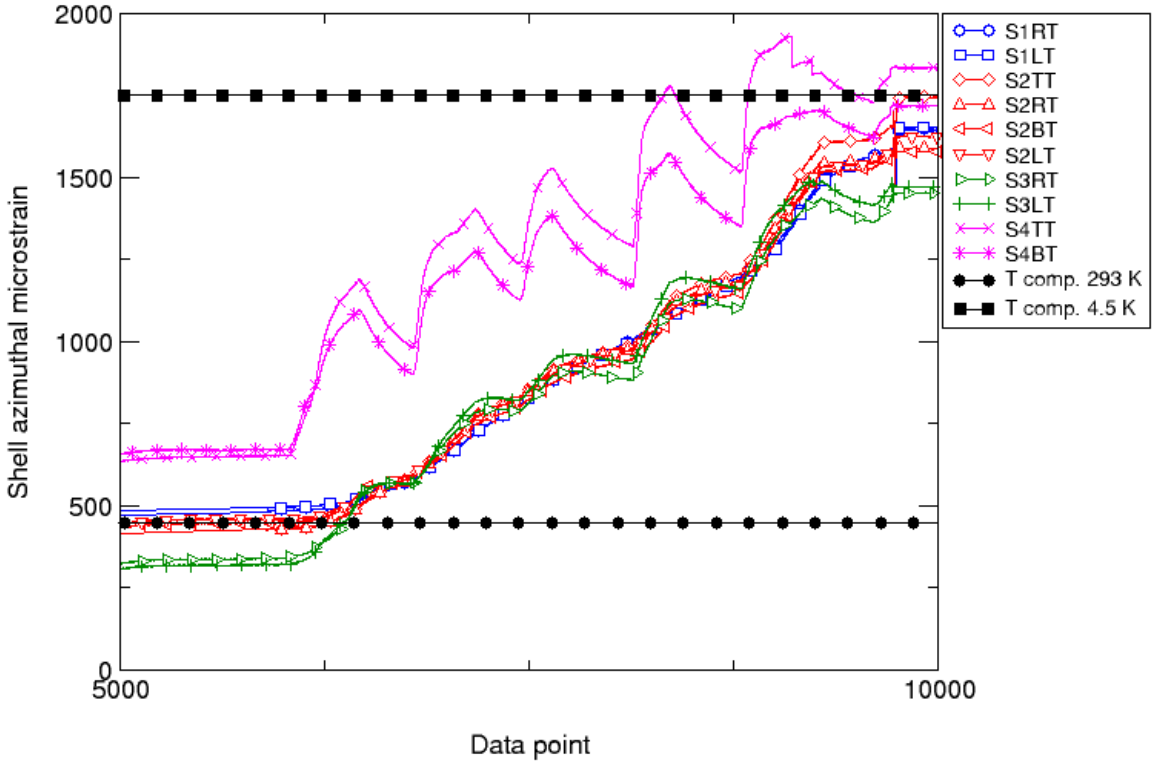

Fig. 19. Azimuthal microstrain in the shell during cool-down: values measured (colored markers) and computed (black markers) from a 3D finite element model.

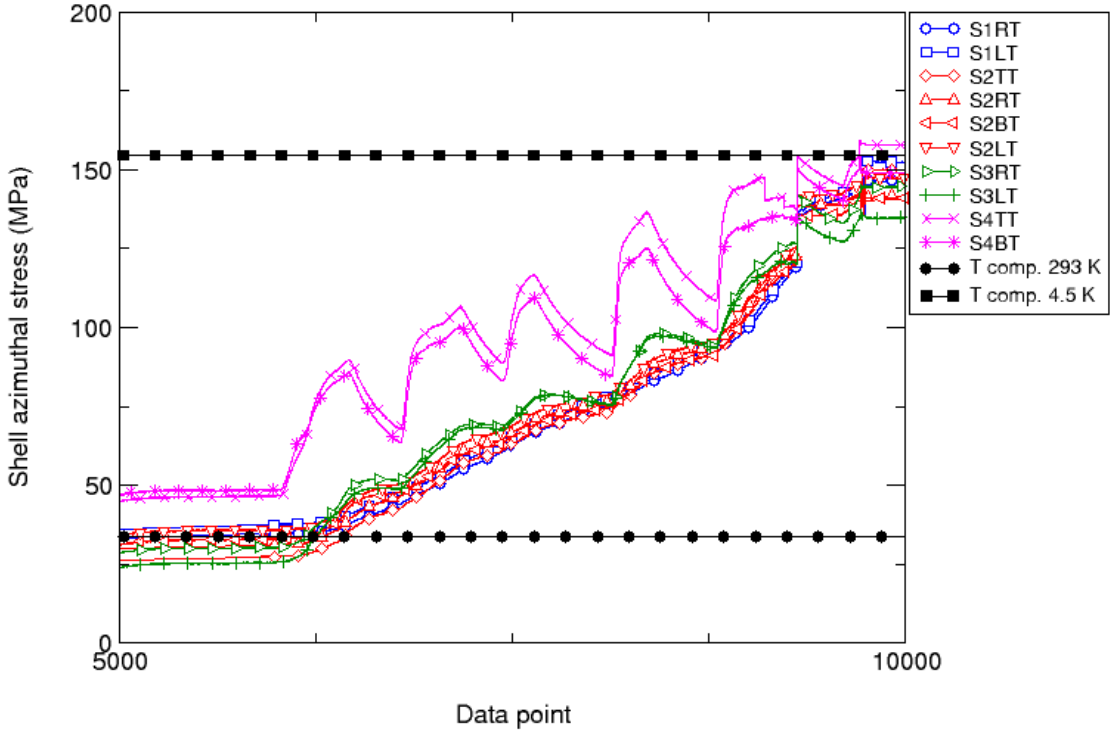

Fig. 20. Azimuthal stress (MPa) in the shell during cool-down: values measured (colored markers) and computed (black markers) from a 3D finite element model.

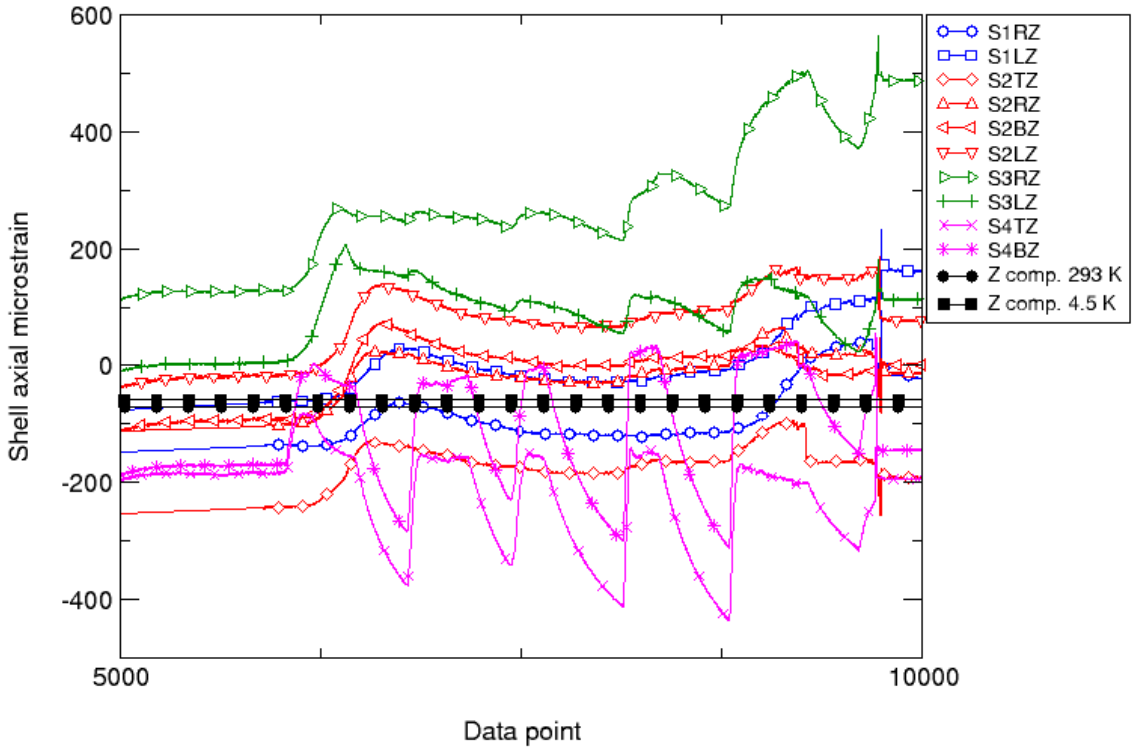

Fig. 21 Axial microstrain in the shell during cool-down: values measured (colored markers) and computed (black markers) from a 3D finite element model.

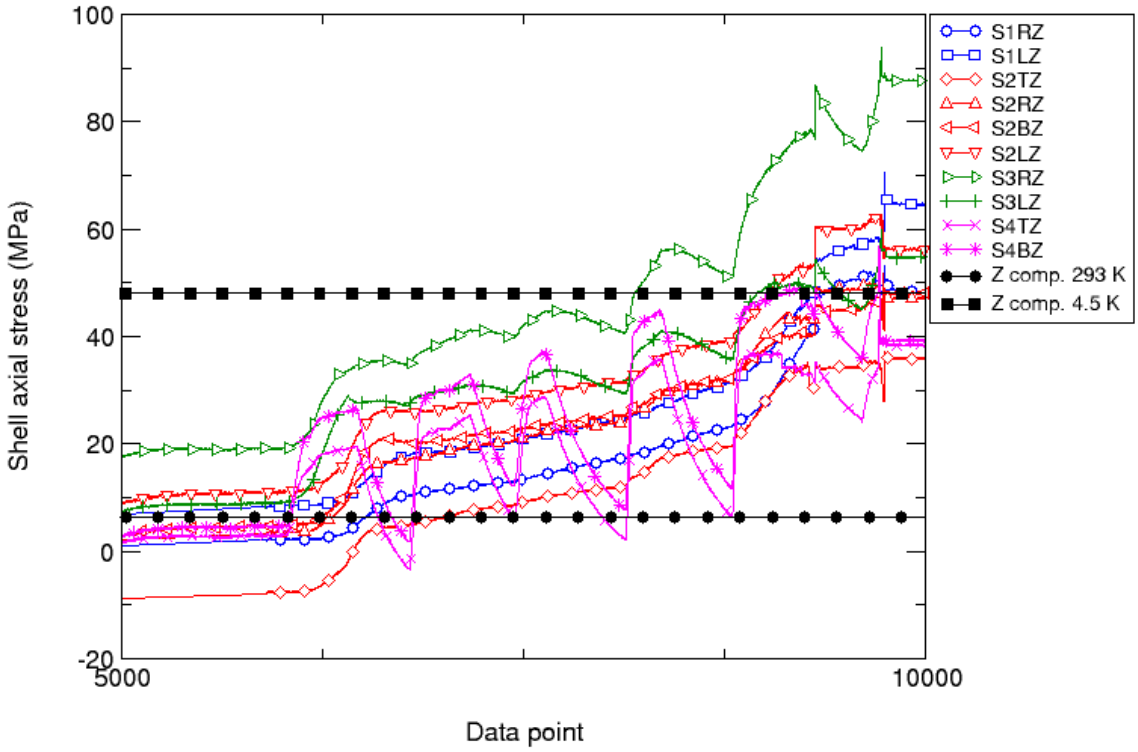

Fig. 22 Axial stress (MPa) in the shell during cool-down: values measured (colored markers) and computed (black markers) from a 3D finite element model.

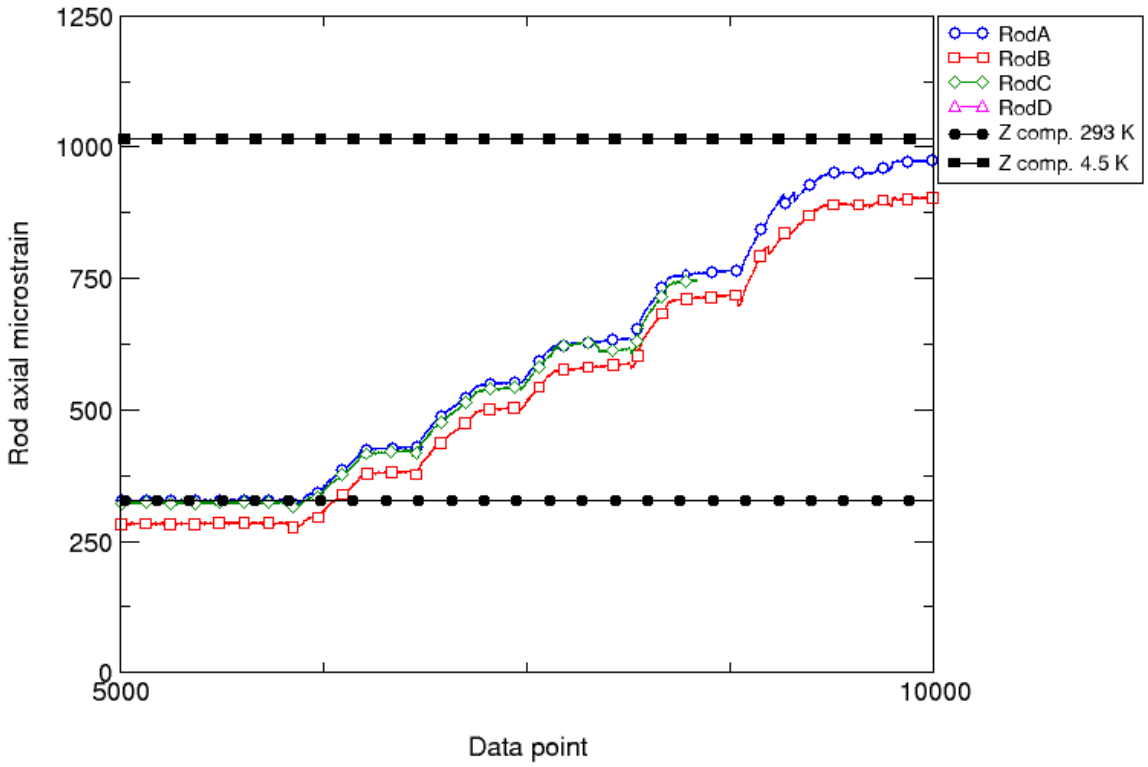

Fig. 23 Axial microstrain in the rods during cool-down: values measured (colored markers) and computed (black markers) from a 3D finite element model.

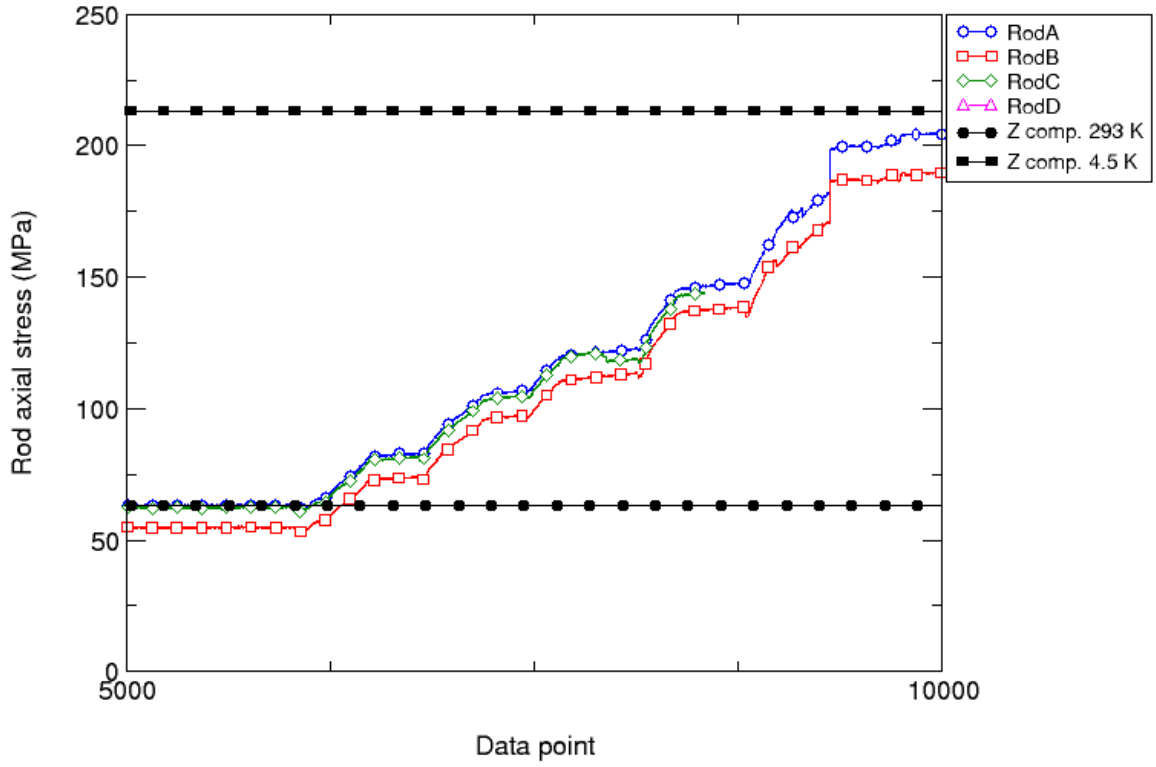

Fig. 24 Axial stress (MPa) in the rods during cool-down: values measured (colored markers) and computed (black markers) from a 3D finite element model.

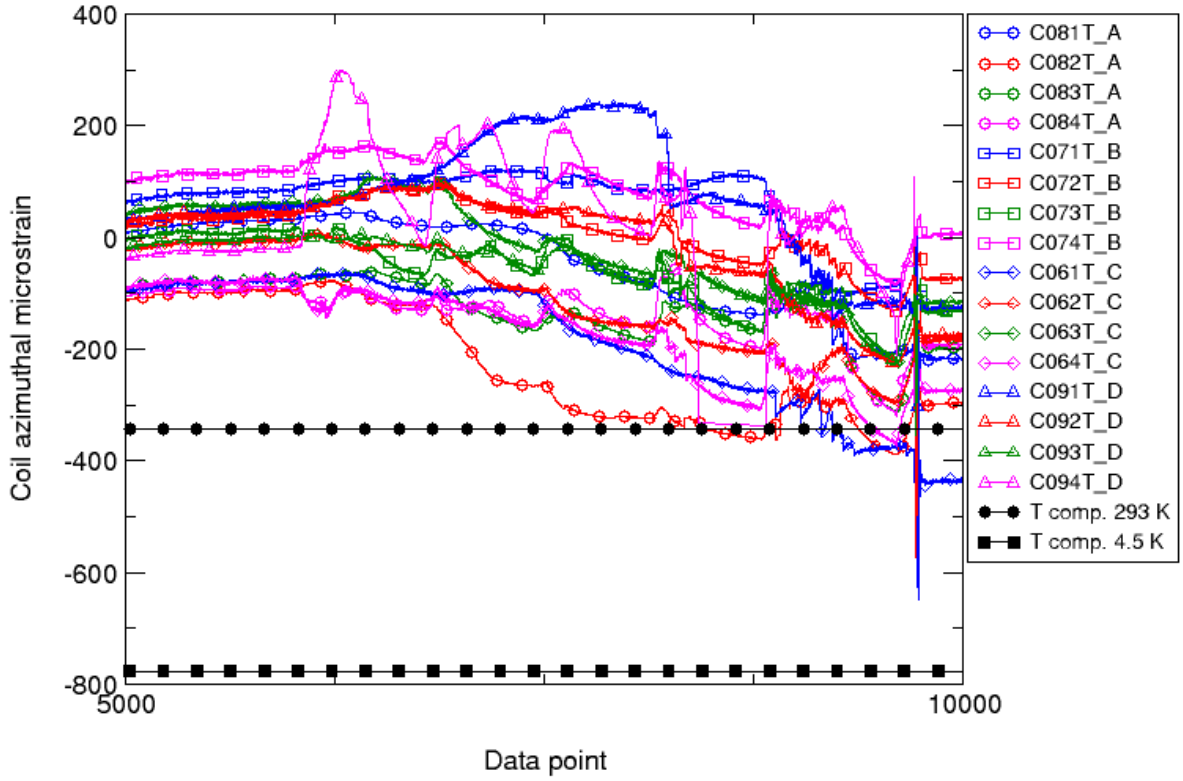

Fig. 25 Azimuthal microstrain in the coil poles during cool-down: values measured (colored markers) and computed (black markers) from a 3D finite element model.

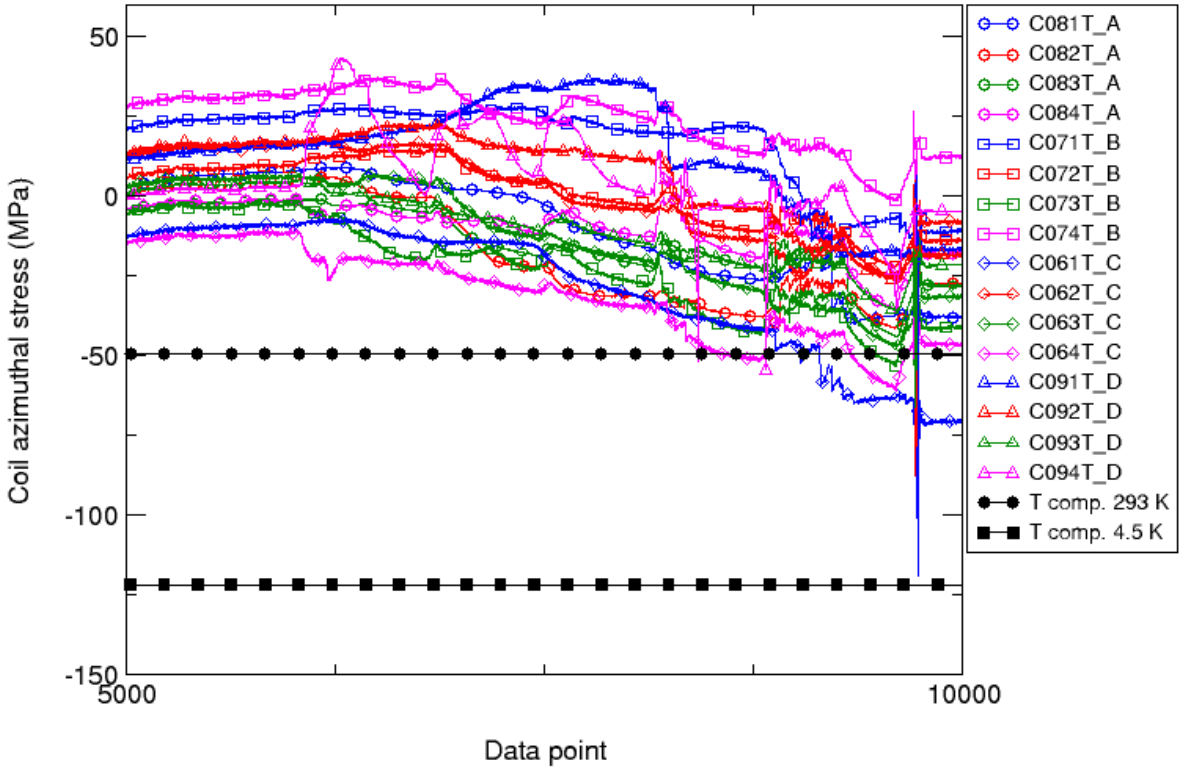

Fig. 26 Azimuthal stress (MPa) in the coil poles during cool-down: values measured (colored markers) and computed (black markers) from a 3D finite element model.

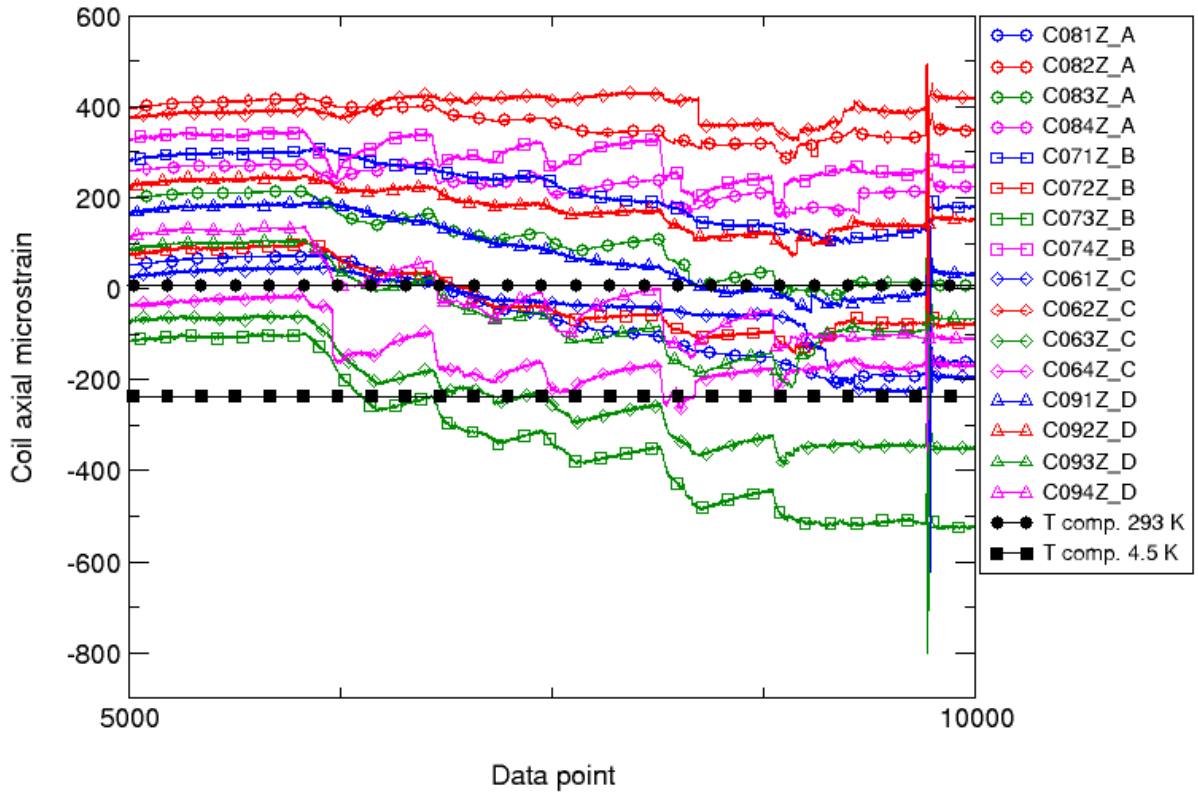

Fig. 27 Axial microstrain in the coil poles during cool-down: values measured (colored markers) and computed (black markers) from a 3D finite element model.

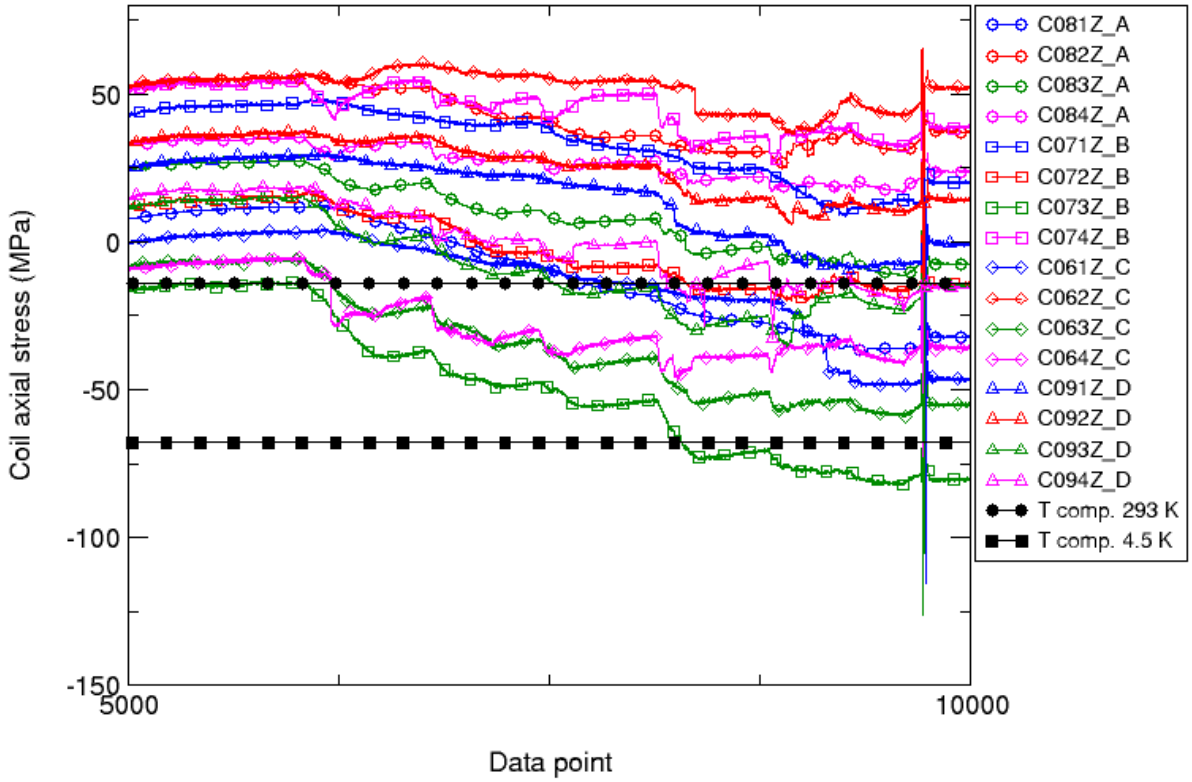

Fig. 28 Axial stress (MPa) in the coil poles during cool-down: values measured (colored markers) and computed (black markers) from a 3D finite element model.

8.2 Excitation

During excitation the axial strain of the coil poles remains constant (Fig. 29). The reduction in azimuthal strain (Fig. 30) induces the reduction of azimuthal stress (Fig. 31-34).

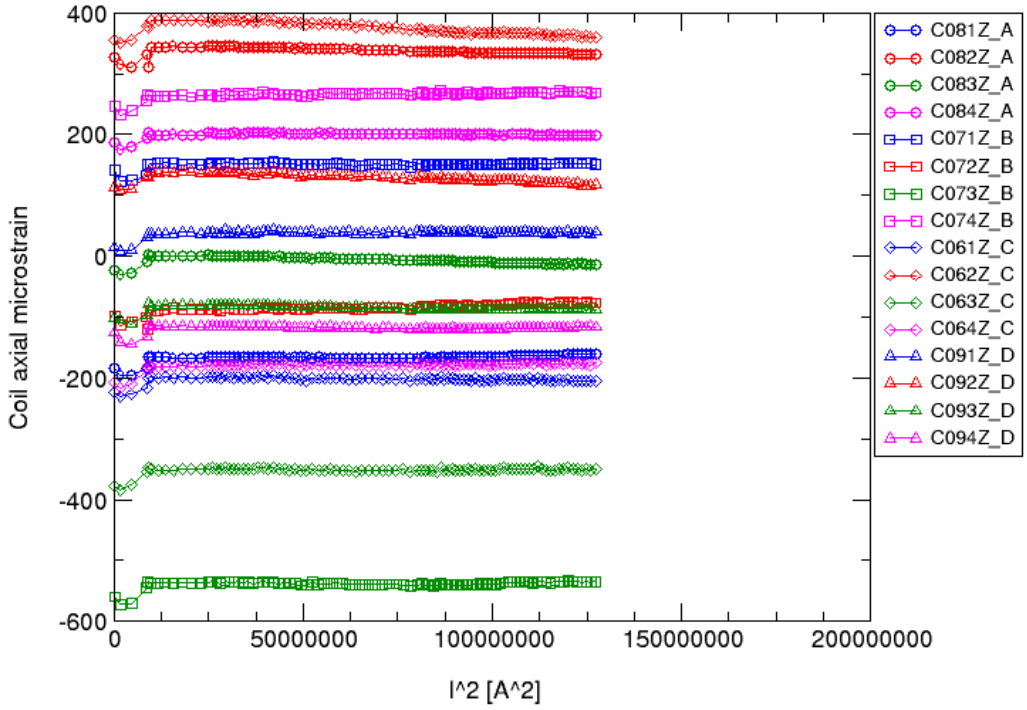

Fig. 29. Axial strain in the coil poles (all stations) vs. I^2 (A^2) for quench # 45 (11372 A).

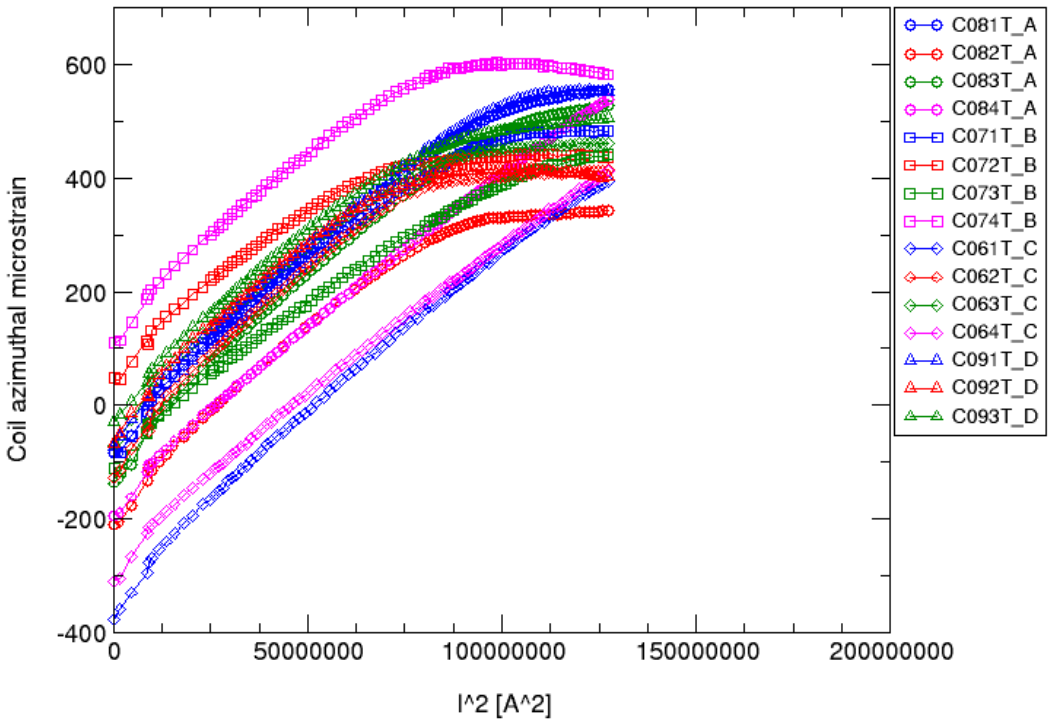

Fig. 30. Azimuthal strain in the coil poles (all stations) vs. I^2 (A^2) for quench # 45 (11372 A).

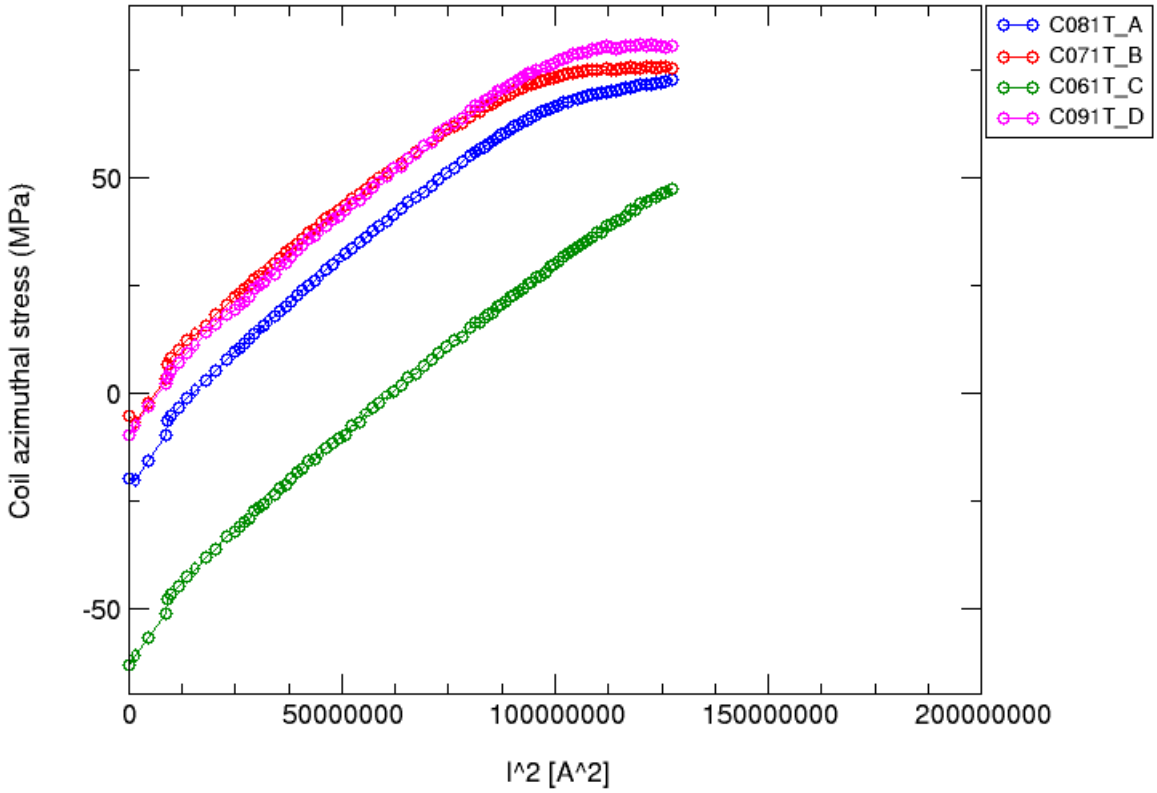

Fig. 31. Azimuthal stress (MPa) in the coil poles (station 1) vs. I^2 (A^2) for quench # 45 (11372 A).

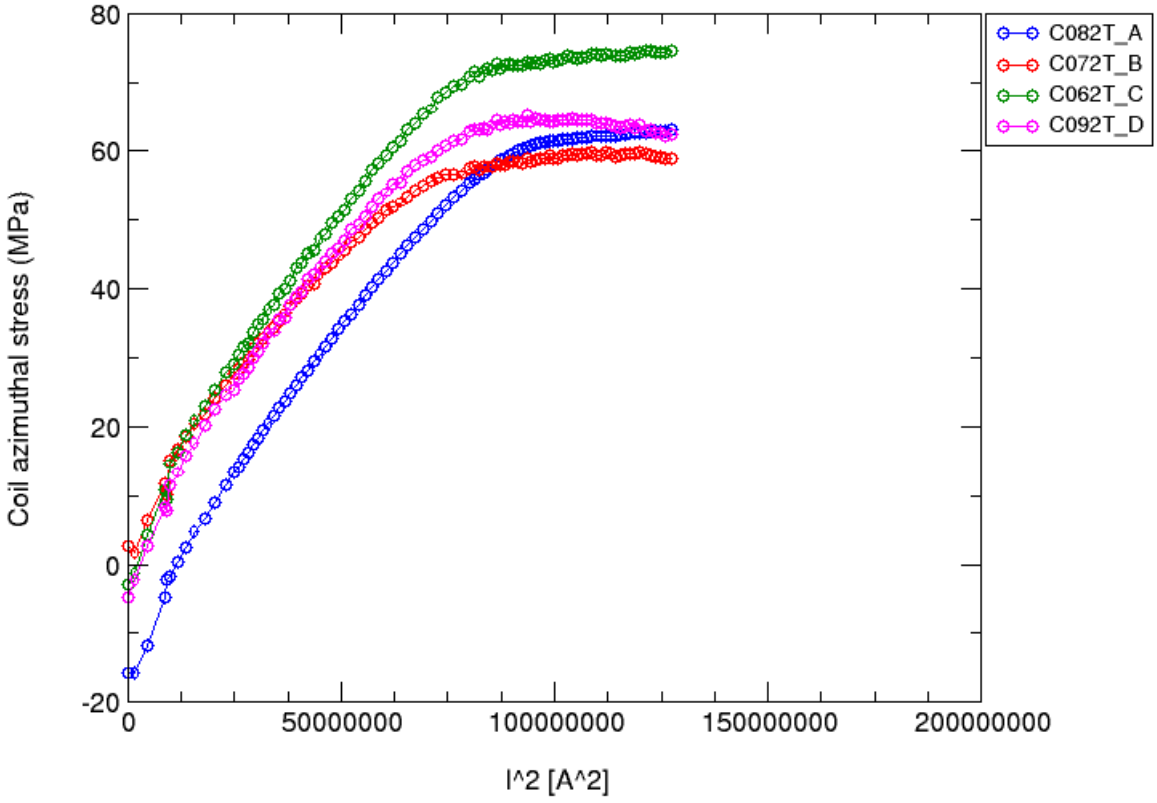

Fig. 32. Azimuthal stress (MPa) in the coil poles (station 2) vs. I^2 (A^2) for quench # 45 (11372 A).

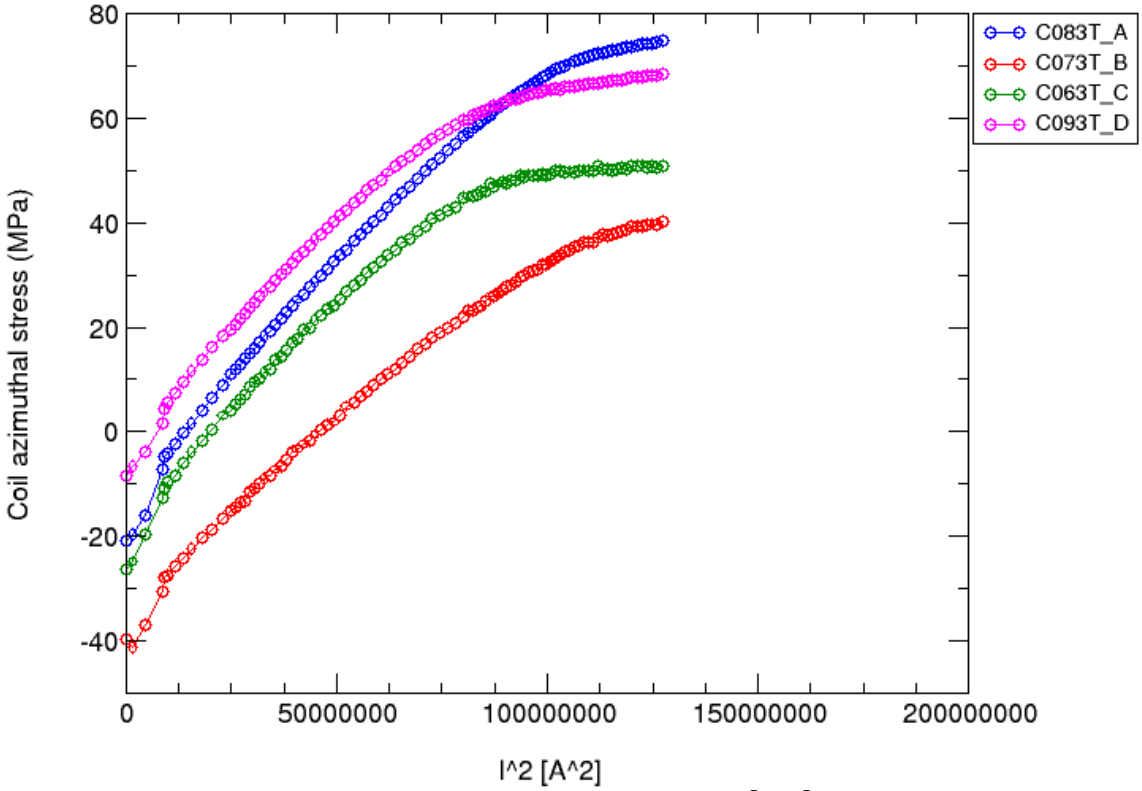

Fig. 33. Azimuthal stress (MPa) in the coil poles (station 3) vs. I^2 (A^2) for quench # 45 (11372 A).

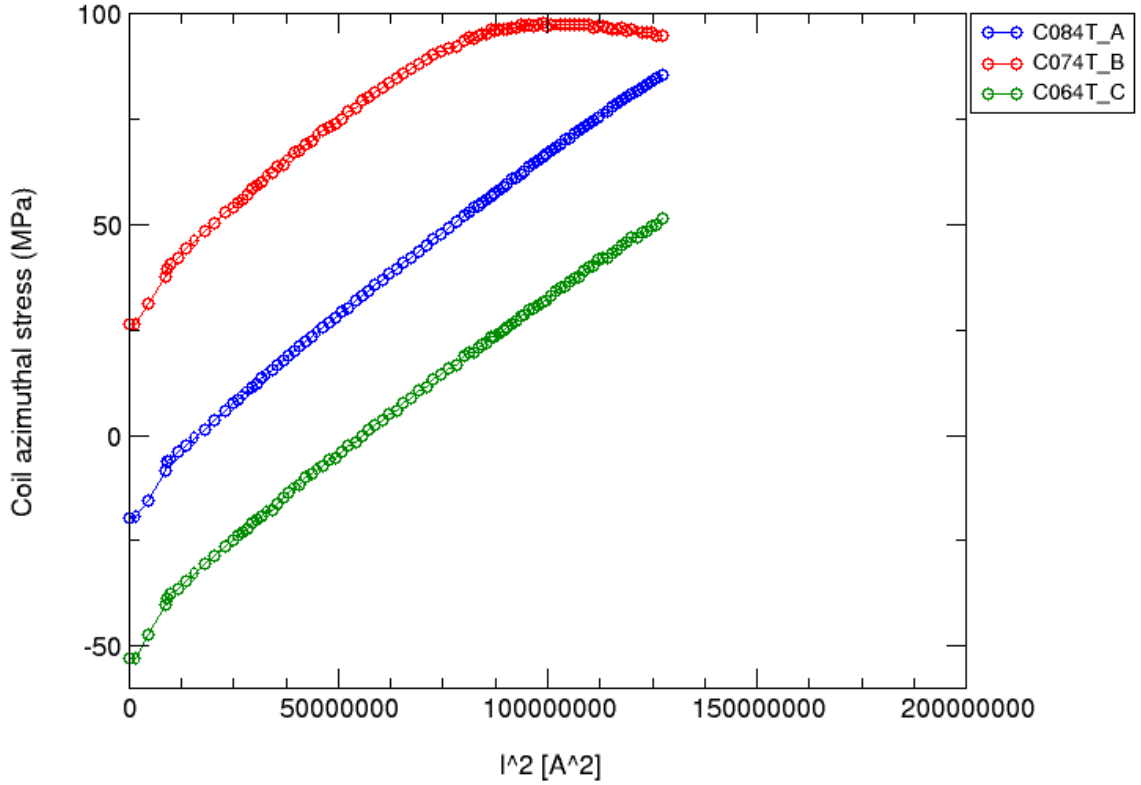

Fig. 34. Azimuthal stress (MPa) in the coil poles (station 4) vs. I^2 (A2) for quench # 45 (11372 A).

8.3 Warm-up

During warm-up (see Fig. 35 and 36)

- the shell strain-stress changed as follows
  - Azimuthal microstrain (Fig. 37): from +1589 ±119 to +338 ±93
  - Azimuthal stress (Fig. 38): from +142 ±7 to +24 ±6 MPa
  - Axial microstrain (Fig. 39): from -9 ±198 to -111 ±94
  - Axial stress (Fig. 40): from +45 ±15 to 0 ±6 MPa
- the rod strain-stress changed as follows
  - Axial microstrain (Fig. 41): from +939 ±51 to +311 ±34
  - Axial stress (Fig. 42): from +197 ±11 to +60 ±7 MPa
- the coil pole strain-stress changed as follows
  - Azimuthal microstrain (Fig. 43): from –89 ±116 to -47 ±70
  - Azimuthal stress (Fig. 44): from -13 ±21 to +1 ±11 MPa
  - Axial microstrain (Fig. 45): from -4 ±251 to +190 ±151
  - Axial stress (Fig. 46): from -3 ±38 to +25 ±22 MPa

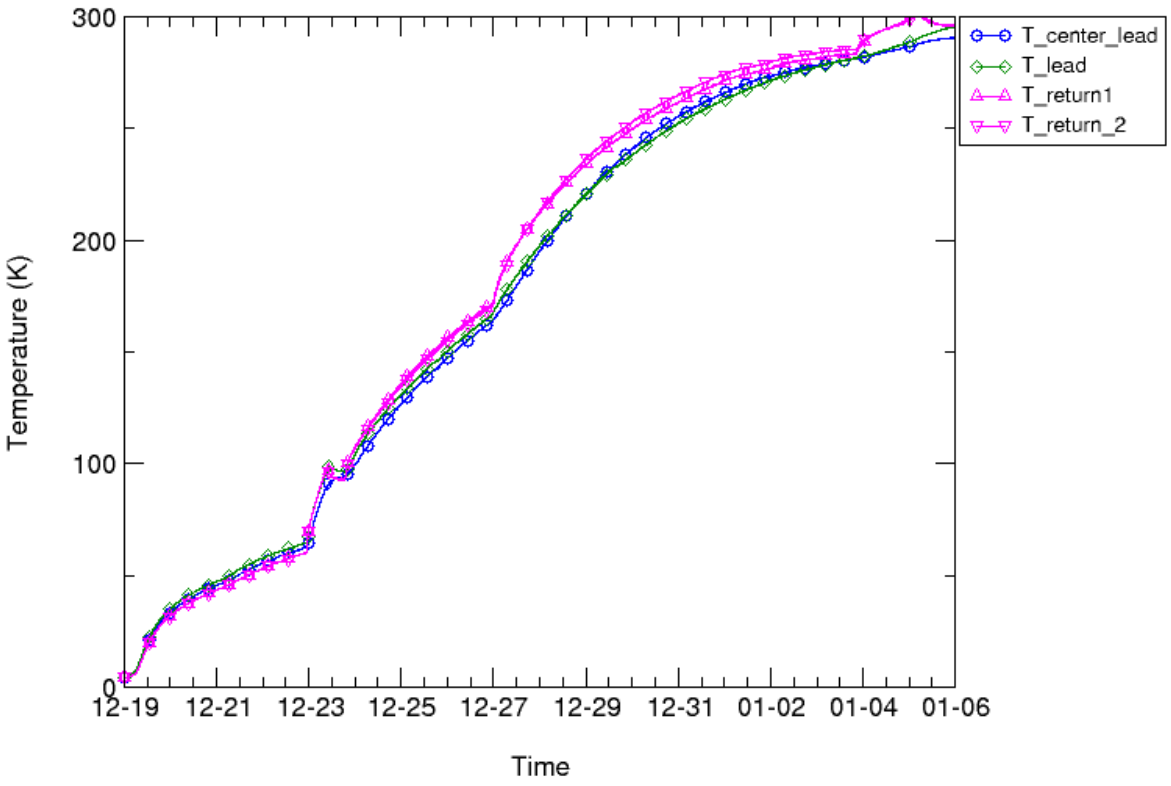

Fig. 35. Temperature of the shell measured during warm-up vs. time

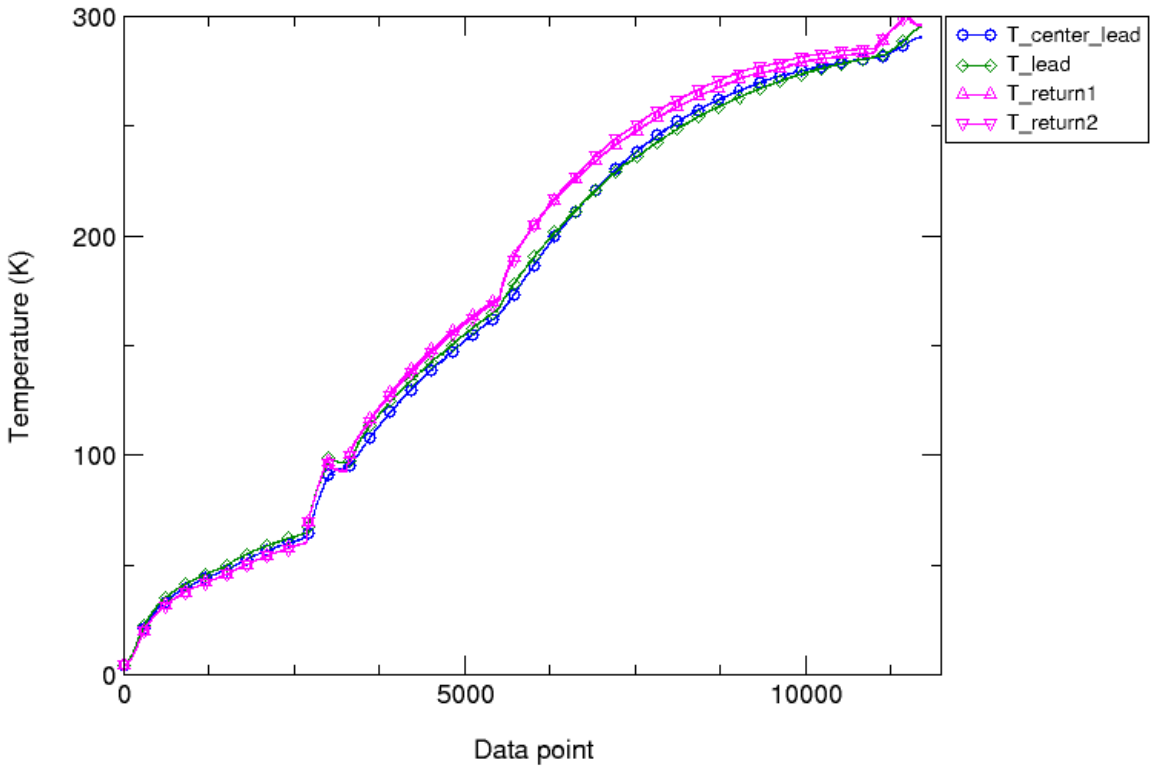

Fig. 36. Temperature of the shell measured during warm-up vs. data point

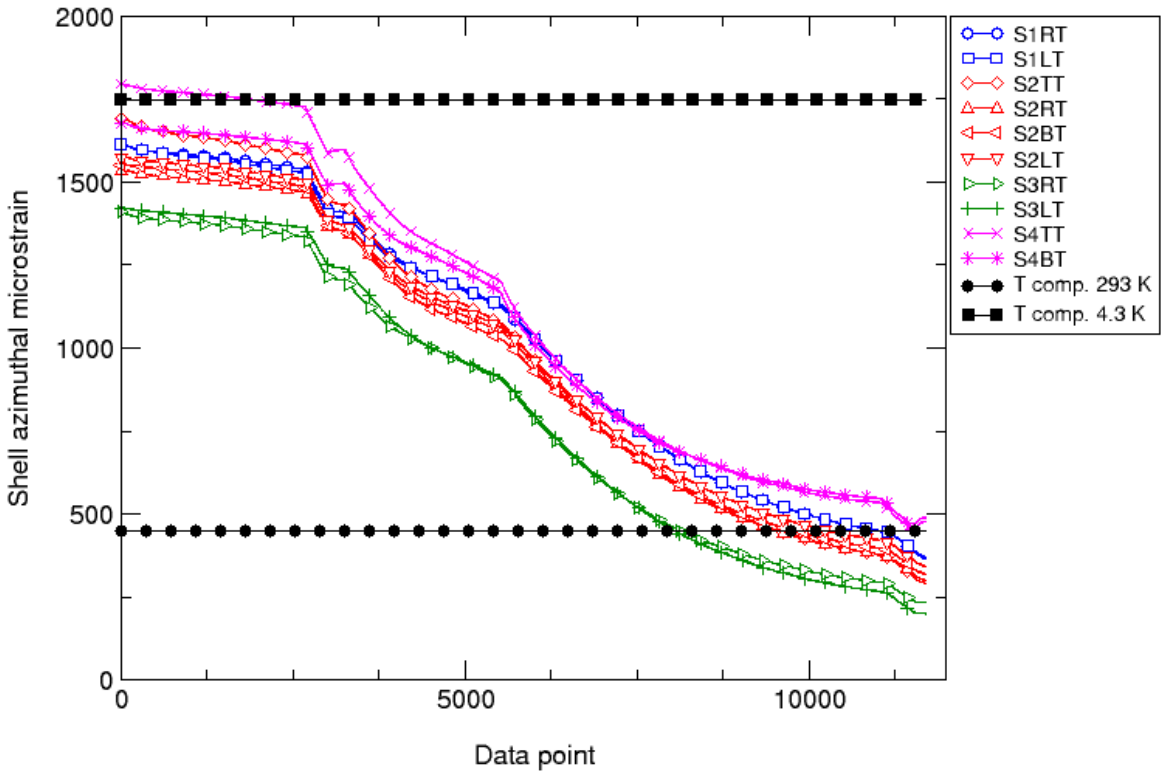

Fig. 37 Azimuthal microstrain in the shell during warm-up: values measured (colored markers) and computed (black markers) from a 3D finite element model.

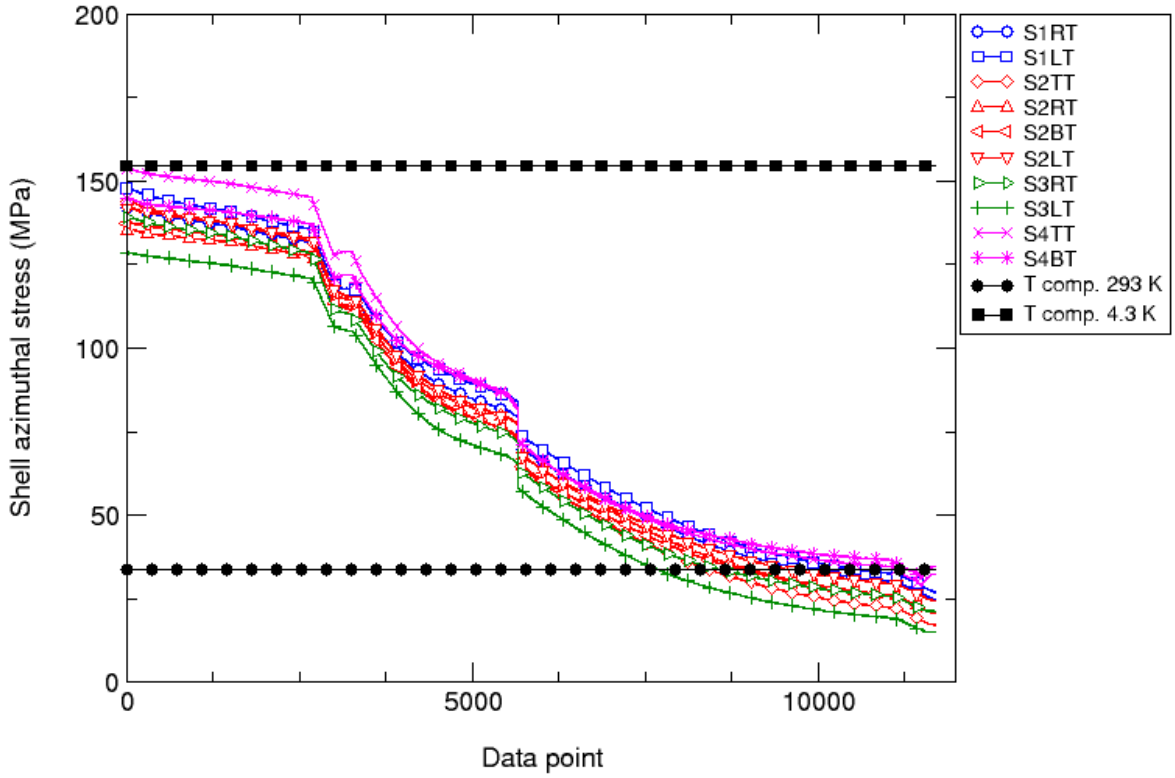

Fig. 38 Azimuthal stress (MPa) in the shell during warm-up: values measured (colored markers) and computed (black markers) from a 3D finite element model.

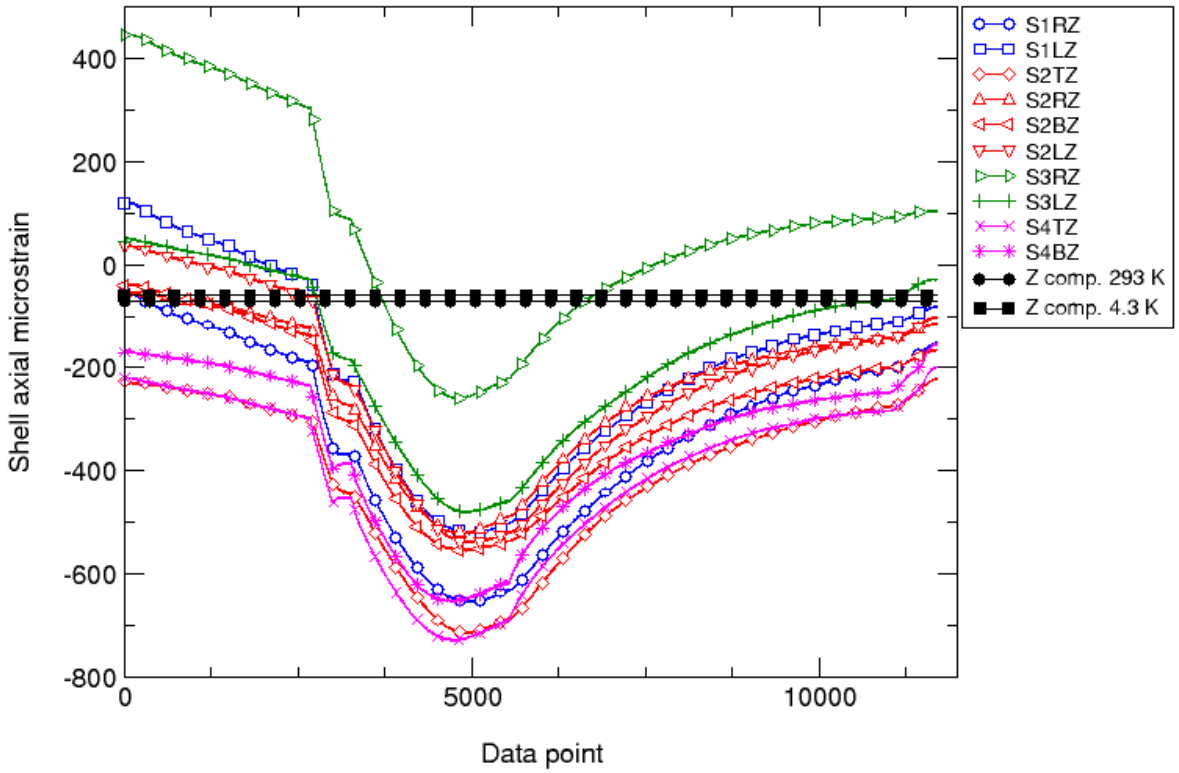

Fig. 39 Axial microstrain in the shell during warm-up: values measured (colored markers) and computed (black markers) from a 3D finite element model.

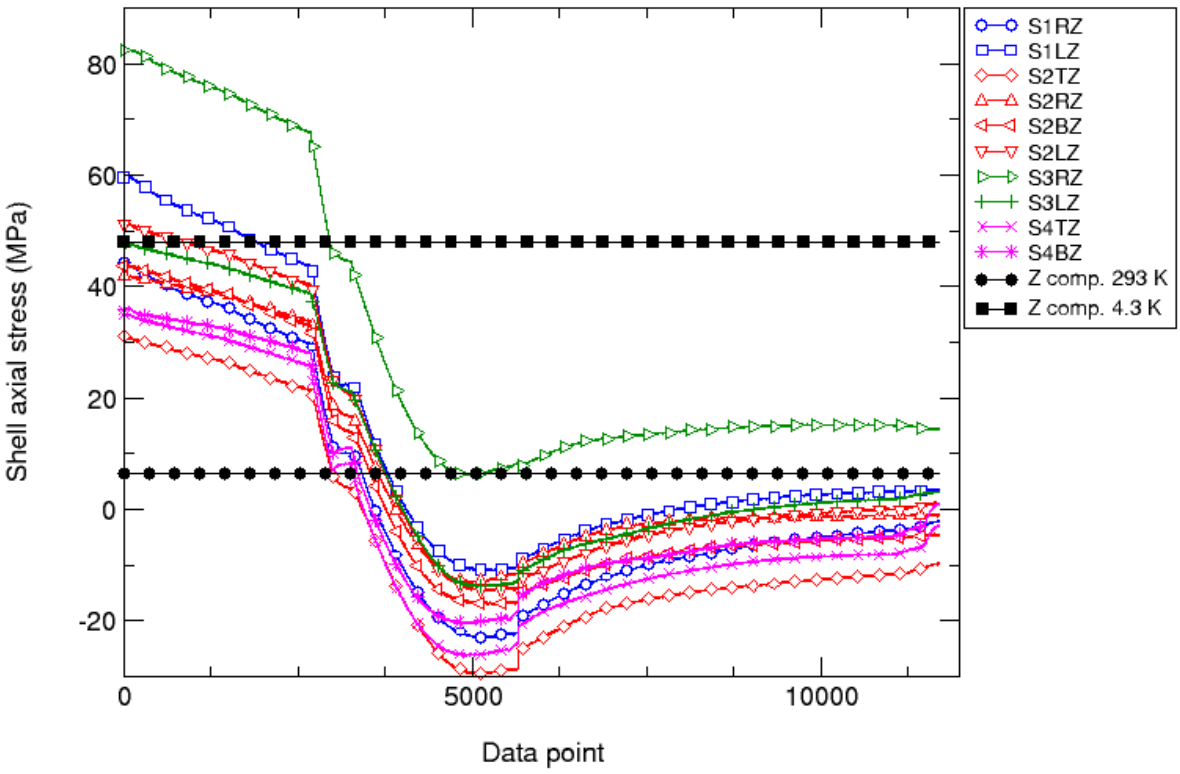

Fig. 40 Axial stress (MPa) in the shell during warm-up: values measured (colored markers) and computed (black markers) from a 3D finite element model.

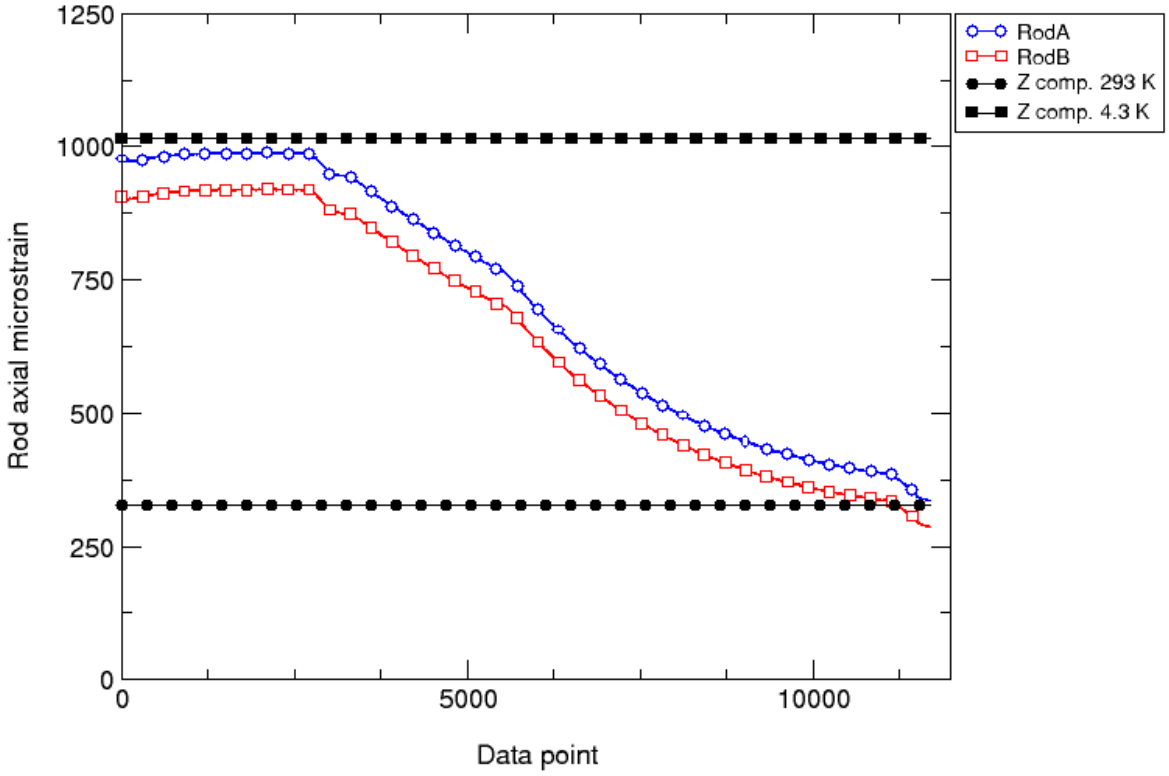

Fig. 41 Axial microstrain in the rods during warm-up: values measured (colored markers) and computed (black markers) from a 3D finite element model.

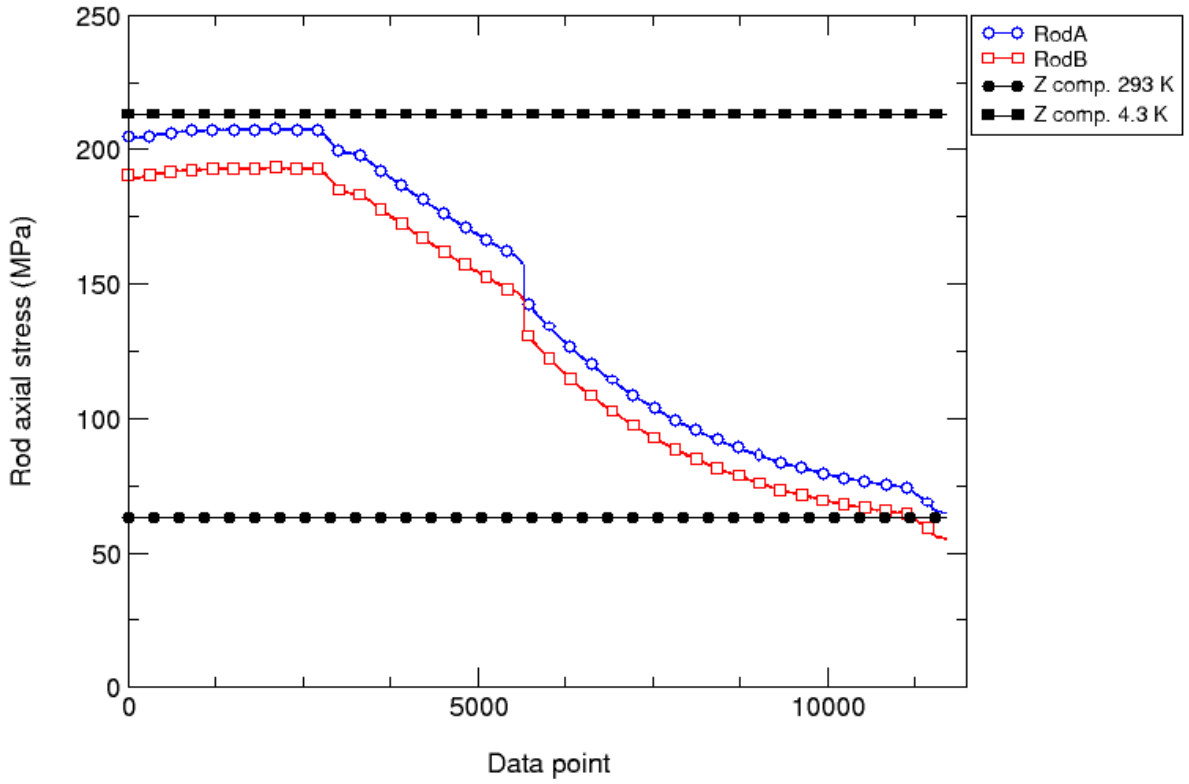

Fig. 42 Axial stress (MPa) in the rods during warm-up: values measured (colored markers) and computed (black markers) from a 3D finite element model.

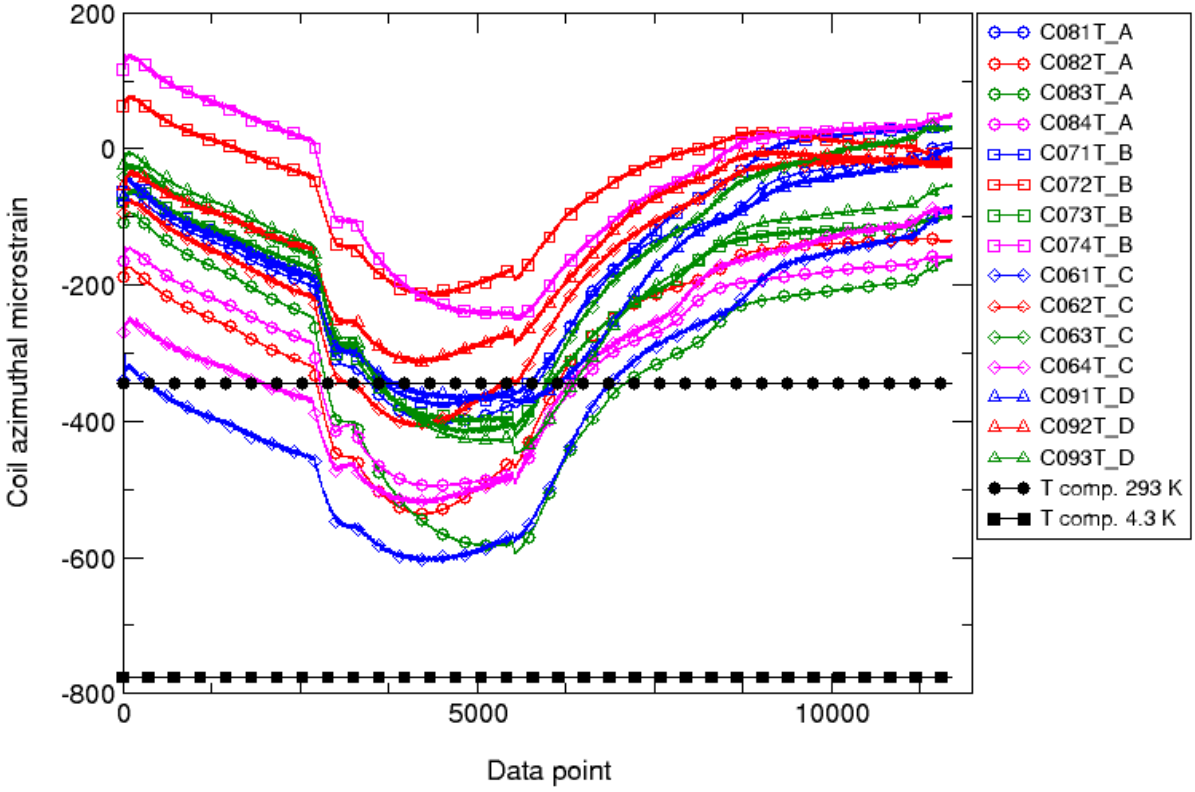

Fig. 43 Azimuthal microstrain in the coil poles during warm-up: values measured (colored markers) and computed (black markers) from a 3D finite element model.

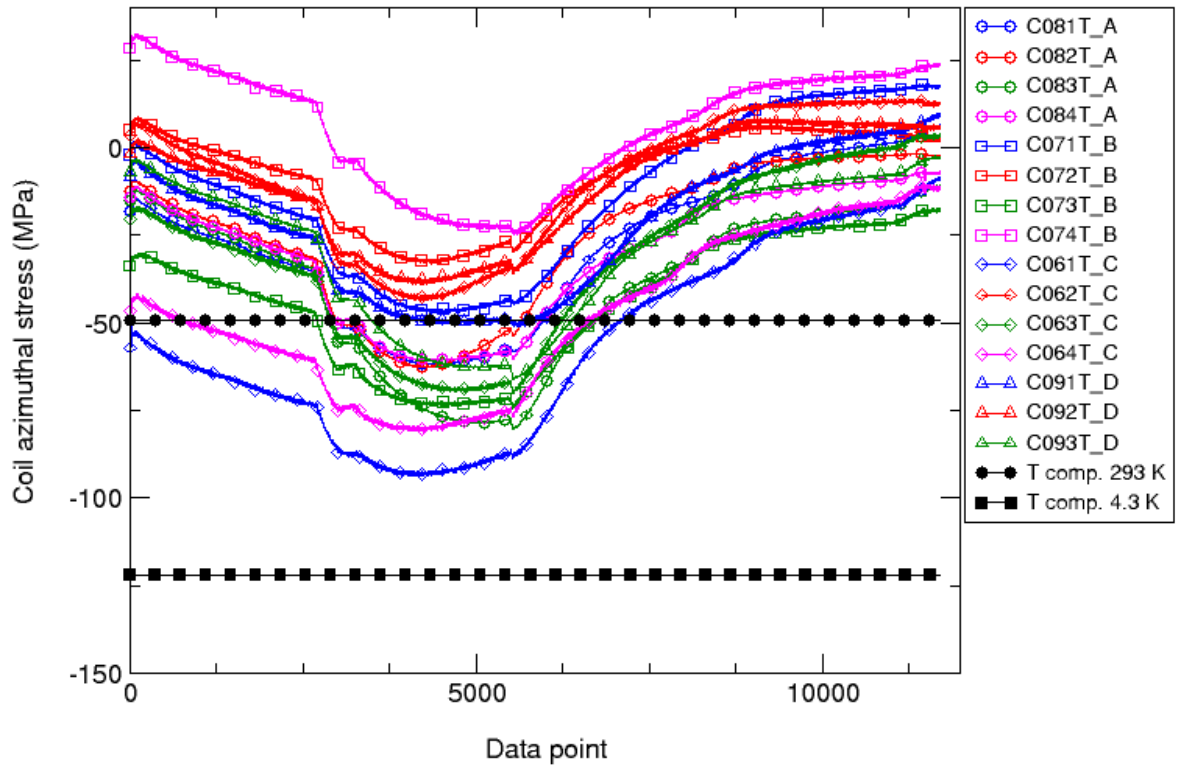

Fig. 44 Azimuthal stress (MPa) in the coil poles during warm-up: values measured (colored markers) and computed (black markers) from a 3D finite element model.

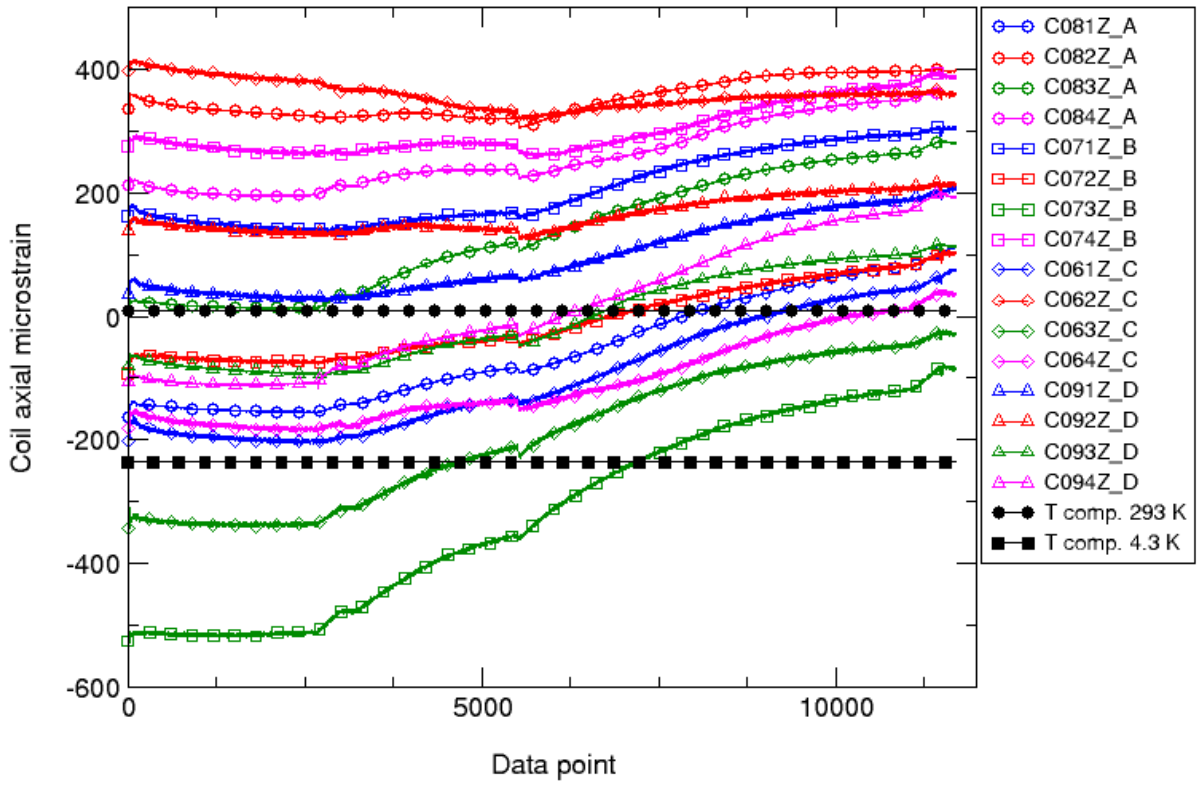

Fig. 45 Axial microstrain in the coil poles during warm-up: values measured (colored markers) and computed (black markers) from a 3D finite element model.

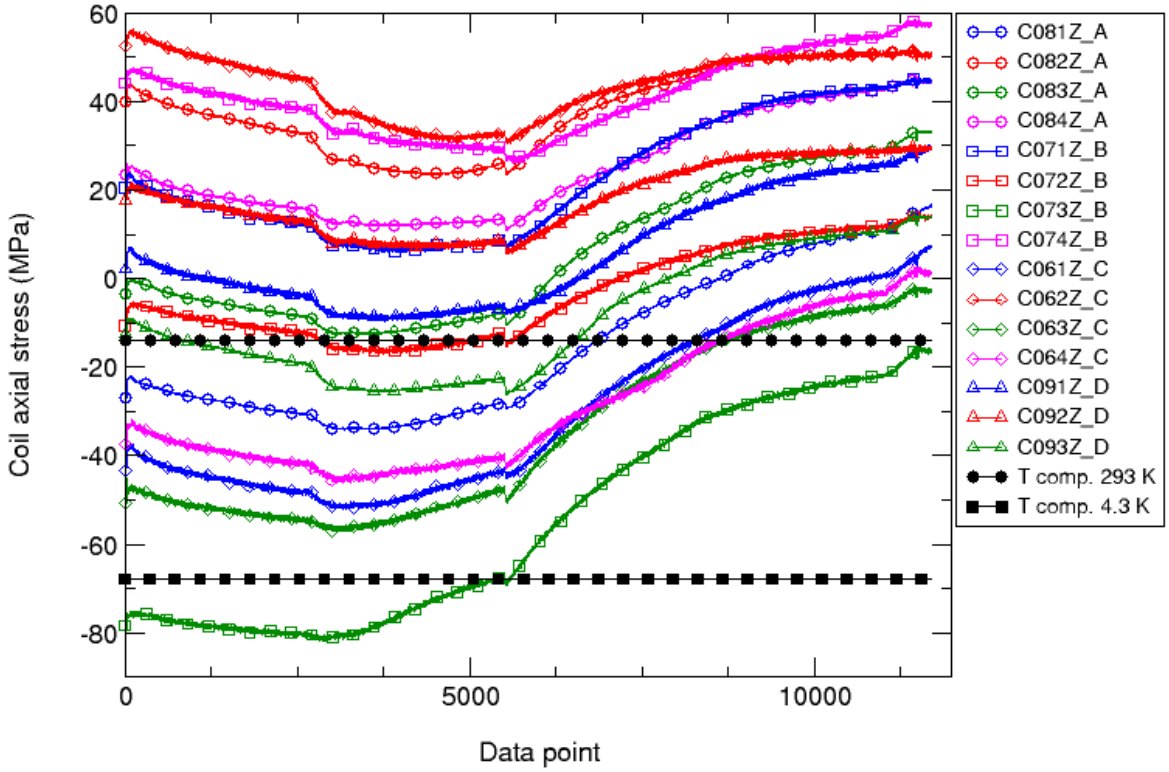

Fig. 46 Axial stress (MPa) in the coil poles during warm-up: values measured (colored markers) and computed (black markers) from a 3D finite element model.

9. Measurement of the Residual Resistance Ratio (RRR)

Estimates of RRR in LQS01 coil segments have been made using data captured during the warm-up after the test. The warm-up was started on December 18th and transition from superconducting to normal occurred at about 11:00 pm of the same day when the temperature gradient along the 4-m long body of the magnet was about 2K. Data captured at 23:40 pm of December 18th was used for the cold RRR measurement. Temperature of the magnet at top, middle and bottom were respectively 19.8 K, 18.6 K and 17.6 K.

Coil voltages across "fixed" and "configurable" voltage tap segments were monitored by the *Pentek* data loggers, while a current of alternating polarity, +/- 5-7 A, was put through the magnet. For both the warm (~ 300 K) and cold (~ 20 K) measurements we used the RRR amplifier gains for the voltage tap segments to maximize the signal levels.

The magnet reached room temperature and warm voltage measurements were captured on January 4th, 2010. Data for all segments, as well as for the whole and half-coils are shown in Table 5. The results are also shown in Fig. 47. Segments around the splices, as well as noisy segments are not shown in the figure.

RRR values for both the configurable and fixed voltage tap segments are reasonably consistent. In average RRR for most of the segments is above 250, and for the half-coil segments it varies from 288 to 296.

Table 5. RRR data for all segments

ΔI=I(+) - I(-) was 14.1 A for the cold and 10.9 A for the room temperature measurements

Segment	V(+)-V(-) cold	R cold	V(+)-V(-) warm	R warm	RRR
	V	Ohm	V	Ohm	
8a2_8a3	0.01038330	0.00073754	2.68309000	0.24435800	331.32
8a3_8a4	0.00201487	0.00014312	0.47954200	0.04367340	305.15
8a4_8a5	0.00364422	0.00025885	0.93723200	0.08535650	329.75
8a5_8a6	0.00006911	0.00000491	0.01736740	0.00158170	322.21
8a6_8a7	0.00005016	0.00000356	0.01179210	0.00107395	301.43
8a7_8a8	0.00034804	0.00002472	0.07777100	0.00708284	286.51
8a8_8a9	0.00006354	0.00000451	0.01477280	0.00134540	298.09
8a9_8a10	0.00002134	0.00000152	0.00499781	0.00045517	300.28
8a10_8a11	0.00006215	0.00000441	0.01472190	0.00134076	303.71
8a11_8a12	0.00034701	0.00002465	0.07793890	0.00709813	287.97
8a12_8a13	0.00005441	0.00000387	0.01172420	0.00106776	276.26
8a13_8b7	0.00005699	0.00000405	0.01256830	0.00114463	282.75
8b7_8b6	0.00049741	0.00003533	0.10846000	0.00987778	279.58
8b6_8b5	0.00003297	0.00000234	0.00754501	0.00068715	293.39
8b5_8b4	0.00053110	0.00003772	0.11170700	0.01017350	269.68
8b4_8b3	0.00603680	0.00042880	1.40370000	0.12783900	298.13
8b3_8b2	0.00844175	0.00059963	2.12424000	0.19346100	322.63
7b2_7b3	0.00945659	0.00067171	2.11101000	0.19225600	286.22
7b3_7b4	0.00667160	0.00047389	1.39447000	0.12699800	267.99
7b4_7b5	0.00062841	0.00004464	0.11097700	0.01010700	226.43
7b5_7b6	0.00003294	0.00000234	0.00755467	0.00068803	294.10
7b6_7b7	0.00061620	0.00004377	0.10774300	0.00981249	224.19
7b7_7a13	0.00007882	0.00000560	0.01266530	0.00115347	206.03
7a13_7a12	0.00005982	0.00000425	0.01171750	0.00106715	251.15
7a12_7a11	0.00039814	0.00002828	0.07731270	0.00704110	248.98
7a11_7a10	0.00006311	0.00000448	0.01478560	0.00134657	300.38
7a10_7a9	0.00002026	0.00000144	0.00504133	0.00045913	319.07
7a9_7a8	0.00006195	0.00000440	0.01458280	0.00132810	301.80
7a8_7a7	0.00039419	0.00002800	0.07749410	0.00705762	252.06
7a7_7a6	0.00006957	0.00000494	0.01269530	0.00115620	233.97
7a5_7a4	0.00411811	0.00029252	0.47370900	0.04314210	147.49
7a4_7a3	0.00212974	0.00015128	0.47615100	0.04336450	286.65
7a3_7a2	0.01145650	0.00081377	2.67190000	0.24333800	299.03
9b2_9b3	0.00926163	0.00065787	2.11414000	0.19254100	292.68
9b3_9b4	0.00649803	0.00046156	1.39773000	0.12729500	275.79
9b4_9b5	0.00062132	0.00004413	0.11097300	0.01010670	229.00
9b5_9b6	0.00002945	0.00000209	0.00756520	0.00068899	329.38
9b6_9a13	0.00067806	0.00004816	0.12031900	0.01095780	227.51
9a13_9a12	0.00006793	0.00000483	0.01185420	0.00107960	223.74
9a12_9a11	0.00039750	0.00002824	0.07760400	0.00706763	250.31
9a11_9a10	0.00006030	0.00000428	0.01472310	0.00134088	313.07
9a10_9a9	0.00001790	0.00000127	0.00494899	0.00045072	354.58

9a9_9a8	0.00005645	0.00000401	0.01475150	0.00134347	335.07
9a6_9a5	0.00009671	0.00000687	0.01735580	0.00158065	230.09
9a5_9a4	0.00408211	0.00028996	0.93398600	0.08506100	293.36
9a4_9a3	0.00211140	0.00014998	0.47829300	0.04355960	290.44
9a3_9a2	0.01170630	0.00083151	2.67390000	0.24352000	292.86
6a2_6a3	0.01110150	0.00078856	2.65208000	0.24153300	306.30
6a3_6a4	0.00214936	0.00015267	0.47369900	0.04314120	282.57
6a4_6a5	0.00392143	0.00027854	0.92535600	0.08427500	302.56
6a5_6a6	0.00007662	0.00000544	0.01716270	0.00156306	287.21
6a8_6a9	0.00006005	0.00000427	0.01371860	0.00124939	292.94
6a9_6a10	0.00001970	0.00000140	0.00470567	0.00042856	306.22
6a10_6a11	0.00005879	0.00000418	0.01406400	0.00128085	306.75
6a11_6a12	0.00034249	0.00002433	0.07590230	0.00691265	284.15
6a12_6a13	0.00005404	0.00000384	0.01133740	0.00103254	268.99
6a13_6b7	0.00005664	0.00000402	0.01213170	0.00110487	274.62
6b7_6b6	0.00051014	0.00003624	0.10544700	0.00960335	265.02
6b6_6b5	0.00003312	0.00000235	0.00729307	0.00066420	282.35
6b5_6b4	0.00052271	0.00003713	0.10804700	0.00984018	265.03
6b4_6b3	0.00582486	0.00041375	1.37608000	0.12532400	302.90
6b3_6b2	0.00847377	0.00060190	2.07037000	0.18855500	313.26
Wcoil	0.0821443	0.00583482	18.7896	1.71122	293.28
Hcoil1	0.0567253	0.00402927	13.1262	1.19544	296.69
Hcoil2	0.0568354	0.00403709	12.7882	1.16466	288.49

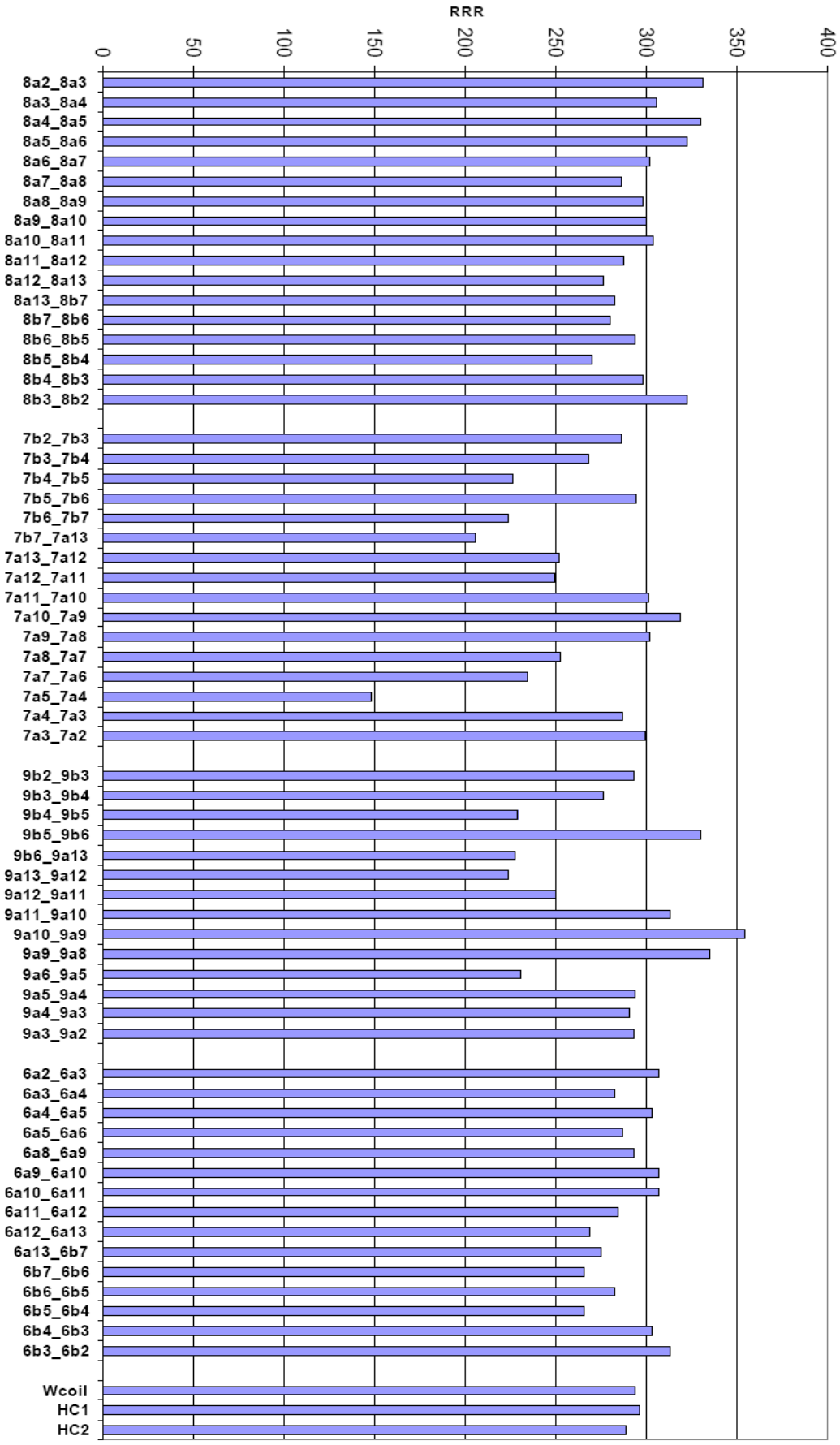

Fig. 47. RRR measurements for CVT and FVT segments.

10. Magnetic Measurements

Field quality magnetic measurements were made with the VMTF vertical drive system and DSP rotating harmonic coil readout cart [5]. Measurements at room temperature - "warm" measurements were done before and after the cold test.

The full cold measurement program is described below. An 81.8 cm long tangential probe (this is the length of the tangential winding), with 2 dipole, 2 quadrupole and 1 tangential windings, was utilized. This probe was specially built for LHC program and it was used extensively in the HGQ program and production measurements of LQXBs. The radius of the probe is 1.95 cm, optimized to the diameter of the LHC warm bore, used in this test. Because of the limited length of the warm bore, the probe could not reach the return end of the magnet. For the first measurement point, labeled as a position 1, the probe center was located at 1.4 inches above the magnet geometrical center. Two more longitudinally translated measurements were taken, where the probe was moved vertically by steps of 81.8 cm (length of probe).

The positive direction of the z-axis for the scans is pointing from the magnet center to the lead end, from which the probe was inserted. Each measurement contains data from at least ~180 full rotations of the probe.

The cold magnetic measurement program was performed at 4.5 K only and consisted of the following measurements:

a. Pre-quench Z-scans, from the magnet center to the lead end, at 6.5 kA,
b. Z-scans at 12.3 Tm/m (LHC injection, estimated to be 0.655 kA), 100 Tm/m (estimated to be 5.3 kA) and 10.0 kA. Two more measurements were done at 3 kA, 4.5 kA and 8 kA.
c. Eddy current loops with the ramp rates 20 A/s, 40 A/s and 80 A/s up to 9.0 kA with the probe positioned in the center of the magnet.
d. Dynamic effects measurement, which included a current accelerator profile, similar to the one used in LHC LQXB quads (15 min. duration of the injection plateau and the probe positioned in the center of the magnet).
e. A stair step measurement, stopping 2 min at 1.5, 2, 4, 6, 8 and 9 kA and back.

All magnetic measurement results are presented at 22.5 mm reference radius, which corresponds to the official radius adopted for LHC (17 mm) corrected for the expected increase in the magnet aperture from ~70 mm to ~90 mm.

Table 6 summarizes the geometrical harmonics at 12.3, ~ 100 and 179 T/m field gradient. Unallowed harmonics of several units are observed almost in all currents, especially for the low order ones.

Fig. 48 shows the quadrupole strength (T/m) versus current (kA). The line represents the fit to the first 3 points only $y = 1.9 + 19.5 \cdot x$. One may conclude that the iron saturation starts at a really low current.

This statement is confirmed by the result shown in Fig. 49. The transfer function (TF) starts significantly to decrease in the region between 2-3 kA. The linear fit returned a result: $y = 21.6 - 0.4 \cdot x$.

Fig. 50 shows the transfer function (TF) versus z coordinate (the center of the probe was positioned at 0.034 m, 0.85 m and 1.67 m) at 0.66 kA (estimated injection current), 5.3 kA (estimated 100 T/m) and 10.0 kA. The effective length of the magnet was not calculated, no full body scan was performed due to limited length of the warm bore.

Fig. 51 shows the dodecapole versus time. The current profile used in this measurement was derived from the profile of production inner triplet LHC quadrupole (LQXB) measurements. The duration of the injection porch was set to 15 min at 12.8 T, accordingly to the LHC specifications. One can observe that the b6 *decay* and *snapback*, which are commonly observed in NbTi magnets, are not present (see the time interval from ~1000 s to ~1080 s). The fine scale inset confirms the flatness of the injection region. This phenomenon needs an independent study for Nb_3Sn magnets.

Table 6. LQS01 body harmonics at different currents

#	Injection (0.66 kA)	100 T/m (5.3 kA)	10 kA
b_3	3.34	2.29	2.61
b_4	7.72	6.73	6.93
b_5	0.06	0.17	-0.08
b_6	-33.31	9.89	7.47
b_7	0.05	-0.06	-0.11
b_8	-0.28	-0.98	-0.38
b_9	0.08	0.19	0.13
b_10	0.56	0.35	-0.47
a_3	2.03	2.28	2.28
a_4	6.28	1.94	2.11
a_5	-0.50	-0.51	-0.65
a_6	-1.14	-0.12	-0.29
a_7	0.17	0.29	0.14
a_8	0.12	0.08	0.06
a_9	-0.29	-1.09	-0.16
a_10	0.05	0.37	0.12

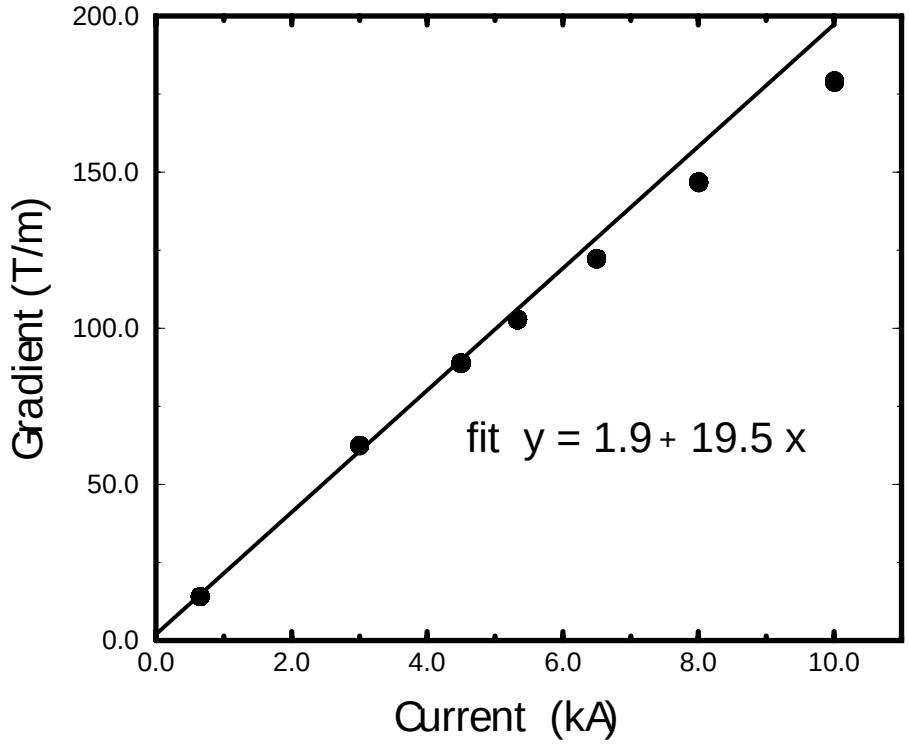

Fig. 48. LQS01 magnet gradient vs current, with linear fit to three lowest current points.

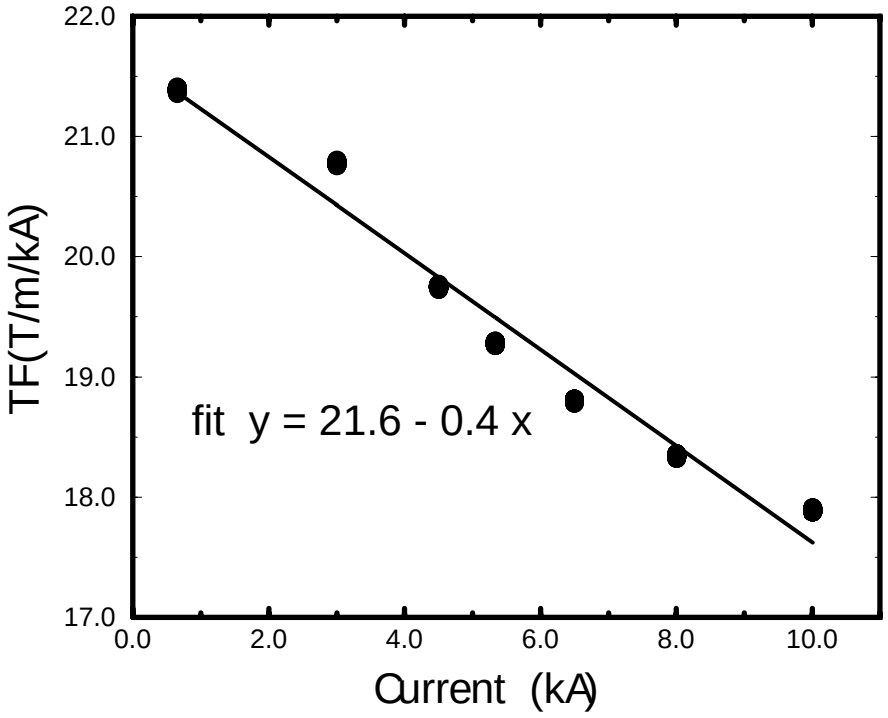

Fig. 49. LQS01 gradient magnetic field transfer function vs current.

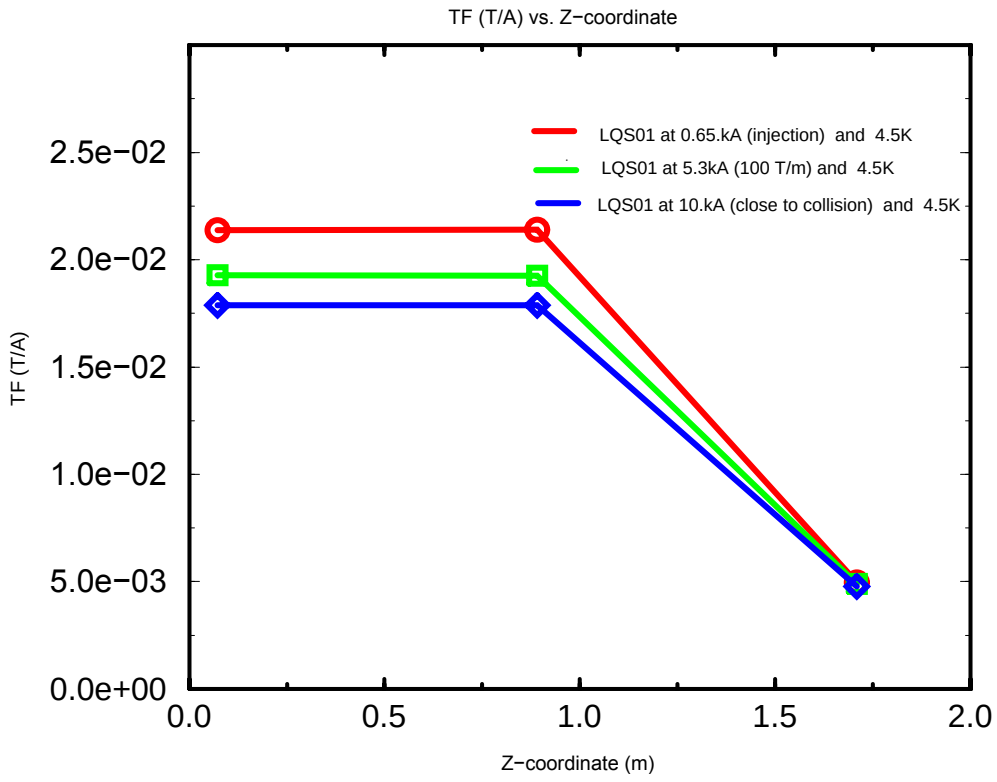

Fig. 50. LQS01 transfer function, integrated over probe length, vs z-coordinate at 0.65 kA, 5.3 kA and 10.0 kA.

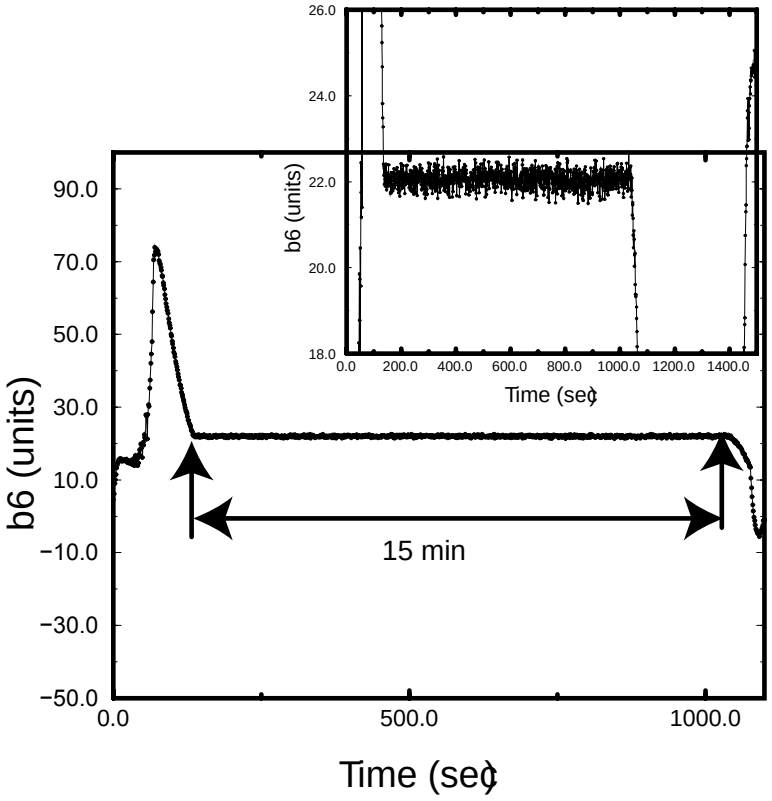

Fig. 51. Dodecapole (b6, in units) vs time (s) in a modified LHC accelerator current profile. The inset shows the injection plateau with fine scale for b_6.

Current loops at 20 A/s, 40 A/s and 80 A/s ramp rates for LQS01 quadrupole have been executed. The b_6 difference between the ramp rate loops is small, indicating small or negligible eddy current effect on the hysteresis loop, similar to what was observed in TQS measurements. The b_6 hysteresis loops are shown in Fig. 52. The blue dots in the figure represent the results from the stair-step measurement, which describes the magnet hysteresis loop.

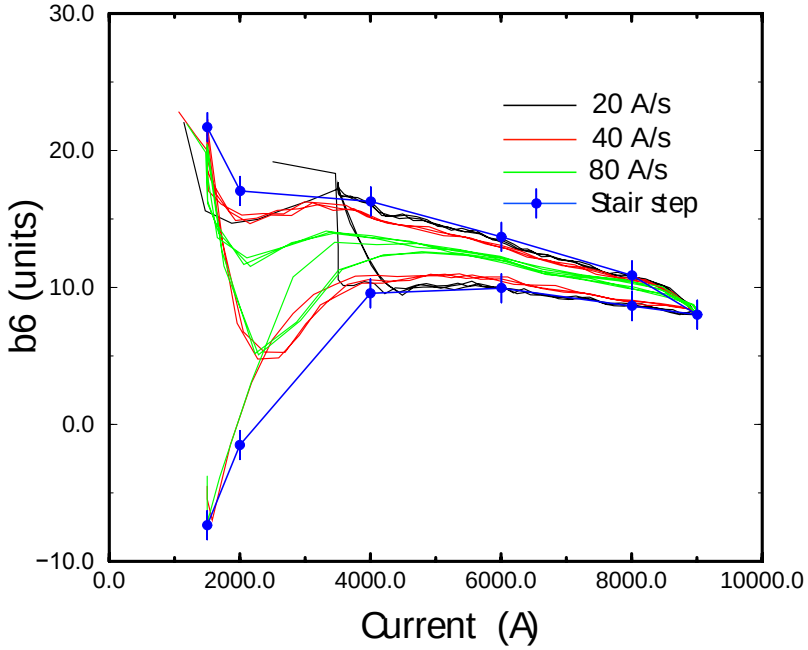

Fig. 52. Dodecapole (b6) vs excitation current at different ramp rates.

11. Spike Data Analysis

The voltage spike detection system (VSDS) based on a National Instruments PXI multifunction DAQ was used for study of thermo-magnetic instabilities in LQS01 magnet. The VSDS captures half-coil signals at a sampling rate of 100 kHz. More details on this system are presented in [6]-[7].

Voltage spikes captured during quench training ramps, as a function of the magnet current and at different temperature, are shown in Fig. 53-55.

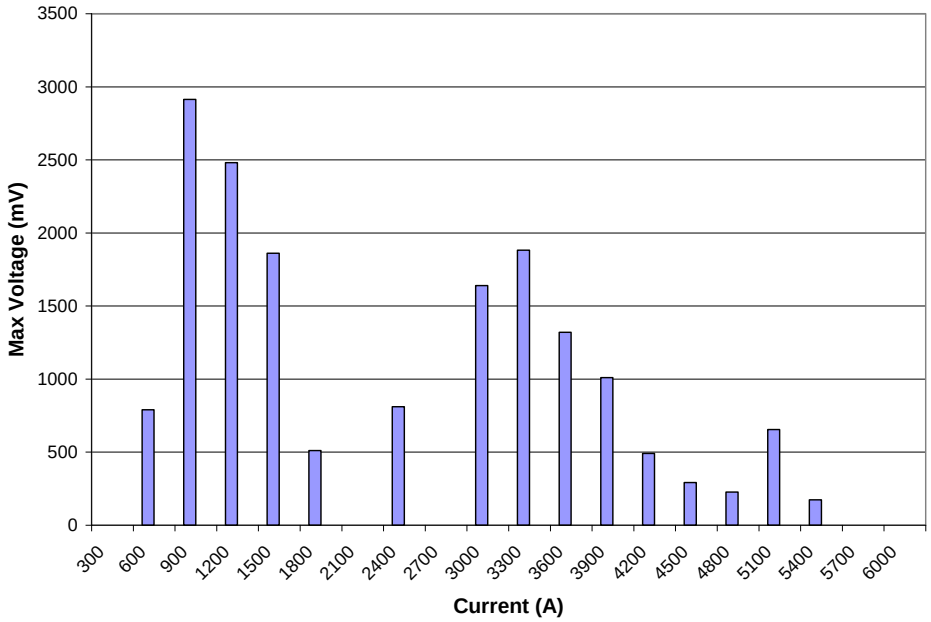

Fig. 53. Voltage spike maximum amplitude as a function of the magnet current at 4.5 K. Two-peak structure is a result of using different ramp rates: 200 A/s ramp rate up to 3 kA and 50 A/s above 3 kA.

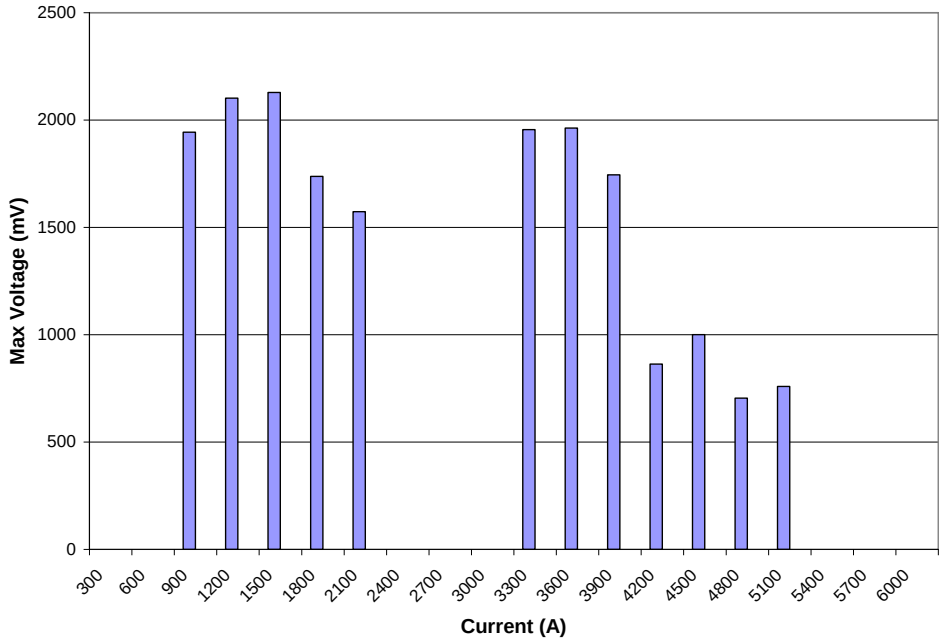

Fig. 54. Voltage spike maximum amplitude as a function of the magnet current at 3 K. Two-peak structure is a result of using different ramp rates: 200 A/s ramp rate up to 3 kA and 50 A/s above 3 kA.

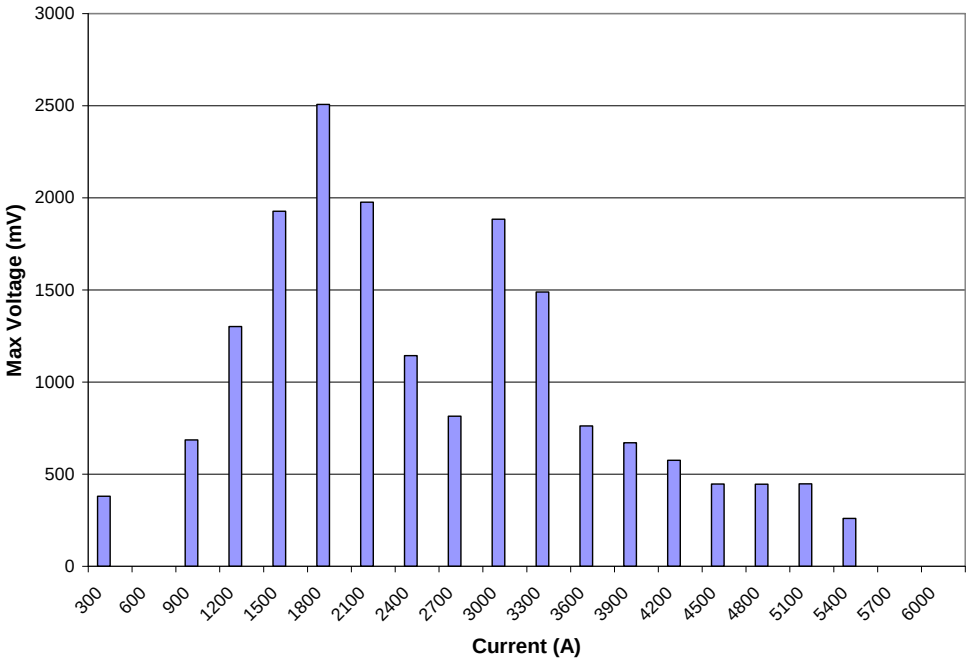

Fig. 55. Voltage spike maximum amplitude as a function of the magnet current at 1.9 K. Two-peak structure is a result of using different ramp rates: 200 A/s ramp rate up to 3 kA and 50 A/s above 3 kA.

Threshold for the voltage spike detection varied between 200 mV and 400 mV. Noise level in half-coil signal of LQS01 magnet at high currents reaches +/- 250 mV, which is significantly larger than +/- 10 mV we observed in short TQ magnets with the same conductor. Long cable could be a source of increased noise, although in the long (4-m) dipole mirror magnet LM02, with the advanced 108/127 RRP strand, the noise level was just +/- 20 mV.

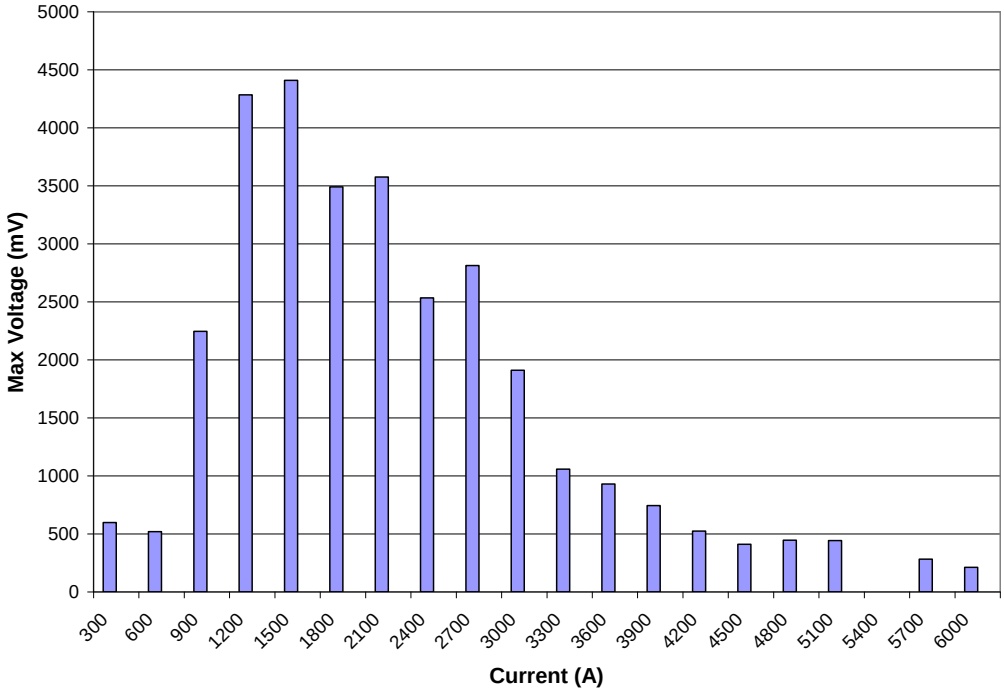

Fig. 56. Voltage spike maximum amplitude vs current at 4.5 K for a ramp rate of 50 A/s.

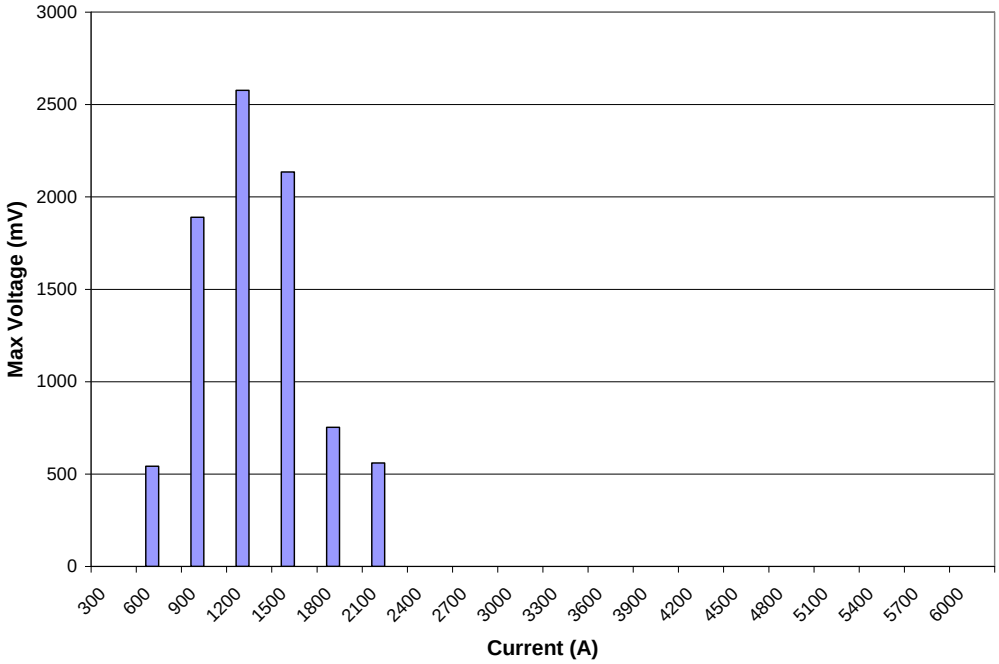

Fig. 57. Voltage spike maximum amplitude vs current at 4.5 K for a ramp rate of 150 A/s.

Two-peak structure in spikes (Fig. 53-55) is caused by different ramping rates we used during the test. For the training quenches we were using 200 A/s ramp rate up to 3000 A and 50 A/s above 3000 A. Different ramp rates result in the different voltage spike distribution. Voltage spikes for 50 A/s and 150 A/s ramp rates are shown in Fig. 56 and 57. One can see that spikes are more localized and have smaller amplitude at 150 A/s. This was the main motivation for using high ramp rate (200 A/s) up to 3000 A during the LQS01 training – to pass through the high amplitude voltage spike region from 800 A to 3000 A for LQS01. At high ramp rates there are almost no spikes above the threshold (400 mV) for the magnet currents 3000 A and more. Peak location also is slightly shifted left (to the lower currents) at high ramp rates.

Number of voltage spikes as a function of magnet current at different temperature is shown in Fig. 58.

12. Summary

The first LARP shell-type Nb_3Sn Long Quadrupole made of 0.7-mm RRP strand with 54/61 sub-elements was tested at the Fermilab's Vertical Magnet Test Facility. The magnet reached target field gradient of 200 T/m several times at both 3 K and 1.9 K temperatures.

Magnet training was interrupted in order to avoid coil degradation due to possibly non-optimal pre-stress distribution in the magnet. The maximum quench current reached in this test was 11372 A at 1.9 K (quench #45). At 4.5 K magnet reached 11.1 kA quench current which is ~ 80 % of the predicted short sample limit.

Ramp rate dependence study confirmed that quench training was not completed and there is margin for improving in the magnet performance.

Magnetically, this is a quadrupole with fairly large non-allowed harmonics, and in which iron saturation sets in at very low current. Ramp rate dependence shows little or no eddy current contribution to the b_6 hysteresis loop, similar to TQS magnet behavior. Also, no decay and snapback are observed in the dodecapole for this conductor.

LQS01 test will be resumed after disassembly and reassembly of the magnet to improve the coil stress distribution.

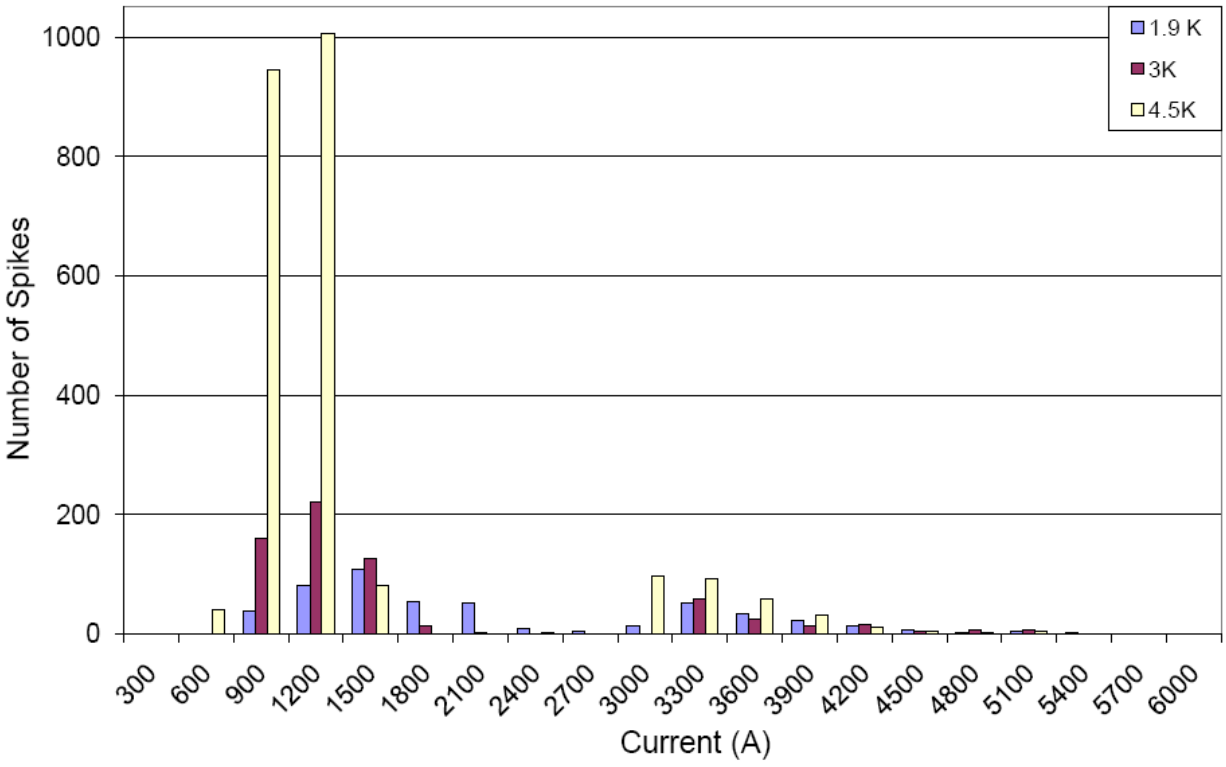

Fig. 58. Spike multiplicity at different temperatures. Two-peak structure is a result of using different ramp rates: 200 A/s ramp rate up to 3 kA and 50 A/s above 3 kA.

References

1. G. Ambrosio, et al., "Final Development and Test Preparation of the First 3.7 m Long Nb_3Sn Quadrupole by LARP", *IEEE Trans. Appl. Supercond.*, accepted for publication
2. P. Ferracin, et al., "Assembly and Loading of LQS01, a shell-based 3.7 m Long Nb_3Sn Quadrupole Magnet for LARP", *IEEE Trans. Appl. Supercond.*, accepted for publication.
3. G. Ambrosio, et al., "Long Quadrupole Design Report", LARP report available on-line: https://plone.uslarp.org/MagnetRD/longquad/LQ_DR.pdf
4. LQS01 Magnet Description at http://tiweb.fnal.gov/website/controller/491
5. G.V. Velev et al., "A Fast Continuous Magnetic Field Measurement System based on Digital Signal Processors", IEEE Trans. Appl. Superconduct., Vol. 12, Issue 2, June 2006, pp 1374-1377
6. B. Bordini et al., "Voltage spikes in Nb_3Sn and NbTi Strands", IEEE Trans. Appl. Superconduct., Vol. 16, Issue 2, June 2006, pp 366-369
7. D.F. Orris et al., "Voltage Spike Detection in High Field Superconducting Accelerator Magnets," IEEE trans. Appl. Superconduct., Vol. 15, Issue 2, June 2005, pp 1205-1208

Attachment I

LQS01 heater powering **10/30/2009**

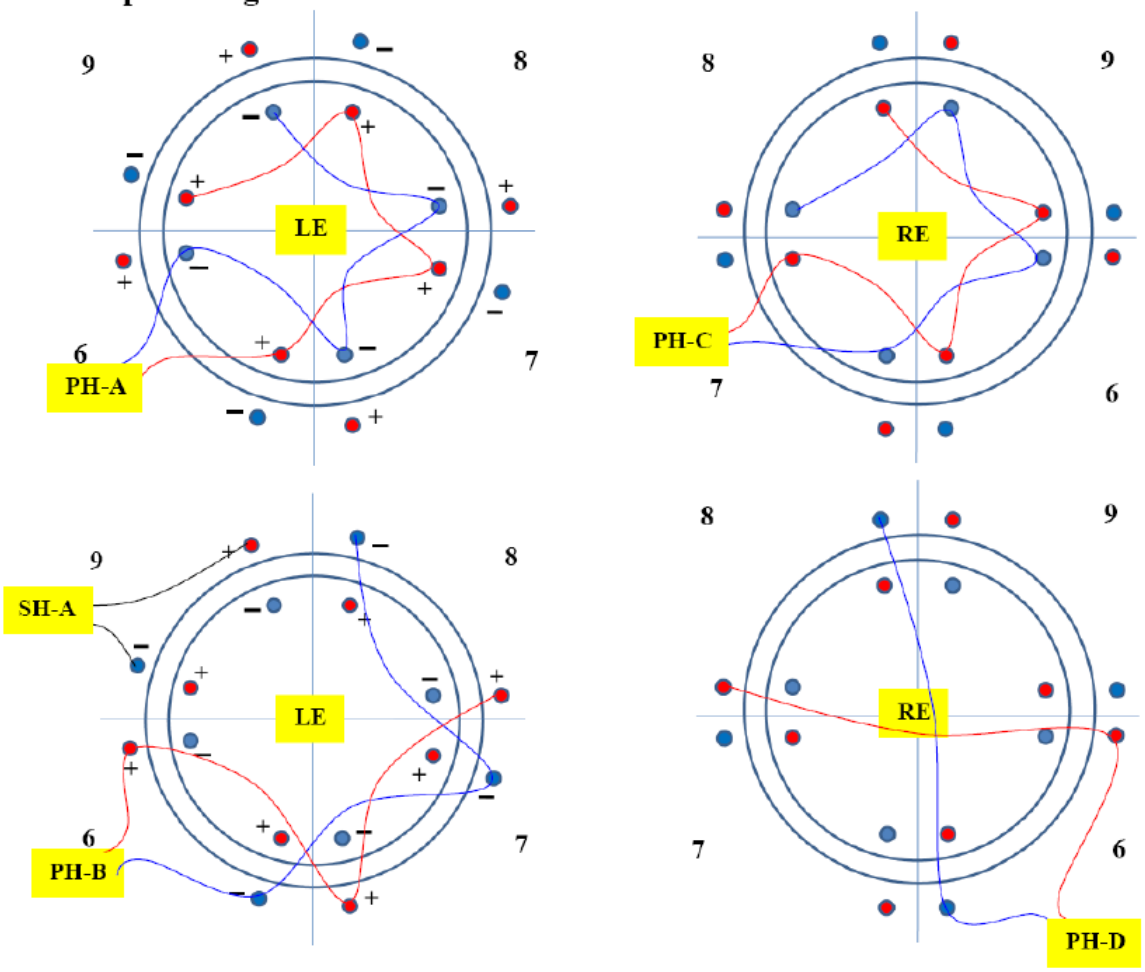

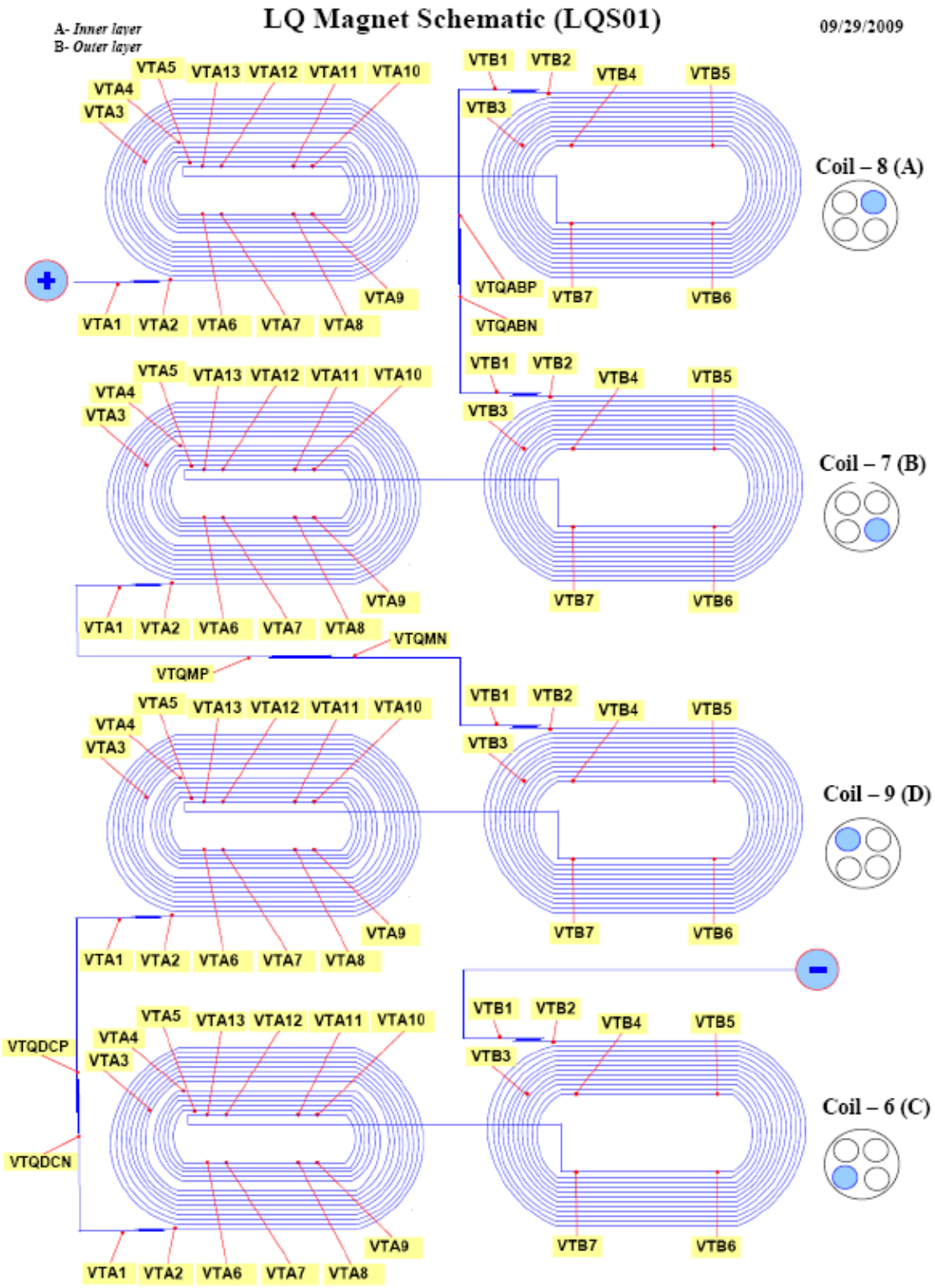
LQ Magnet Schematic (LQS01)
09/29/2009
A- Inner layer
B- Outer layer
VTA5 VTA13 VTA12 VTA11 VTA10
VTA4
VTA3
VTB1 VTB2 VTB4 VTB5
VTB3
Coil – 8 (A)
VTA9
VTA1 VTA2 VTA6 VTA7 VTA8
VTQABP
VTQABN
VTB7 VTB6
Coil – 7 (B)
VTQMN
VTQMP
Coil – 9 (D)
Coil – 6 (C)
VTQDCP
VTQDCN